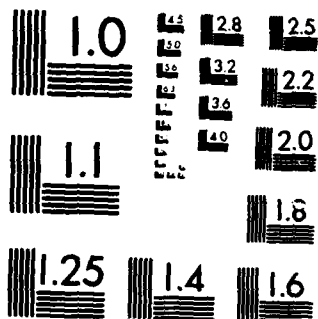


AD-A163 949 STUDY OF BIPOLAR NICKEL-CADMIUM BATTERIES AS PULSED
LOAD FILTERS(U) AIR FORCE INST OF TECH WRIGHT-PATTERSON
AFB OH SCHOOL OF ENGI.. R W CHEDISTER ET AL. NOV 85
UNCLASSIFIED AFIT/GE/ENG/85D-6 F/G 18/3

UNCLASSIFIED

NL

F/G 10/3



MICROCOPY RESOLUTION TEST CHART
NATIONAL BUREAU OF STANDARDS-1963-A

AD-A163 949



DTIC
ELECTE
FEB 12 1986
S D

Study of Bipolar Nickel-Cadmium
Batteries as Pulsed Load Filters

Thesis

Robert W. Chedister
Major, USAF

John M. Ulmer
Captain, USAF

AFIT/GE/ENG/85D-6

DISTRIBUTION STATEMENT A

Approved for public release;
Distribution Unlimited

DEPARTMENT OF THE AIR FORCE
AIR UNIVERSITY

AIR FORCE INSTITUTE OF TECHNOLOGY

Wright-Patterson Air Force Base, Ohio

FILE COPY

AFIT/GE/ENG/85D-6

DTIC
ELECTE
FEB 12 1986
S D D

Study of Bipolar Nickel-Cadmium
Batteries as Pulsed Load Filters

Thesis

Robert W. Chedister John M. Ulmer
Major, USAF Captain, USAF

AFIT/GE/ENG/85D-6

Approved for public release; distribution unlimited

AFIT/GE/ENG/85D-6

STUDY OF BIPOLAR NICKEL-CADMIUM
BATTERIES AS PULSED LOAD FILTERS

THESIS

Presented to the Faculty of the School of Engineering
of the Air Force Institute of Technology
Air University
In Partial Fullfillment of the
Requirements for the Degree of
Master of Science in Electrical Engineering

Robert W. Chedister
Major, USAF

John M. Ulmer
Captain, USAF

November 1985

Approved for public release; distribution unlimited

Preface

We would like to recognize and thank a few of the many people who provided guidance and assistance to us during this study effort. Our thesis committee helped us professionally with their guidance and support. Mr. Carl Shortt and Mr. Ron Ruley from the Model Fabrication Division of the Air Force Institute of Technology helped us making the battery parts. Mr. Scott Bishop, Mr. Irv Luke, and Mr. Mel French from the Air Force Wright Aeronautical Laboratories, Aero Propulsion Laboratory provided excellent sponsorship and assistance. Also from the Aero Propulsion Laboratory, our guru, Dr. David Fritts provided daily technical guidance while Mr. John Leonard showed us how to actually do most things. Without the help of the aforementioned few, among many, and the support of our families, this effort would not have been possible.

Robert Chedister

John Ulmer

Accession For	
NTIS CRA&I	<input checked="checked" type="checkbox"/>
DTIC TAB	<input type="checkbox"/>
Unannounced	<input type="checkbox"/>
Justification	
By	
Distribution /	
Availability Codes	
Dist	Avail and/or Special
A-1	

Table of Contents

	Page
Preface	ii
List of Figures	vi
List of Tables	viii
Abstract	ix
I. Introduction	1
Background	1
Purpose	3
Approach	3
Sequence of Presentation	5
II. Battery Theory	6
Background	6
Nickel-Cadmium Cell	7
Chemical Reactions	8
Bipolar Design	9
Capacitance and the Double Layer	10
Electrode Structure	13
Battery Parameters	14
Battery Testing	17
Acceptance	17
Performance	18
Endurance	19
III. Experimental Battery	21
Background	21
Design	21
Fabrication	22
Metal Work	22
Electrodes	23
Sinter	23
Impregnation	24
Seals	26
Assembly	27
Specifications	28
Theoretical Capacity	28
Battery Equivalent Weight	29
IV. Test Network	30
Background	30

	Page
Test Equipment	30
Test Circuit Designs	30
Test Circuit Operation	31
Conditioning Test Circuit	31
Charging Circuit	32
Performance Test Circuit	32
Endurance Test Circuit	35
V. Experimental Test Procedures	38
Background	38
Acceptance Testing	38
Charging	38
Conditioning	39
Capacity Checking	40
Performance Testing	42
Current Load	42
Cycle Rate	42
End of Discharge Voltage	43
Endurance Testing	44
Cycle Life Capacity	44
Cadmium Electrode Study	44
VI. Results and Discussion	46
General	46
Battery Mechanics	46
Design	46
Electrodes	47
Seal	49
Test Network	52
Operator Interface	52
Data Collection	52
Circuit Control	52
Program Structure	53
Measurement Inaccuracy	53
Battery Response	53
Acceptance Testing	54
Charging	54
Capacity	54
Internal Resistance	55
Performance Testing	56
Current Load	56
Cycle Rate	57
End of Discharge Voltage	63
Endurance Testing	64
Cycle Life	64
Cadmium Electrode Study	66

	Page
VII. Conclusions and Recommendations	70
Conclusions	70
Recommendations	72
Appendix A. Capacitance From Voltage Waveform . .	74
Appendix B. Sample Calculations of Battery Parameters	76
Appendix C. Battery Components	79
Appendix D. Electrode Sintering Checklist . . .	85
Appendix E. Electrode Impregnation Checklist . .	87
Appendix F. Battery Equivalent Weights	92
Appendix G. Equipment	94
Appendix H. Computer Program	101
Appendix I. Electrode Specifications	104
Appendix J. Internal Resistance	106
Appendix K. Performance Data	109
Appendix L. Scanning Electron Microscope Photographs	114
Bibliography	118
Vita	121

List of Figures

Figure	Page
2-1 Simple Nickel-Cadmium Cell	7
2-2 Current Path Through a Four-Cell Battery . .	10
2-3 Ni-Cd Battery Equivalent Circuit	11
3-1 Battery Inter-cell Seal	27
4-1 Conditioning and Charging Circuit	32
4-2 Performance and Endurance Test Network . . .	33
5-1 Battery Voltage and Charging Current . . .	40
6-1 Energy Density of Test Battery #1	58
6-2 Current Load Test - Temperature	59
6-3 Current Load Test - Efficiency	60
6-4 Current Load Test - Capacitance	61
6-5 Current Load Test - Discharge Voltage . . .	62
6-6 Endurance Test - Capacity Versus Cycles . .	65
6-7 Cadmium Electrode Interior Before Cycling . .	68
6-8 Cadmium Electrode Interior After Ten Thousand Cycles	68
6-9 Cadmium Electrode Interior After Ten Million Cycles	69
A-1 Capacitance From Voltage Waveform	75
B-1 Typical Waveforms	78
C-1 Dimensions of Battery Components	80
C-2 Inner End Plate for Removeable Electrode Battery	81
C-3 Standard Electrode Substrates	82
C-4 Expanded View of a Test Bipolar Battery . .	83

Figure		Page
C-5	Expanded View of a Removeable Electrode Battery	84
E-1	Electrode Impregnation Apparatus	90
E-2	Impregnation Mount Components	91
G-1	Test Equipment Layout	97
G-2	Bipolar Ni-Cd Battery	98
G-3	Bipolar Ni-Cd Battery Parts	99
G-4	Miscellaneous Battery Parts	100
H-1	Endurance Test Battery Control Parameters . .	102
H-2	Endurance Test Control Logic	103
J-1	Internal Resistance of Battery #1 at Full Capacity	107
J-2	Internal Resistance of Battery #1 at One-Half Capacity	108
K-1	Battery #1 Capacitance Versus Cycle Rate . .	110
K-2	Battery #1 Efficiency Versus Cycle Rate . .	111
K-3	Battery #2 Capacitance Versus End of Discharge Voltage	112
K-4	Battery #2 Efficiency Versus End of Discharge Voltage	113
L-1	Cadmium Electrode Blister - Top View . . .	115
L-2	Cadmium Electrode Blister - Side View . . .	115
L-3	Cadmium Electrode Surface Before Cycling . .	116
L-4	Cadmium Electrode Surface After Ten Million Cycles	116
L-5	Cadmium Electrode Back Before Cycling . . .	117
L-6	Cadmium Electrode Back After Ten Million Cycles	117

List of Tables

Table	Page
I. Bipolar Battery Capacities	55
II. Electrode Specifications	105

ABSTRACT

Bipolar nickel-cadmium batteries were designed, built, and tested for possible use as capacitive filter elements in pulsed power applications. Electrodes were made by electrochemically impregnating sintered sides of nickel cell walls. Four-cell batteries were constructed by compressing the electrodes together with Teflon seals. A computer controlled test circuit charged and discharged the test batteries at frequencies of 1 to 50 Hertz and at depths of discharge of less than one percent. A special test battery was constructed with a removeable cadmium electrode for scanning electron microscope study. Battery energy density, effective capacitance, and efficiency were investigated as a function of current load or depth of discharge, cycle rate, and end of discharge voltage. Energy densities of nearly 75 joules per pound were demonstrated. Current loads of up to a 100 C-rate were demonstrated and an average capacitance of 6 farads was achieved. Cadmium electrode morphology was photographed and studied as a function of the charge and discharge cycle life with no crystalline anomalies discovered. Sinter corrosion, nickel electrode overcharging, and individual cell voltage imbalances were discovered as areas for further study.

Study of Bipolar Nickel-Cadmium Batteries as Pulsed Load Filters

I. Introduction

Background

Recent space endeavors requiring increased power have accentuated the need for lighter power sources which can operate reliably for extended periods of time. Spacecraft power systems account for typically one third of the total weight of a satellite with capacitive filters a significant part of the power system weight (1:250). These filters provide high load current pulses that reduce the peak demand on the power source. Space planners have recognized the need for innovative and significant advances in the space power systems of the near future to keep pace with the advancing technology of spacecraft subsystems (1,2). One such innovative idea is to use batteries, instead of capacitors, as pulsed load filters.

Batteries have a demonstrated capability to provide higher energy densities than the capacitors currently used in space power systems (3:59). This increased energy density can be translated into a direct weight reduction of the power source. Recent investigations have been made at the Aerospace Power Division, Aero Propulsion Laboratory, Air Force Wright Aeronautical Laboratories, Wright-Patterson

AFB, Ohio into the use of nickel-cadmium (Ni-Cd) batteries as filter elements for pulsed loads. D.C. Stumpff and W.S. Bishop demonstrated a ten-fold increase in energy density over capacitors using typical Ni-Cd aircraft batteries in 1982 (4). A cycle life of 10 million charge/discharge cycles was achieved at an energy density of 5.4 joules per pound. Cimino and Gearing continued this investigation, in 1984, through an Air Force Institute of Technology thesis sponsored by the Aero Propulsion Laboratory (5). They constructed a pseudo bipolar Ni-Cd battery in an attempt to optimize the capacitive efficiency of the battery. Energy density, cycle life, and electrode characteristics were investigated. They concluded that the bipolar design significantly increased the available energy density and successfully cycled their batteries for 10 million cycles with an equivalent energy density of 14 joules per pound. However, they had difficulty monitoring and adjusting their batteries during testing and suggested a computer controlled test network would enhance any further investigations.

In this study, a true bipolar battery was constructed for testing. A bipolar battery is one in which the normally separate positive and negative electrodes are combined on opposite sides of a single conducting substrate. The substrate acts as an inter-cell connector (6:3). Batteries are constructed by stacking numerous bipolar plates into battery cells. The advantages of the bipolar battery design over

the standard monopolar battery are reduced internal resistance and inductance, and a significant weight and size reduction for equivalent battery energy densities.

Purpose

The goal of this thesis was to continue the Aero Propulsion Laboratory's investigation into the use of nickel-cadmium batteries as filter elements for pulsed load applications. The objectives of this thesis were to design, construct, and test bipolar Ni-Cd batteries to determine their suitability for use as relatively high frequency filter elements. Battery performance, expected service life, and specific battery failure mechanisms were investigated. A computer controlled test network was developed to facilitate and control the evaluation of the test batteries.

Approach

Presently, there are few, if any, large research efforts studying true bipolar batteries and no known bipolar batteries are being commercially manufactured. However, there is some related work being conducted. Dunlop Batteries of Australia has developed and produced a quasi-bipolar lead-acid battery for use in automobiles. The Jet Propulsion Laboratory has worked on a bipolar lead-acid battery for electric vehicle applications. NASA Lewis Research Center has investigated bipolar nickel-hydrogen batteries for space applications. Gulton Industries, in 1966, developed a workable bipolar Ni-Cd battery which was proposed for use in

laser and pyrotechnic activation (7). The Gulton batteries were not rechargeable or utilized as filter elements. However, their design was similar to the bipolar batteries independently designed and manufactured for this thesis effort (8:976).

The first of three major areas of concern in this thesis was the manufacturing of the test batteries. The test bipolar batteries were designed and built to minimize electrolyte leakage, and to facilitate electrode production, assembly, and evaluation. No attempt was made to optimize the batteries for commercial applications or to minimize overall weight. The batteries were specifically built to explore the performance of the bipolar design in a capacitive application and to demonstrate a higher energy density than previously tested batteries at the Aero Propulsion Laboratory.

The second major effort in this thesis was to set up a semi-automated test circuit to test the bipolar batteries. The test network was controlled by a Hewlett Packard HP-85A computer and test battery parameters were monitored with an HP-3497A data acquisition and control system. The test circuit alternately charged and discharged the test batteries at varying cycle rates from 1 to 50 Hertz and controlled the battery parameters used in evaluating battery performance. Battery testing was divided into acceptance, performance, and endurance phases. The computer controlled test network was partially used for performance testing and

extensively used for the long term, endurance testing.

The final area of concern in this study was to design and build a bipolar test battery with a removeable cadmium electrode. This electrode was periodically examined with a scanning electron microscope to investigate the effects of this cyclic filter application of the test battery on the structure of the cadmium electrode.

Sequence of Presentation

Chapter 2 presents battery theory. The nickel-cadmium electrochemical process and a discussion of the Helmholtz region or capacitance capability of the battery is also presented. Important battery parameters are defined and explained. Chapter 3 describes the design and manufacture of the test batteries. The process of making electrodes and the electrolyte sealing effort are outlined. Chapter 4 describes the semi-automated test network used to test the batteries. Key circuit control elements are identified and explained. Chapter 5 details the experimental procedures followed to accomplish battery acceptance, performance, and endurance testing, and cadmium electrode examinations. Chapter 6 presents the results and discussion of the data collection and analysis. Chapter 7 contains conclusions and recommendations resulting from this thesis effort. Finally, the appendices provide specific details and explanations in several areas.

II. Battery Theory

Background

The electrochemical process fundamental to a battery's operation may have been known for thousands of years. Archaeological discoveries of copper-iron wet cells near Baghdad, Iraq are thought to be 2000 years old. Chemical energy stored in a battery is converted into electrical energy when the battery is discharged. The quantity of electrical energy is a function of the inherent potential and efficiency of the electrochemical reactions, as well as the amount of chemically active material within the battery.

The fundamental element of a battery is a cell. A simple cell, like the monopolar nickel-cadmium (Ni-Cd) cell shown in Figure 2-1, is made up of a positive nickel hydroxide (NiO(OH)_2) electrode, a negative (Cd) electrode, and an aqueous solution, or electrolyte, of potassium hydroxide (KOH). The positive and negative electrodes accept and furnish electrons to an electrical circuit while the electrolyte completes the circuit internally by furnishing ions for conductance. The chemical process is reversible for rechargeable or secondary batteries. The choice of electrode materials determines the fundamental potential difference or electromotive force of the cell. The type of electrolyte, efficiency of the chemical reaction, and the cell design are major determinants in the performance of a battery (2,9).

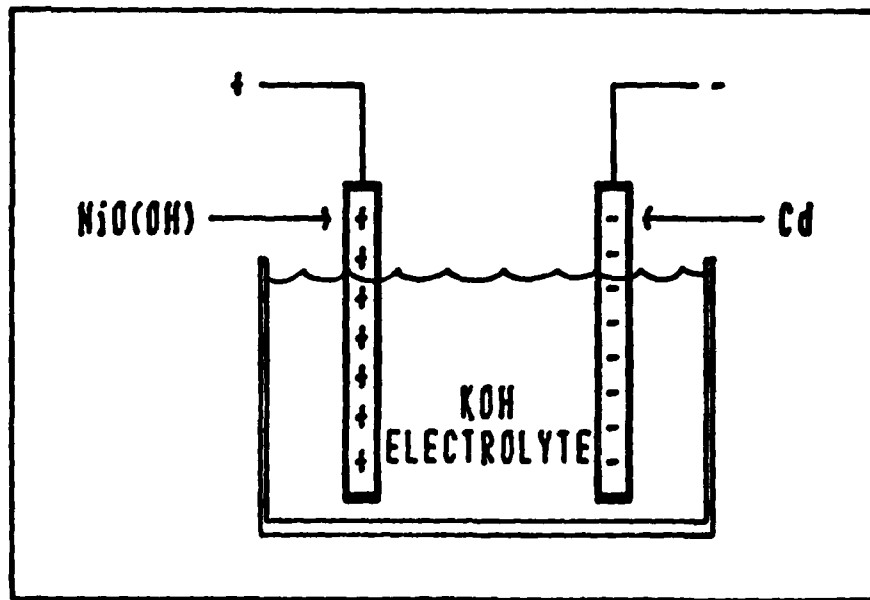


Figure 2-1. Simple Nickel-Cadmium Cell

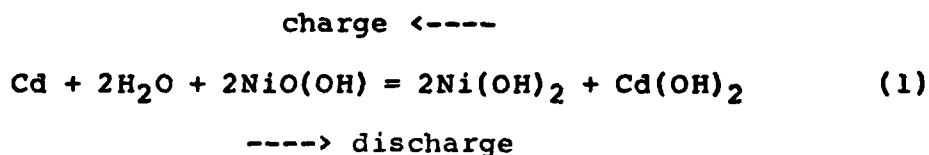
Nickel-Cadmium Cell

There are many types of rechargeable batteries available today with specific characteristics that makes one type better than another for certain applications. However, this study dealt solely with the nickel-cadmium (Ni-Cd) battery first built by Waldeman Junger, a Swedish chemist, in 1890 (10:69). The Ni-Cd battery has been the workhorse for the United States space program since its inception and is the most widely used battery aboard United States Air Force aircraft (2:255,11:28). Ni-Cd batteries emit no noxious fumes or gasses during use. There are no specific gravity tests required for the electrolyte and the batteries can be stored in any state of charge for long periods of time. Ni-Cd batteries have demonstrated superior cycle life characteristics as compared to other available batteries (12).

Ni-Cd batteries are mechanically rugged and can operate over a wide temperature range. They are good for high magnitude, short duration currents and have excellent quick charging characteristics. These factors, in addition to the results of earlier work in this area accomplished at the Aero Propulsion Laboratory, led to the selection of the Ni-Cd battery for this study (4,5).

Chemical Reactions

In a Ni-Cd battery, the electrochemical reaction is the oxidation and reduction of the active material on the electrodes. During discharge nickelate hydroxide $\text{NiO}(\text{OH})$ at the positive electrode changes to nickel hydroxide $\text{Ni}(\text{OH})_2$ by accepting electrons from the external circuit and taking a proton from a water (H_2O) molecule. The remaining OH^- ion is released and is passed by the KOH electrolyte to the negative cadmium electrode. There it combines with cadmium to produce cadmium hydroxide $\text{Cd}(\text{OH})_2$ and release two electrons to the external circuit. The potential between the two electrodes provides the impetus for the movement of the ions. When the cell is recharged the process is reversed. An overall chemical reaction equation (10,13:70) can be simply represented by :



During overcharge, or when the battery is fully charged and charging current is still being applied, Oxygen (O_2) is released at the positive ($NiO(OH)_2$) electrode and migrates to the negative (Cd) electrode to combine with hydrogen (H_2) to produce water (H_2O). To reduce this gassing effect, the capacity of the cadmium electrode is made greater than the nickel hydroxide electrode (14). Gassing is a major problem in sealed cells and can create high internal battery pressures. Pressure vents are utilized to relieve pressure buildup in the cells of many Ni-Cd batteries.

Bipolar Design

The relatively long current path and the non-uniform current density through the electrodes are two disadvantages of the monopolar cell design of conventional batteries like that shown in Figure 2-2. The ohmic losses limit power density, reduce voltage efficiency, and generate excess heat. The non-uniform current density distribution over the electrodes does not fully or evenly utilize the active material and thus limits the useful life of the cell (6).

The bipolar cell design alleviates these two monopolar cell design disadvantages. It was first utilized when Volta built his original battery (15:710). The bipolar battery derives its name from its electrode configuration. The positive electrode of one cell and the negative electrode of the next cell are on opposite sides of a conducting substrate. Figure 2-2 shows how the current path through a

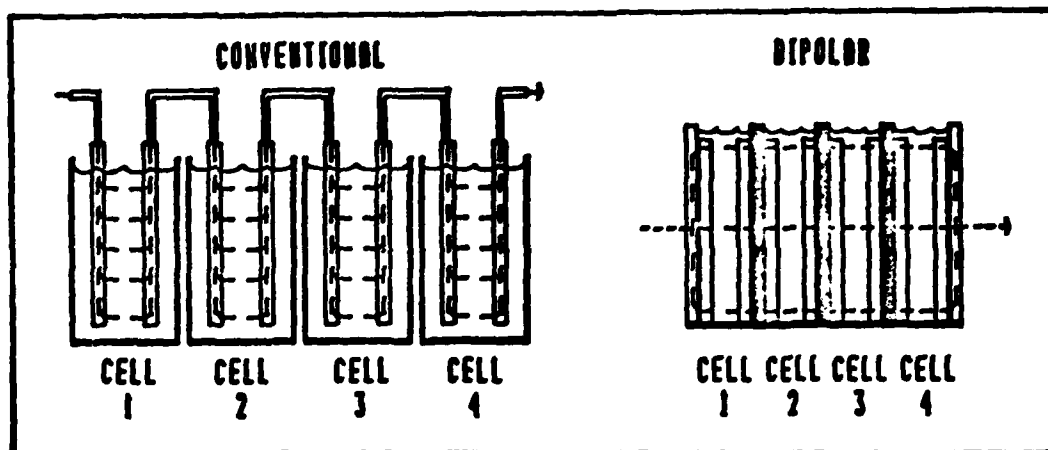


Figure 2-2. Current Path Through a Four-Cell Battery

bipolar cell differs from a monopolar cell. The current is uniformly distributed over the surface of the electrodes and its current path is shortened considerably. Previous testing of bipolar Ni-Cd batteries provided about six times the current density of conventional, monopolar batteries (6:A-14). Bipolar batteries, with a lower internal resistance, are capable of providing higher energy densities than capacitors and are believed to be an optimum cell design for pulsed power applications.

Capacitance and the Double Layer

When the battery is used to filter a pulsed load the instantaneous current and voltage changes through the battery are effected by its short-term or transient characteristics. These characteristics are dominated by the battery's internal resistance and capacitance. A common

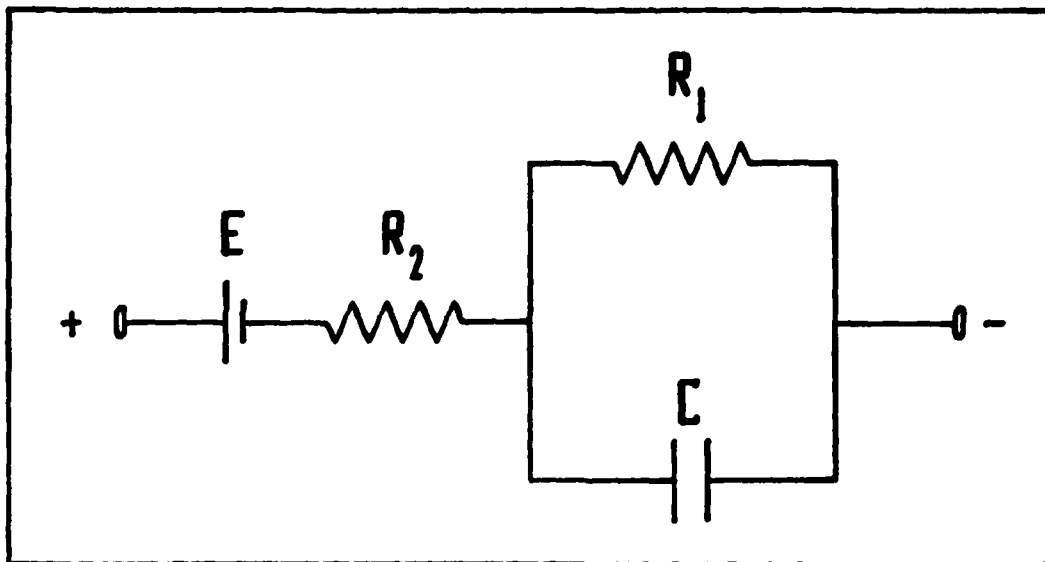


Figure 2-3. Ni-Cd Battery Equivalent Circuit (5:11)

equivalent circuit model of a Ni-Cd battery is shown in Figure 2-3. The circuit parameters are the ideal voltage, E , the effective delayed internal resistance, R_1 , the effective instantaneous internal resistance, R_2 , and the effective capacitance of the electrodes, C .

Capacitance is normally considered an electrostatic phenomenon of storing energy between two conductors separated by a dielectric material. The narrow region between a metallic electrode in a battery and its electrolyte behaves like an electric capacitor in that it is capable of storing charge. Electrodeics, or the study of this narrow region in electrochemistry, was conducted by Helmholtz almost a century ago (16:xiii,1-3). He, along with many others who followed, attempted to describe this capacitive nature of batteries as a double layer of ions. These charged ions,

separated by dielectric water molecules, act as miniature capacitors with the cell voltage across them. This "double layer" capacitance is an important factor in the transient response of a battery operated in a cyclic charge/discharge manner and is the basis for its proposed use as a filter element for pulsed loads.

Initially, when a Ni-Cd battery is discharged, the double layer capacitance of the cadmium and nickel electrodes discharge quickly. This initial voltage decay is due to the capacitive discharge of the battery electrodes and is followed by the much slower classical electrochemical, or faradic, discharge of the battery through the electrolyte (17:7). The effective capacitance of a battery can be calculated by assuming the capacitance remains constant and picking values for the current (I) and corresponding values for the voltage change (dV/dT) from battery output waveforms. Using the well-known equation

$$C = I / (dV/dT) \quad (2)$$

the effective battery discharge capacitance (C) can be calculated from the measured data.

The internal resistance of a Ni-Cd battery can be approximated by measuring the impedance with an a-c ohmmeter (18:6). It can also be calculated by assuming the instantaneous voltage change when the battery is switched from charge to discharge is strictly an IR drop (14). The resistance is then the change in voltage divided by the change in

current. Internal resistance for this study was based on ohmmeter readings and it was only used to quantify the internal resistance of the test bipolar batteries.

Where and how you measure the change in voltage on the voltage discharge curve is very important in determining the average capacitance of the battery. This study determined a pulse capacitance and a load capacitance. The pulse capacitance was based on the slope of the voltage curve at the point where the instantaneous voltage changes from a straight line path due to IR (current times resistance) drop; hereafter called the knee. The load capacitance was based on the slope of the voltage curve from the knee to the end of discharge value. This load capacitance is similar to the previously presented capacitance values of Cimino and Gearing (5:12). Figure A-1 illustrates these voltage points.

Electrode Structure

Failure mechanisms in Ni-Cd batteries include the general categories of total abrupt failure, loss of capacity, and shortened service life. One specific failure mode that impacts all of the above general categories is a change in the crystalline structure of the cadmium electrode. During discharge, the cadmium metal is changed into cadmium hydroxide crystals that form in the pores of the electrode plaque or sintered nickel. During charging, the cadmium hydroxide at the electrode surface changes to cadmium metal through a solid state reaction. The size of the deposited cadmium

crystals during the electrode manufacture and subsequent charge and discharge cycle life have a major impact on the performance of the battery. Large crystals or dendrites can cause inter-cell shorts (19). Heavy crystallization of the outer surface of a porous electrode reduces the available active material and reduces the capacity and service life of the battery by blocking the passages for electrolyte flow to the active material within the porous plaque. This study examined how rapid charging and discharging of a Ni-Cd battery affects the crystalline structure of the cadmium electrode. Scanning electron microscope photographs were used to record the cadmium crystalline structure changes as a function of the charge/discharge cycle life of a test bipolar Ni-Cd battery.

Battery Parameters

Numerous battery parameters are utilized to compare and evaluate battery performance. Unfortunately, many of these parameters have non-standard definitions within the electrochemical and scientific community. This section will establish the definitions for some of the important parameters used in this study. Sample calculations are provided in Appendix B to illustrate some of these parameters.

The "cycle life" of a secondary battery refers to the number of times it can be charged and discharged before its available current or voltage drops below a required minimum (20:6-2). Normally Ni-Cd batteries are expected to last up

to a few thousand cycles depending on their design and utilization. This study will address the expected performance of a battery that has been cycled millions of times.

The "depth of discharge" (DOD) of a battery is the ratio of the capacity removed from the battery during discharge to the specified capacity of the battery (21:1). Normal Ni-Cd utilization involves discharging the battery from 10 to 75% of its capacity over a few hours and slowly recharging it over many more hours (22:ii). This study involved depths of discharge under 1% for charge and discharge cycles of 20 to 1000 milliseconds. Previous research in this area dealt with DODs of hundredths of a percent (4,5:33).

The "capacity" of a battery is the amount of charge that it can deliver to the load, normally expressed in ampere-hours (a-h) (20:6.12). This study defined theoretical capacity as the capacity of a battery electrode based on electrochemical considerations. Each gram of cadmium or nickel hydroxide impregnated into a porous plaque yields 0.366 a-h or 0.289 a-h of capacity, respectively. A test battery's theoretical capacity was then equal to that of the minimum capacity electrode within its four cells. The measured capacity of the test battery was based on charging the battery for 1.75 hours at a current of 60% of its theoretical a-h capacity until the voltage reached 6.2 volts. The battery was discharged at its theoretical capacity amperage until the discharge voltage reached 1 volt per cell. The amperes multiplied by the hours of discharge time yielded

the measured ampere-hour capacity of the battery. This capacity amperage is sometimes called the C-rate and is used to refer to the rate at which a battery is being charged or discharged. For example, a 5 a-h battery discharged at 5 amps, at a 1 C-rate, would last one hour. Similarly, if the same battery is discharged at 1 amp, a 0.2 C-rate, it would last 5 hours.

The "energy density" of a battery is a common figure of merit expressing the stored energy as a function of weight. Capacitors used on spacecraft are expected to provide 1 joule per pound of energy density (23). An important part of this study was to demonstrate higher energy densities from Ni-Cd bipolar batteries than those provided from capacitors or previous Ni-Cd batteries tested. Energy density is calculated by multiplying the battery voltage by the battery current and discharge time and then dividing this value by the battery weight.

The "efficiency" of the test batteries was approximated by multiplying the average discharge voltage by the discharge current and then dividing this value by the average charge voltage multiplied by the charge current for an equal charge and discharge time (10:24). This serves as a figure of merit for the battery's response to charging and is an indication of the battery's operational status, internal losses, and the functional state of the electrodes.

Battery Testing

Acceptance. Acceptance testing involved the charging and conditioning of the test batteries. There are a number of methods for effectively charging vented Ni-Cd batteries. Charging involves putting energy into the battery in the form of electricity and then storing it as chemical energy. The methods differ in the amount of current supplied as compared to the ampere-hour capacity of the battery, the amount of time the battery is charged, and how the charging current, voltage or both are maintained during the charge. The charging current and time are combined into the C-rate parameter. For example, if a 10 ampere-hour battery is charged at a constant 5 amperes it is charged at a 0.5 C-rate. To fully charge it at this rate would require 2 hours. To charge it to 75% of its capacity would require charging it for only 1.5 hours.

Charging of the test batteries, as described in the discussion of the capacity parameter, was fundamental to the conditioning of the test batteries. Once a battery was assembled it was charged and discharged a number of times to determine its capacity and to condition the battery or optimize its operation. This conditioning process was the result of years of experience with Ni-Cd batteries and is based on the fact that Ni-Cd batteries initially improve with use. Researchers believe the improvement in performance is due to a further improvement in the nickel electrode similar to that resulting from the formation process

described later in the experimental battery chapter.

Performance. Performance testing was conducted on the bipolar batteries to ascertain how well they functioned when used as a capacitive element under a pulsed load. The first test involved determining how much current the battery could handle without overheating. From this test the energy density capability of the batteries was established to compare with past battery designs similarly tested. Average capacitance, efficiency, and energy density versus the battery discharge current were computed. A computer controlled test network was used to monitor battery temperature. All the battery testing was done at a 75% state of charge. This first test was done at a cycle rate of 5 cycles per second (cps).

The second performance test investigated the battery's response to different cycle rates. Cycle rates from 1 to 50 cps were performed at various current levels. Battery parameters such as average capacitance, efficiency, and energy density versus battery discharge current, were computed. Test battery response was studied to determine its characteristics over the range of cycle rates for future application possibilities.

The third and final performance test was done to determine the effect the end of discharge voltage had on the performance of the test battery as a capacitive element. Cimino and Gearing previously proposed that the average value of the voltage at the end of discharge in each cycle

effected the average capacitance, efficiency and voltage regulation (5:36). Test batteries were cycled at 5 and 10 cps at various current levels with the end of discharge voltage adjusted up and down by controlling supply current. Battery performance data were computed and analyzed to determine the effects if any of the end of discharge voltage on capacitance and efficiency.

During all of the performance testing, a test circuit was used to control the load current demanded from the charging source and the battery. A 50% duty cycle load (load on half the time and off half the time) ensured that the batteries were alternately charged and discharged as desired. Raw data recorded from the testing were the battery voltage waveform and the source, battery, and load currents. The measured capacity of the test batteries was also checked periodically to determine how battery performance degraded with use.

Endurance. The two purposes of the endurance tests were to gather data on the cycle life of the test batteries and to study the effects of the rapid cycle application on the cadmium electrode. One test battery was run in a computer controlled test circuit with the goal of one billion charge and discharge cycles. Its capacity was periodically measured in addition to its average capacitance and efficiency in order to gather data on the cycle life performance of the battery. The computer control test circuit continuously monitored the end of discharge voltage and automatically

adjusted the supply current to maintain this voltage relatively constant.

A test battery specially designed with a removeable cadmium electrode was cycled using the endurance test circuit to study the effects on the cadmium structure within the electrode. After a number of cycles, samples of the removeable cadmium electrode were photographed by a scanning electron microscope. This pictorial history of the cadmium structure after the electrode's use in this high cycle rate application was studied to better understand Ni-Cd battery failure mechanisms associated with the cadmium electrode. The test circuit required for this test was almost identical to the other endurance test circuit.

With the preceding theory as a basis, the study of a bipolar Ni-Cd battery as a pulsed power filter was begun by designing, manufacturing, and testing batteries. Chapter 3 explains the test battery design and manufacture in an attempt to optimize the battery's performance for pulsed power applications.

III. EXPERIMENTAL BATTERY

Background

The bipolar cell design was selected due to its low internal resistance, its capacity for higher and evenly distributed current loads, and its potential for lighter total weight. An Australian, commercial, quasi-bipolar automotive battery boasts of an almost 30% reduction in size and weight over a standard automotive battery (6:iii).

A recommendation arising from previous efforts in evaluating the capacitive filter ability of Ni-Cd batteries was to use the bipolar battery design (4,5). In addition, the sponsor of this study was interested in the bipolar design for the capacitive filter application.

Design

The design of the test bipolar battery used in this study resembles a design used by Seiger (et al) at Gulton Industries in connection with pyrotechnic work (8). While the designs are similar in size and shape, the use of the battery and its construction procedures are quite different. The earlier work does serve as a useful comparison to the batteries built for this study.

Figure C-4 presents an expanded view of a regular bipolar test battery. The test batteries were designed to facilitate simple construction and testing, in addition to the development of an effective electrolyte seal. The lack

of a good electrolyte seal is a recognized pitfall in the bipolar design. Size and weight considerations were sacrificed in an attempt to effect the seal.

The circular design was chosen in an attempt to evenly distribute the current through the battery and to minimize the ratio of seal area to active electrode area as compared to that of a rectangular design. The larger the diameter of the electrode, the less significant is the wasted area used for seals and the lighter the battery becomes as compared to its electrode weight.

The design of the removeable electrode battery involved a minor alteration in the regular test battery design. The fourth nickel electrode in the normal stack of five electrodes was enlarged and designed to allow the end electrode (cadmium) to be removed for examination while maintaining the integrity of cells 1 through 3. Figure C-5 is an expanded view of the removeable electrode test battery. These battery designs allowed the test batteries to be easily assembled, repaired, or examined throughout the study effort. Battery component failures could be more easily isolated and repaired as needed, using spare components.

Fabrication

Metal Work. The battery superstructure (or cell walls) and the end plates were made of 200 grade nickel. Nickel was chosen because of its high electric conductivity, resistance to reaction with KOH, and its availability. These

nickel plates or slugs were machined according to detailed drawings made during the design phase of this effort. The removeable electrode battery contained an oversized nickel slug used to maintain the seals on three of the four cells of the battery. The machining of the active electrode area was identical to that of the regular test battery slugs with the exception of the drilled and tapped holes used in establishing the intermediate seal. The end slugs, with only a single machined surface, had nickel tabs welded to them which served as battery terminals. Appendix C contains detailed battery component drawings.

Electrodes. The following paragraphs describe the steps used to fabricate and impregnate the electrodes used in the battery.

Sinter. The first step in making an electrode was to sinter (heat without melting) nickel powder in a Linberg tube furnace until it became an 80-90 percent porous sponge-like structure attached to the nickel slug. This porous structure, referred to as plaque, is where active electrode materials are later impregnated. Early attempts at keeping the sintered nickel plaque attached to the slug failed when no special preparations of the nickel slug surface were made and the standard patented procedures were followed (24). After a month of experimentation, a combination of spiral grooving (10 mils deep) and acid etching of the surface resulted in securely attaching the plaque to the nickel slug.

A special procedure was required to sinter both sides of a nickel slug without losing the powder from the inverted side of the slug as it lay in the furnace. The method used was a "soft" sinter of the first side for 8 minutes at 980° Celsius and then a full sinter of the other side for 10 minutes. The side sintered twice was then used as the cadmium side since that electrode was mechanically stressed the least in the impregnation process. A detailed sintering checklist is provided in Appendix D.

The special removeable cadmium electrodes were made with a commercial plaque material to facilitate the removal of small pieces to study with a scanning electron microscope. The commercially manufactured nickel sintered plaque was spot welded onto the slug. This reduced the current path area through this last battery cell but it allowed the removal of electrode pieces without destroying the entire electrode.

Impregnation. The electrochemical impregnation of cadmium and nickel hydroxide into the nickel powder plaques was achieved by a minor variation of patented procedures (25,26). The positive nickel hydroxide electrode was impregnated by immersing a prepared sintered slug into 1.8-molar (molecular weight in grams per liter) nickel nitrate and 0.2-molar cobalt nitrate solution. A direct current of 0.175 amperes per square inch of electrode surface or 0.875 amperes was passed through a nickel plate, the solution and the electrode slug for four hours. The negative cadmium

electrode was impregnated by immersing a sintered slug into a 2-molar cadmium nitrate solution. A current of 0.1 ampere per square inch of electrode surface or 0.5 amperes was run through the slug, solution, and a cadmium metal plate. The current was run from the cadmium plate to the slug 50 seconds and then reversed through the circuit for 10 seconds for a total of four hours to impregnate cadmium crystals into the nickel plaque. Both impregnation baths were kept at a pH of 3.5 by a nitric acid drip and maintained at 80° Celsius (C). Figure E-1 shows the impregnation apparatus. Figure E-2 is a drawing of the special mount used to impregnate only one side of the bipolar electrodes at a time.

After the electrochemical impregnation, the cadmium electrode was placed in a distilled water rinsing bath to remove any solution left in the sintered plaque. The nickel electrode was removed from the impregnation bath and quickly placed in a KOH formation bath. Here, a 0.5 ampere current was passed through the slug, the KOH electrolyte, and a nickel plate in one direction for 20 minutes and then reversed for 20 minutes for a few cycles. This formation process was done to convert the nickel hydroxide to a more electrochemically active form and improve the coulombic or charge transferring efficiency of the electrode (8:975). Upon completion of the formation cycle, the nickel hydroxide electrode was rinsed in a distilled water bath and then dried in a vacuum oven to remove moisture from the electrode for accurate weighing. A detailed impregnation checklist is

provided in Appendix E.

Seals. A major design consideration was an attempt to make a temporary compression seal on the test batteries that would eliminate leakage of the KOH electrolyte, but allow periodic assembly and disassembly of the test batteries. Historically, sealing problems have been one of the major limitations of bipolar batteries. Therefore, battery design and weight concessions were made in an attempt to effectively solve the leakage problem and prevent the failure of the test batteries due to a loss of electrolyte or exterior short circuit from the leaked conductive fluid. The material used between the nickel slugs or cell walls had to be an electrical insulator, relatively impervious to the corrosive effects of KOH, and compressible. Teflon was selected as the seal material. Thin (.035 inch or 35 mil) washers of this insulating and sealing material were compressed between the nickel slugs by sixteen stainless steel bolts and nuts around the outer diameter of the battery slugs. They were each tightened to at least 60 inch-pounds of torque. Since the Teflon was somewhat compressible, the test batteries were assembled a few hours prior to their use to insure a good seal and minimize any "cold flow" or delayed compression of the insulator.

To take advantage of this "cold flow" property of the Teflon, the outer edges of the battery slugs were lightly grooved one mil deep and then had two 10 mil circular grooves cut into them. These grooves were attempts at

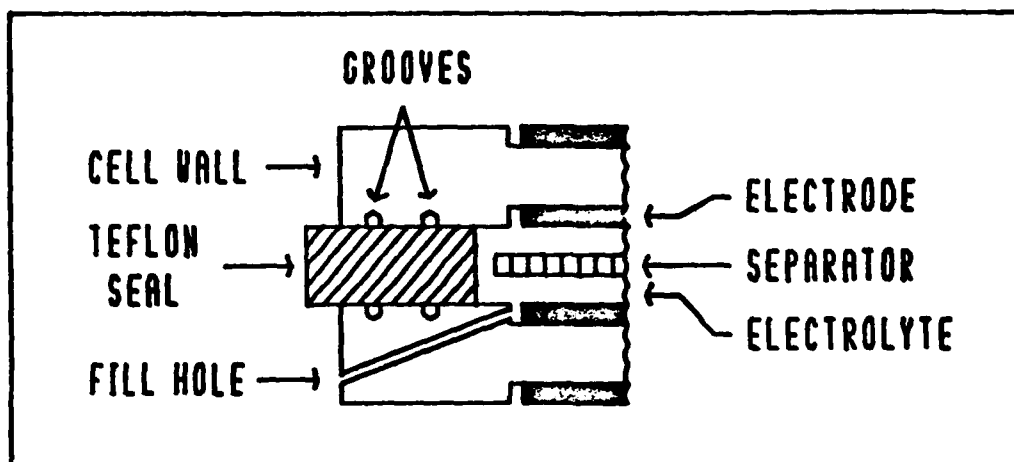


Figure 3-1. Battery Inter-cell Seal

providing tighter barriers to prevent the ubiquitous KOH from leaking out when the cells were under pressure. Figure 3-1 shows a sideview of the seal utilized in this study.

Assembly

Once the electrodes were prepared and the seals, cell separators, and various other battery parts were gathered, a test battery was easily assembled in a matter of minutes. As shown in Figure C-4, each cell had a Pellon 2506, unwoven, fibrous nylon separator in it to prevent the cell electrodes from shorting out by forming a crystalline bridge or dendrite between the two electrodes. The separator also serves to keep a uniform amount of KOH electrolyte dispersed throughout the cell. The battery compression was achieved using two stainless steel end plates torqued down with sixteen bolts and nuts. Electrical conductivity checks

insured that no mechanical short was caused during construction.

After torquing the compression bolts down to insure an effective electrolyte seal, the battery was placed with its fill holes immersed in KOH and then vacuum filled using a bell jar leak detector. This vacuum filling was done several times to insure that the cells were filled as fully as possible with KOH. A hypodermic needle was used to top off each cell with KOH and then the exterior of the battery was cleaned and dried to eliminate any residual KOH that might short the cells.

Specifications

Theoretical Capacity. The theoretical ampere-hour capacity of a test battery was based on the weight of the active materials impregnated into the porous plaque of the electrodes. By multiplying the weight (to the nearest milli-gram) of the cadmium and nickel metal impregnated by the factors of 0.366 a-h per gram of cadmium and 0.289 a-h per gram of nickel, respectively, the ampere-hour capacity of the electrode was found (16). Each test battery electrode was carefully weighed with a Gram-attic balance before and after impregnation and its theoretical ampere-hour capacity computed. A particular battery's capacity was then based on the lowest capacity electrode. This theoretical capacity value was used to determine battery charging and

discharging currents utilized in measuring actual ampere-hour capacity and in conditioning the test batteries.

Battery Equivalent Weight. The weight of the battery is a primary consideration for computing the energy density of the battery. Since the batteries for this study were not optimized for weight or for a commercial application, an equivalent weight was used to compare the energy density of the bipolar batteries with previously tested batteries. The actual weight of the plaque and active material, plus an allowance for cell walls based on Seiger's work (8:975), was used to compute the electrode weight for the battery. This actual electrode weight was considered to be 57.9% of the total battery weight; based on a study of standard Ni-Cd aircraft batteries (4). This allowed a direct comparison of this study's results to those of Cimino and Gearing (5). Appendix F shows the actual calculations and equivalent weights of the test batteries.

The design and manufacture of the test bipolar batteries was only the first segment of this study. A test network for evaluating the capacity, performance, and endurance of these batteries was required. The next chapter describes the test networks assembled and utilized in the testing of the bipolar batteries.

IV. Test Network

Background

Evaluation of the operational characteristics of the bipolar battery used for this study was divided into three types of testing: capacity, performance, and endurance. Capacity testing was performed using a timed, semi-automated network. Performance testing was performed using manually adjusted test equipment because the individual tests required frequent and non-periodic adjustments of the test equipment. Endurance testing was accomplished using a computer controlled test network which automatically adjusted the test equipment to obtain the desired operating parameters.

Test Equipment

The equipment used for the various types of testing is listed in Appendix G. It is grouped by type of test. A test log of calibration data and test apparatus photographs are also given in Appendix G.

Test Circuit Designs

Two basic test circuit designs were used in performing the required tests. The first test circuit design was used for capacity testing and charging the batteries to the desired state of charge. The second test circuit design was used for performance testing and with the addition of the computer control elements, was also used for endurance

testing.

Test Circuit Operation

Conditioning Test Circuit. A schematic of the circuit used for conditioning the batteries is shown in Figure 4-1. During a charge cycle, the dc power supply provided a voltage limited, constant current to the battery. Charging time was controlled by a countdown timer/relay device. When the countdown timer reached zero, a relay switched the charging power supply out of the circuit and connected the discharge power supply and the discharge load of 30 ohms across the battery to force the battery to discharge.

During a discharge cycle, the discharge power supply was in series with the battery and the load resistor. The power supply adjusted its voltage such that the battery provided the desired current load. When the discharge timer reached zero or the battery voltage dropped below a preselected cutoff voltage, the discharge power supply and load were disconnected by relays. This charge/discharge cycle was repeated until two consecutive discharge cycles resulted in similar measured battery capacities.

During both charge and discharge cycles, the corresponding battery voltage and current were recorded using a two-channel chart recorder. This recorded data was used to determine the battery's ampere-hour capacity as well as provide useful information to analyze any malfunctions during the conditioning process.

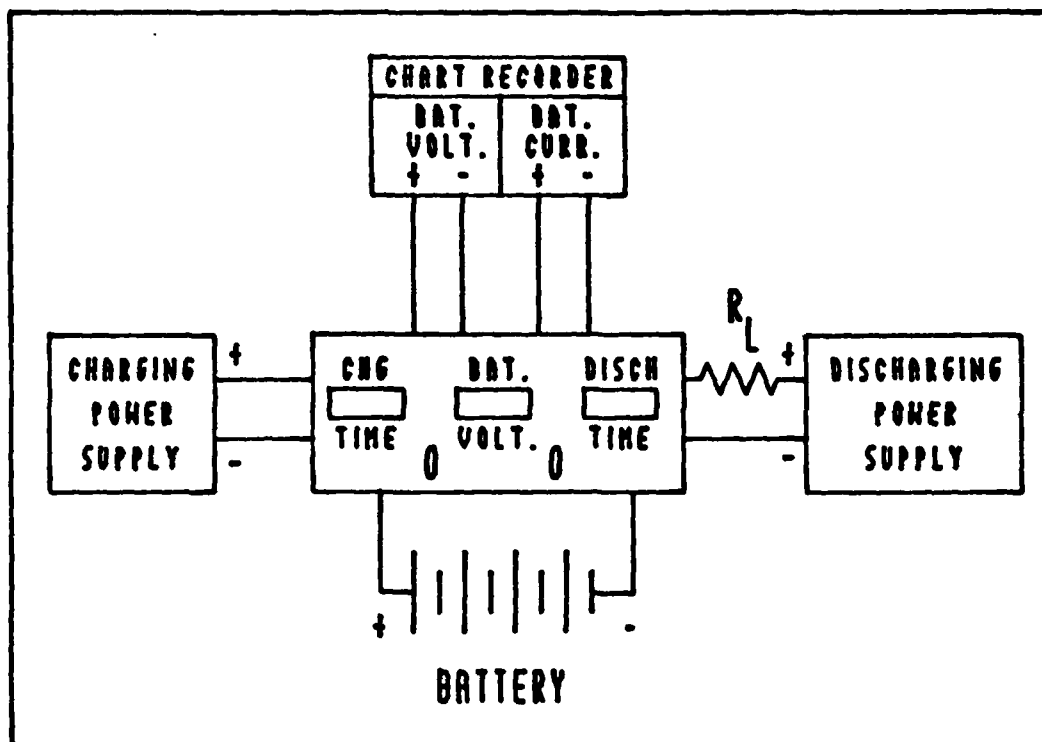


Figure 4-1. Conditioning and Charging Circuit

Charging Circuit. The same circuit used in conditioning the battery was also used to charge the battery to the desired operating state of charge. The theory of operation is the same as that described in the previous section. The difference between charging and conditioning is the number of charge and discharge cycles applied to the battery. When charging, the battery is initially charged and discharged once and then recharged to 75% of the battery's measured ampere-hour capacity.

Performance Test Circuit. A schematic of the circuit used during performance testing is shown in Figure 4-2.

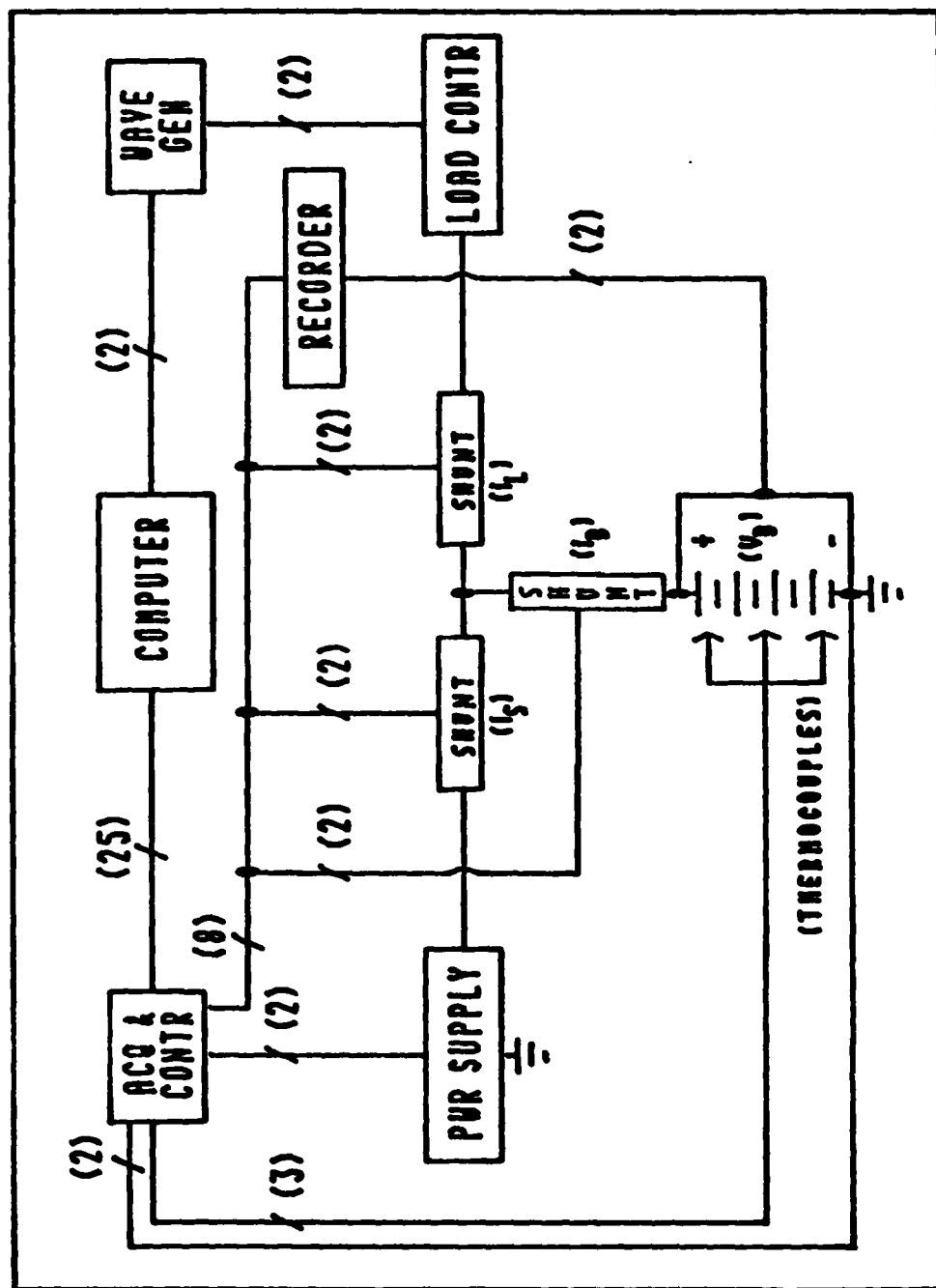


Figure 4-2. Performance and Endurance Test Network

This circuit provided a means of controlling the current demanded from the battery by adjusting the charging supply current. All circuit control adjustments were made manually during this test.

A solid state load controller, modulated by an external wave generator, alternately connected and disconnected its internal load to the test circuit. The wave generator supplied a 50% duty cycle square wave at various frequencies used during testing. The load controller was controlled by an input voltage of 0-6 volts which corresponded to 0-60 amperes of load current from the battery. The load current was initially adjusted to twice the charging supply current. This forced the battery to provide a current equal to the supply current. The charging supply current was applied to the battery when the load was off and applied to the load and the battery when the load was on. Adjustments to the charging supply current were made manually at the power supply. As an example, when the load was on and it demanded 6 amperes of current, the charging power supply provided 3.1 amperes and the battery would provide 2.9 amperes. When the load was off, the charging power supply just charged the battery with 3.1 amperes of current.

The current shunts provided chart recorder inputs for recording supply current (I_s), battery current (I_b), and load current (I_l) during testing. Battery voltage (V_b) was also monitored using the chart recorder.

Since the individual tests within performance testing required high currents (compared to the battery's ampere-hour capacity), the temperature of the battery at each end cell and at a center cell was monitored using an HP-85A computer and iron/constantan thermocouples. This temperature was used to determine the maximum current the battery could withstand and not exceed 80° Celsius. This value permitted a high operating temperature without exceeding the boiling temperature of the KOH electrolyte; about 100° Celsius. Elevated temperatures also produce other undesirable effects on Ni-Cd batteries such as reduced efficiency and shorter cycle life (20:68).

Endurance Test Circuit. The circuit used for endurance testing is shown in Figure 4-2. The basic circuit is the same as the circuit used in performance testing, but a computer and computer controlled test equipment were added to monitor and control various circuit parameters. The computer and computer controlled equipment utilized the HP-IB interface bus. Use of this interface greatly simplified circuit control and data acquisition.

A primary concern was maintaining the battery's end of discharge voltage at a particular value without exceeding a maximum end of charge voltage limit. Using an HP-85A computer and an HP-3497A data acquisition and control unit, software was developed which allowed the user to select a desired battery current, maximum charge voltage, minimum

discharge voltage, operating discharge voltage, and to monitor battery temperature. The program first initialized the wave generator to modulate the load controller, and then turned on the charging and discharging power supplies, and the data acquisition/control unit to their power-on condition (no input or output). Next, load and supply currents were applied at the operating frequency and the battery voltage was monitored for three minutes to allow battery operation to stabilize. Once the three minute warmup was complete, the computer reported the maximum end of charge and minimum end of discharge voltages. The computer would then request desired limiting charge and discharge voltages and an operating discharge voltage.

With warmup and initialization complete, the battery was then alternately charged and discharged at the desired frequency. The battery voltage was monitored and sampled using the HP-3497A to determine an average end of discharge voltage. The decision logic used to control the test battery is outlined in Figure H-1. Charging current was controlled to maintain the battery voltage between desired limits and avoid overcharging as illustrated in Figure H-2. Automatic test termination was commanded whenever established operating or safety limits were exceeded.

For temperature monitoring, the computer measured the thermocouple voltages and using a software compensation utility program supplied with the HP-3497A, the battery

temperature was computed and compared to the maximum allowable value. If the measured temperature exceeded this value the test was terminated and the operator was alerted of the over temperature condition by a printed message containing the date and time of day the test was terminated. If the measured temperature was less than the maximum value, the computer repeated the voltage sampling, charge current adjustment (if necessary) and temperature measurement process until the desired number of cycles had been completed.

Program information is given in Appendix H. The program made use of several utility routines supplied with the HP-3497A data acquisition/control unit. The program was designed to be user friendly and once initiated required no operator intervention except to terminate a test when desired

This chapter presented a descriptive explanation of the equipment and test circuits used and their operation in the three major testing areas of this study -- conditioning and charging, performance, and endurance. Each of these categories consisted of several specific tests. A more detailed explanation of these specific tests and the procedures used in their performance is given in the next chapter.

V. Experimental Test Procedures

Background

After the bipolar batteries and a test network were constructed, it was necessary to evaluate the batteries for their suitability as pulsed load filters. Battery testing was divided into acceptance, performance, and endurance test phases. Acceptance testing covers the procedures used to charge and condition the test batteries. Performance testing determined the efficiency, energy density, and average capacitance of the batteries. Finally, the endurance testing was done to determine the overall capacity of the battery as a function of cycle life and to investigate battery failure mechanisms associated with the deterioration of the cadmium electrode.

Acceptance Testing

Charging. After a battery was assembled and filled with electrolyte, it was fully discharged across a resistive load to bring each individual cell down to an approximately equivalent state of discharge. A dc ohmmeter was used to insure the assembled battery had no internal mechanical short circuits. An ac ohmmeter was used to measure the resistance of the battery as a function of the battery's state of charge.

A modified constant potential charging method was used to charge the test batteries. This method was a compromise

between a slow or fast charge time to facilitate testing procedures and standardize the charging process. The circuit described in Chapter 4 and shown in Figure 4-1 was used. Charging was done at the 0.6 C-rate of the battery or electrode. For example, a battery with a 0.5 ampere-hour theoretical capacity, based on the active material in the weakest electrode, was charged at 0.3 amperes of current. This constant current was held until a battery or cell voltage of 1.55 volts per cell was reached (i.e. 6.2 volts for a four cell battery). The charging current was then reduced to maintain this battery voltage and to avoid overcharging and gassing of the battery or cell. Charge time to full capacity normally averaged 1 hour and 45 minutes. Full capacity was based on the leveling of the battery voltage and charging current as shown in Figure 5-1.

The charging circuit was also used to discharge the test batteries or individual cells. Discharge current was always the C-rate of the battery or cell. For example, a 0.5 ampere-hour capacity battery was discharged at 0.5 ampere. The test batteries were normally discharged down to 1 volt per cell, or in the case of the removeable cadmium electrode, down to 0.3 volt for the single cell.

Conditioning. As previously mentioned, Ni-Cd batteries initially improve with use because of the increase in the nickel electrode's capacity. The test batteries in this study were conditioned by charging and discharging them several times. This was done until the discharge time for

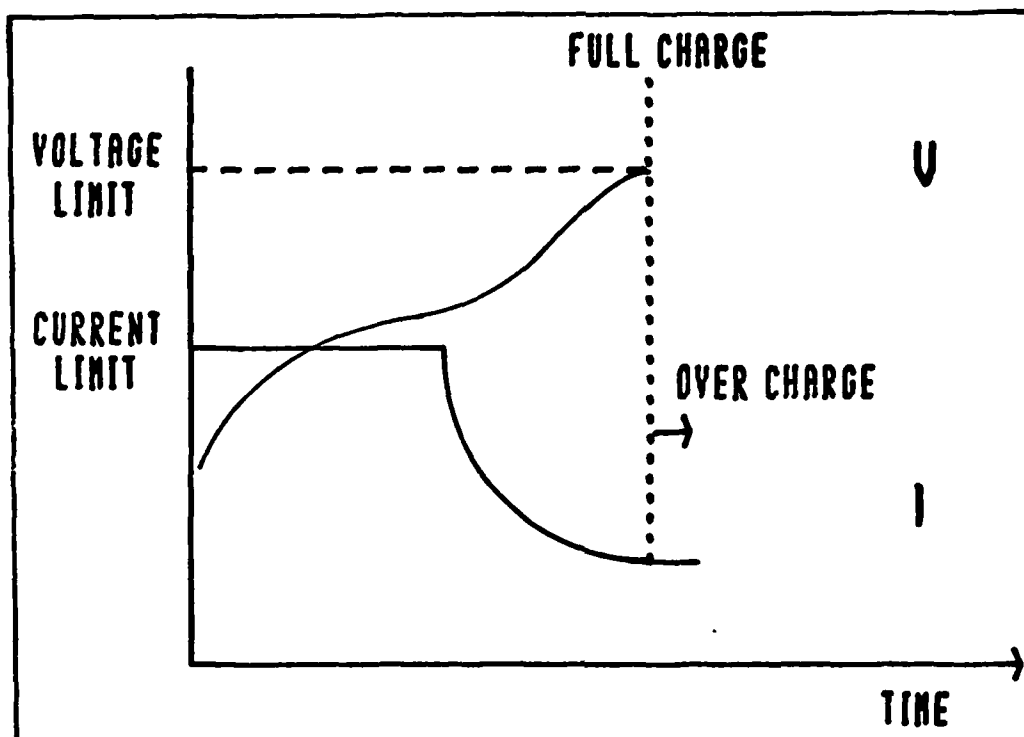


Figure 5-1. Battery Voltage and Charging Current

each cycle stabilized and any leakage or assembly problems were resolved.

Capacity Checking. The measured capacity of the test batteries or electrodes was obtained from the conditioning process. The theoretical capacity of a Ni-Cd battery is seldom actually obtained for a number of reasons, including imperfect electrodes, assembly flaws, electrolyte problems, and internal losses. The measured capacity of the test battery was based on the discharge time and current to a battery voltage of 4 volts. Since a constant current discharge was used, the measured capacity of the battery was determined by multiplying the discharge current by the discharge time in hours. For example, a battery discharged at

0.5 amperes for 30 minutes had an actual capacity of 0.25 ampere-hours. Once a battery's initial measured capacity was determined, it could be charged to a specific state of charge. All batteries were tested using a 75% state of charge based on measured capacity. For example, a battery with a 0.25 ampere-hour measured capacity would be charged for 45 minutes at 0.25 amperes to obtain a 75% state of charge.

The capacity measurements of the removeable electrode were done differently. The removeable cadmium electrode was removed from a fully discharged battery and a sample of the electrode was taken for scanning electron microscope study. The cadmium electrode was then placed in a beaker of KOH electrolyte with a commercial nickel plate of greater capacity. This open Ni-Cd cell was charged at a 0.6 C-rate for two hours to thoroughly overcharge the cell. The cell was then discharged at the theoretical capacity 1 C-rate, or at a current of 0.974 amperes, down to 0.3 volts. The current times the discharge time yielded an electrode capacity. This electrode capacity was tracked as a function of the number of times the battery was charged and discharged. The capacity of the cadmium electrode was physically reduced each time a portion of the electrode was removed for study. The degradation in capacity was considered and accounted for geometrically in the presented data by reducing the capacity directly proportional to the reduction of electrode surface.

Performance Testing

Two of the test bipolar batteries were used during this phase of the study to determine how well a bipolar Ni-Cd battery could function as a capacitive element under a pulsed load. Performance testing involved determining how much current the battery could handle without overheating, how the capacitive nature of the battery changed as the cycle rate changed, and how the battery efficiency and average capacitance changed as the end of discharge voltage was varied.

Current Load. The test network shown in Figure 4-2 was used to test battery #1 for maximum current capacity. The battery current demanded by the load was systematically increased from 3 to 28.5 amperes. All current adjustments were made manually while the HP-85A computer was used to monitor the temperature of the battery. Battery voltage, load current, source current, and battery current were recorded along with the measured temperatures and run times at each different current load. A cycle rate of 5 cycles per second was maintained and a total of 60,000 charge/discharge cycles were made on battery #1 during this phase of testing. Each different current rate was maintained for over 20 minutes and until the operating temperature stabilized.

Cycle Rate. Bipolar battery #1 was cycled at rates of 1, 5, 10, 25, and 50 Hertz and current loads of 5 and 10 amperes. The cycle rate or charge and discharge frequency was controlled by a wave generator cycling the load on and off.

The battery's state of charge at the start of cycle testing was 75% of the total measured capacity. Battery voltage, load current, source current, and battery current were recorded during the approximately 20 minute periods of each combination cycle rate and current load. A total of about 232,000 cycles were accomplished on battery #1 during this phase of testing. Temperature was monitored as before by the HP-85A computer while all other test circuit control functions and adjustments were done manually. The test circuit shown in Figure 4-2 was again used for this performance test.

End of Discharge Voltage. Bipolar test battery #2 was used for the end of discharge voltage performance testing. The charging or supply current was varied along with the demanded load current to change the current supplied to or by the test battery. The difference between the current going into the battery when the load was off and the current coming out of the battery when the load was on, determined whether the battery was being charged or discharged. Over time, this charge or discharge status would raise or lower the end of discharge battery voltage. Therefore, the end of discharge voltage could be controlled simply by changing the supply current for a set load current. Cycle rates of 1, 5, and 10 hertz (cycle per second) and load currents from 4 to 10 amperes were examined. Supply current was manually varied to investigate battery performance at end of discharge voltages of 3.6 to 5.2 volts. Battery voltage

along with load, supply, and battery currents were recorded to enable comparison computations of battery efficiency and average capacitance at various end of discharge voltages.

The capacities of batteries #1 and #2 were periodically checked during testing to gather capacity versus cycle life data. The internal resistance of battery #1 was measured using an ac ohmmeter and plotted as a function of its state of charge. Performance test results presented in the next chapter were used to determine a battery current, cycle rate, and end of discharge voltage to operate the test bipolar batteries during the endurance phase of testing.

Endurance Testing

Cycle Life Capacity. Test battery #3 was tested at a battery current of 3 amperes , a cycle rate of 10 cycles per second and an end of discharge voltage held around 5 volts. The battery was tested using the computer controlled test circuit shown in Figure 4-2. Periodically, the battery was removed from the test circuit and its capacity checked as described earlier. Battery voltage and load, supply, and battery currents were recorded. The battery was left running in an attempt to reach at least 10 billion charge/discharge cycles or until total failure of the battery occurred.

Cadmium Electrode Study. Test battery #2, with the removeable cadmium electrode, was cycled at 5 hertz, a battery current of 3 amperes, and an end of discharge voltage

around 5.15 volts using the test circuit shown in Figure 4-2. The capacity of the uncycled, removeable cadmium electrode was initially measured and its crystalline structure photographed. At various cycle points, the removeable cell's capacity and its cadmium crystalline structure were again photographed and examined. Battery voltage and load, supply and battery currents were recorded periodically to compute and track battery performance parameters. The capacity of the cadmium electrode versus cycle life was also tracked. Scanning electron microscope pictures showing the changes in the cadmium crystalline structure were correlated with the capacity checks and cycle life history.

The next chapter presents a discussion of the results of the acceptance, performance, and endurance testing. A prelude to these results is a discussion of the bipolar battery construction accomplished during this study and an assessment of the overall effectiveness of the test networks.

VI. RESULTS AND DISCUSSION

General

The results of this study are presented in a chronological sequence that begins with the design of the test batteries and ends with endurance testing. Data from previously explained procedures and methods is presented with little discussion. Other data is discussed in detail, as needed, to clarify an idea. Tabulated, graphical and pictorial data is presented in the appendices.

Battery Mechanics

Design. The basic design of the bipolar test batteries was successful in that the batteries were functional and they were easily assembled and repaired. The modification for the removeable electrode worked very well and made that area of testing go smoothly.

Based on the experience gained from this study and some exploration with other manufacturing techniques, the nickel substrates used for the electrodes could have been much thinner and lighter without sacrificing any performance (27). Even though the heavier design added to the weight and internal resistance of the batteries, it helped to dissipate heat and resist internal pressure distortions of the substrates. It was also considerably easier to manufacture the heavier nickel plates using conventional milling techniques.

Stainless steel compression end plates, nuts and bolts, and impregnation mounting plates were used to resist the caustic effects of the KOH electrolyte. In a few cases the KOH broke through the passivation or protective layer of the stainless steel and caused iron contamination of impregnation baths or electrolyte. To prevent this contamination, the stainless steel parts were replaced frequently and watched carefully during their use.

The cell design required that the electrolyte be introduced into the battery cells through 0.025 inch diameter holes drilled through the cell walls. Electrolyte was introduced by vacuum filling and with hypodermic needles. While this method was functionally acceptable, the holes should have been a little larger to facilitate filling. Considerable difficulties with the cell seals required more use of the fill holes than originally expected and larger holes (0.03-0.04 inch) would have been better.

The actual weight of the test batteries was between three and four pounds. Equivalent weights of under a third of a pound were used based on previous study efforts explained in Chapter 3 and shown in Appendix F.

Electrodes. The electrodes for this study were made by using patented and established procedures (25,26,27). However, due to the requirement for bipolar electrodes, some of the procedures had to be modified. As explained earlier in Chapter 3, the sintering process used for this study worked well. Initially, nickel electrodes were failing during

impregnation because the sinter was separating from the nickel substrate (28). It was discovered that the impregnation of nickel into the sinter caused the plaque to expand against the nickel substrate walls. This mechanical stress was alleviated by cutting a growth ring around the outside diameter of the sinter.

The major problem in the manufacturing of the electrodes was the inconsistent impregnation process. Approximately half of the impregnation attempts ended in too little or too much active material in the electrode plaque. The patented impregnation processes were optimized for two-sided electrode impregnations without the extraneous surfaces in the bath like the special mounts used in this study. The current levels, bath temperature, pH, and time intervals required for correct impregnations were therefore not optimized for this study. Most of the successful electrodes were those that were continuously monitored during impregnation. The process was so inconsistent that repeating a successful impregnation technique did not insure success the next time. Other problems, such as contaminated baths caused by eroded acid pumps or iron from stainless steel corrosion, were encountered throughout the study effort.

Appendix I lists the individual battery electrodes with their ampere-hour capacities. Most of the electrodes had a considerably lower a-h capacity than what is normally expected from the patented processes used for electrode manufacture. This was primarily attributed to the one-sided

instead of two-sided impregnation procedure. The nickel hydroxide electrodes were impregnated with about 1 gram of active material per cubic centimeter (cc) of void volume instead of the expected 1.6 grams per cc. These low a-h capacities limited battery performance, but were not detrimental to the evaluation of the batteries for this study.

The formation process used on the nickel electrodes after impregnation was the cause of one test battery failure. During the study effort, the charge and discharge labels were inadvertently switched on the formation apparatus. As a consequence, fully charged nickel electrodes were assembled into battery #0 instead of fully discharged electrodes. This error led to a severe overcharge of the nickel electrodes in the battery which caused them to shed active material from the electrode surface and short the battery. To minimize nickel electrode overcharging and shedding in the other batteries, the individual cell voltages were checked more often and balanced by discharging when required. All other nickel electrodes were also resubjected to the formation process a second time to insure they were fully discharged before being assembled into a test battery.

Seal. An effective seal was made which minimized leakage, however the classical bipolar battery seal problem needs further work. Originally, the test bipolar batteries were designed to be sealed cell batteries. Preliminary testing with a two cell battery was promising. The battery was filled and the fill holes plugged with Silastic brand

RTV, a rubber cement-like substance. The battery sat uncharged for two weeks without leaking. The battery was then slowly charged and discharged for almost a month with only minor leakage. This initial optimism was soon dashed when the first four cell test battery was tested and began to leak when charged and discharged. The cause of the leakage was identified to be internal pressure build-up resulting from gasses generated during overcharging. To relieve the pressure, in lieu of using pressure valves, the fill holes were left unplugged to vent the gasses. The remaining bipolar test batteries were left unsealed and the leakage was minimized.

The compression plates were held together with 16 nuts and bolts tightened to 60 inch-pounds (in-lbs) of torque. Initially, the compression on the batteries was checked every day and torqued as required to maintain the 60 in-lbs. After the first battery was taken apart, it was discovered that the repeated torquing was causing the electrodes' edges to eventually cut through the Teflon insulators/seals. While the "cold flow" property of the Teflon reduced with subsequent compressions, it was still continuous. It was decided that the repeated torquing of the batteries was not preventing leakage and could cause short circuits. Therefore, the batteries were only torqued tightly during initial assembly.

Numerous ideas to improve the electrolyte seal were tried over the course of three months. One idea implemented

was the grooving of the outside diameter of the nickel slugs. This seemed to reduce leakage but could not fully stop the ubiquitous KOH solution. Polyurethane, instead of Teflon, was tried for the seal material. Initial tests were successful but the electrolyte eventually corroded the polyurethane seals.

The batteries were designed to be assembled dry and then filled with electrolyte. When initial test batteries were disassembled it was discovered that some cells were electrolyte starved or nearly dry. Assembly with the electrodes and separators soaked with electrolyte was then tried, but the seals would not hold as well because the electrolyte had established a path past the seal prior to compression. A battery electrolyte capacity check was performed and it was discovered that the electrolyte volume did not increase using wet assembly over dry assembly. Therefore, dry assembly was used thereafter. In retrospect, more open volume should have been left between the cells for electrolyte. This might have improved battery performance, but probably would have aggravated the leakage problem.

In summary, effective seals were accomplished using Teflon as long as the fill holes were unplugged to vent internal cell gasses. Periodic refills were required to keep the battery cells full of electrolyte and to compensate for the minor leakage and overflow from the fill holes.

Test Network

Automation of the circuit used for endurance testing was accomplished to minimize operator interface and to maintain critical battery parameters near predetermined test values. Both positive and negative attributes of this process are discussed in the next few paragraphs.

Operator Interface. Since portions of endurance testing spanned several days, automation of the test circuit was required to verify that operating parameters were maintained and to eliminate the need for a manned test station. Once the computer program was initialized, no operator intervention was required, except to terminate the test as desired. Another aspect of minimal operator interface was the reduction in error due to the operator's adjustment of test equipment both prior to and during testing. By using the automated network, the computer adjusted all the equipment identically between test segments.

Data Collection. Through the use of the automated network, data collection was performed at predetermined time intervals as needed and stored on tape for later use.

Circuit Control. The computer was able to measure, store, and analyze data in seconds. This capability enabled it to make required test equipment adjustments more quickly than a human operator could. The use of the automated network in controlling the test equipment also minimized error due to incorrect calibration by using iterative sampling and adjusting of test equipment to obtain desired

operating values. This automatic adjustment reduced the required number of highly calibrated devices.

Program Structure. The program was written to be user friendly. The operator was prompted to enter required data, eliminating the need for the operator to know how the program ran in order to use it. The program was written using subroutines (smaller, relocatable programs) which allowed the user to customize it by adding and/or eliminating segments as needed. Utility subroutines provided with the HP-3497A Data Acquisition Unit were also used to perform repetitive, numerically intensive tasks, such as temperature measurement and conversion. Use of these utility programs reduced programming time and increased program efficiency.

Measurement Inaccuracy. Due to the slow sampling time of the HP-3497A's internal voltmeter and the cyclic nature of the signal under measurement, an averaging method was used in determining the peak charge and discharge voltages used as circuit controlling parameters. The inaccuracy introduced was only a few tenths of a volt and was not critical in this particular application.

Battery Response. The response time of the battery to changes in its charging or discharging current was not taken into account in determining the frequency or the size of adjustment. In effect, the battery was forced to stay within the desired voltage limits. By not allowing the battery to respond, the adjustments were more frequent and at times too large. One possible cure to this problem is to

incorporate a time delay between adjustments. Another solution would be to base the adjustment on the magnitude of the change between the current and preceeding battery voltage measurements.

Acceptance Testing

Charging. All battery testing was done with the battery at a 75% state of charge. Due to the rapid cycling of the test batteries, individual cell voltages within a battery would vary after a short time under test. Usually, one cell would become overcharged and begin to gas and adversely effect its nickel electrode. To prevent cell failure, prolong battery life, and maintain the battery state of charge, the test batteries were periodically fully discharged and recharged. This process complicated battery testing, but was a necessary procedure.

Capacity. The way a nickel-cadmium battery is charged and discharged plays a major role in its capacity and performance. Variations in charging would have introduced another variable into the evaluation of the batteries which could have masked changes in capacity or other critical battery parameters. Therefore, as mentioned in Chapter 5, all charging was accomplished using the same procedure. Table I shows the test battery's theoretical capacities, determined by the impregnation of electrodes, and their measured capacities, determined by charging. The measured capacities were disappointingly low. It is not unusual to

Table I
Bipolar Battery Capacities

Battery Number	Theoretical Capacity Ampere-Hours	Measured Capacity Ampere-Hours
0	0.56	0.27
1	0.53	0.34
2	0.49	0.24
3	0.53	0.21

get better than theoretical capacity out of Ni-Cd batteries because of the theoretical model used to determine capacity. The low capacities can be attributed to a summary of such factors as lack of electrolyte, less than optimum impregnation, cell voltage imbalances, and soft or high resistance short circuits due to leaks or mechanical imperfections. Another major factor that caused the low measured capacities was the relatively quick charge and discharge rates utilized in this study for battery charging. This method was selected to accelerate the testing so that it could be completed as planned. The lower capacities only affected the energy density performance testing and probably expedited battery failures during high current testing due to the high C-rate operations. Other aspects of the testing were done at a low current rate to compensate for the low capacities.

Internal Resistance. One of the primary purposes for the bipolar design was to reduce the internal resistance of

the battery. There were no elaborate tests to examine the internal resistance of the test bipolar batteries. However, an ac ohmmeter was used to measure the resistance of a test battery as a function of its state of charge. Figure J-1 shows the internal resistance of bipolar battery #1, new and at full capacity (0.34 a-h), during charge and discharge. Figure J-2 shows battery #1 at half capacity (0.17 a-h) after over one-half million cycles of testing. The internal resistance increased as the state of charge decreased and as expected, as the capacity of the battery decreased.

The relatively high resistance of the test batteries was attributed to the operation of the batteries in a starved electrolyte mode. It was not possible to keep the cells flooded with electrolyte because the design did not allow for much electrolyte and the vented cells leaked.

Performance Testing

Bipolar test batteries #0 and #1 were used exclusively for performance testing, but performance data from batteries #2 and #3 was also obtained. Analysis of the data from batteries #0 and #1 led to the selection of a current rate, minimum discharge voltage and cycle rate for endurance testing of batteries #2 and #3.

Current Load. Bipolar battery #1, with a measured capacity of 0.34 a-h, was operated at 10 to 100 times its C-rate (3-28.5 amps). With an equivalent weight of 0.31 pounds, the energy density supplied by battery #1 is shown

in Figure 6-1. If the energy density was calculated as was done in the study by Cimino and Gearing (i.e. neglecting the inter-cell connector weights) the values would be about double those shown (5:37). An energy density of nearly 75 joules per pound at a rate of one cycle per second was achieved during the cycle rate testing. Figures 6-2 through 6-5 give current load testing results. As expected, the battery temperature increased as the current increased. Efficiency fell below 80% for battery currents at or above 5 amperes. Load capacitance leveled at about 6 farads, while pulse capacitance held around 3 farads at currents above 20 amperes. Average discharge voltage fell to below 5 volts at currents above 3 amperes. There were no failures experienced while testing battery #1 in this phase. Additional performance test data is given in Appendix K.

Cycle Rate. The capacitance and efficiency of battery #1 as a function of cycle rate are shown in Figures K-1 and K-2, respectively. At a current of 5 amperes and cycle rates of 1 to 5 Hertz, the efficiency remained stable at around 90%. At a current of 10 amperes and cycle rate of 50 Hertz, the efficiency dropped off dramatically to nearly 50%. Data collection at the 25 and 50 hertz rates was very difficult because the chart recorder's highest speed was too slow to accurately record the data at these cycle rates. Capacitance fell, as expected, when the cycle rate was increased. At a battery current of 10 amperes and cycle rates of 10 and 25 Hertz, the pulse and load capacitance were

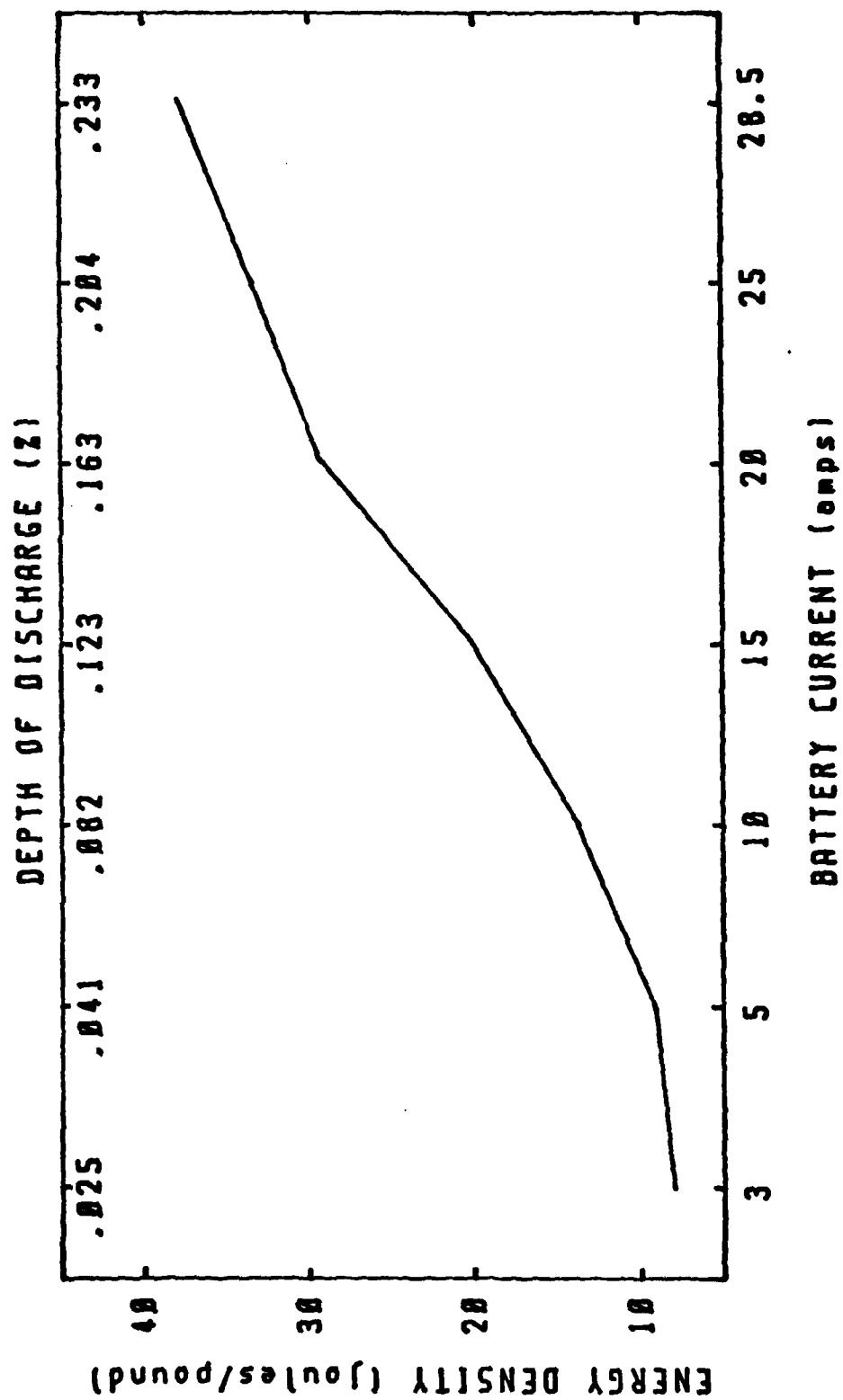


Figure 6-1. Energy Density of Test Battery #1

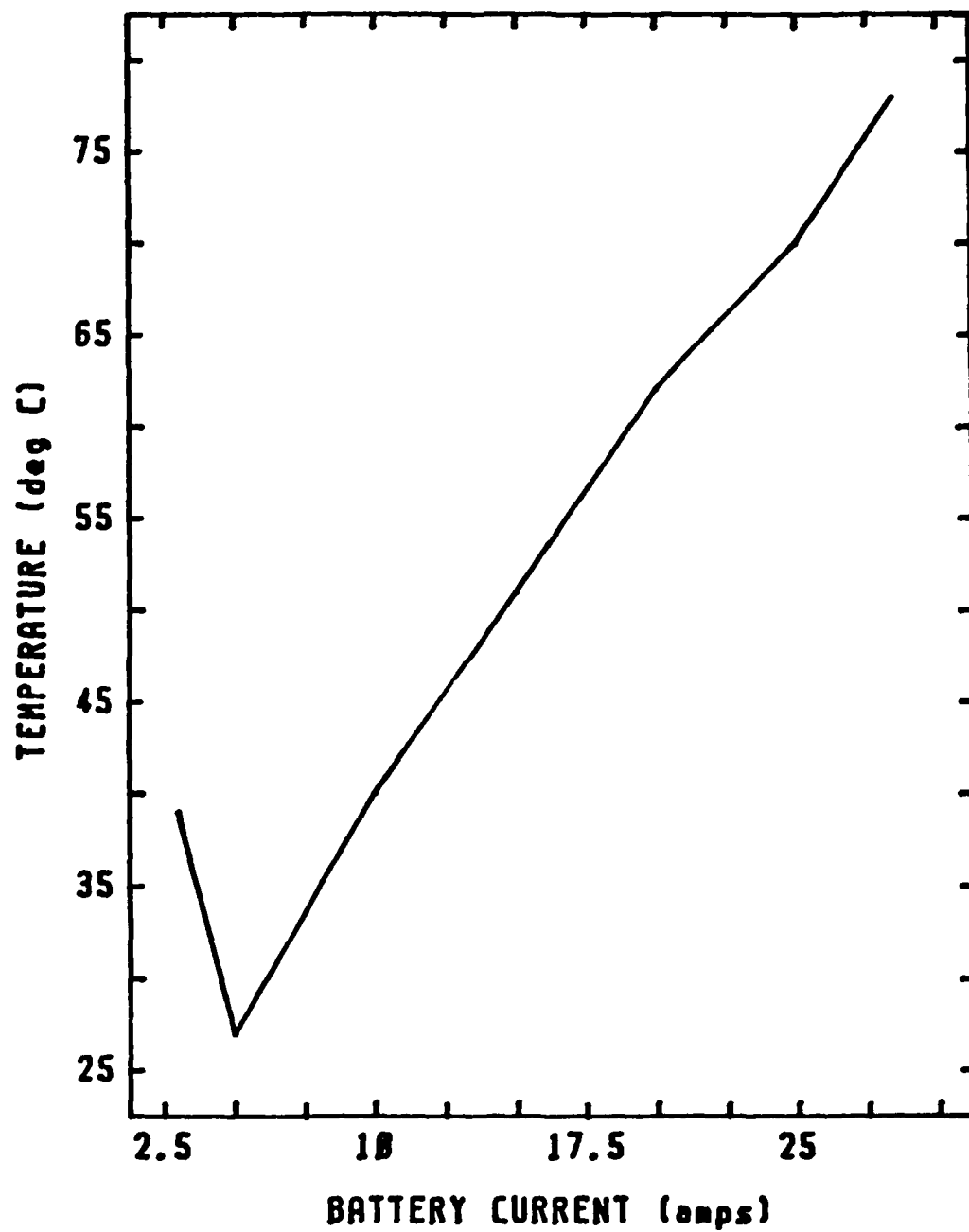


Figure 6-2. Current Load Test - Temperature

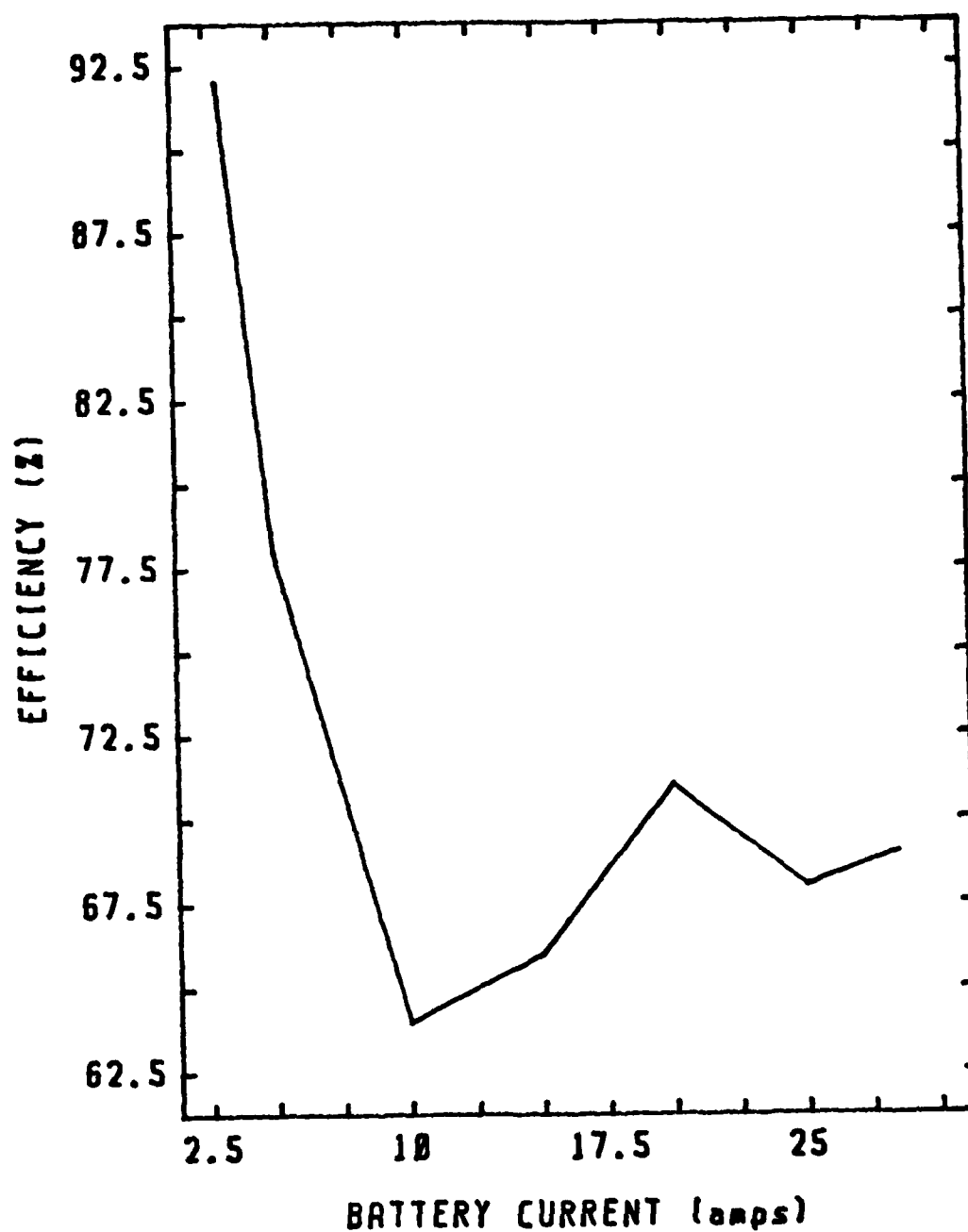


Figure 6-3. Current Load Test - Efficiency

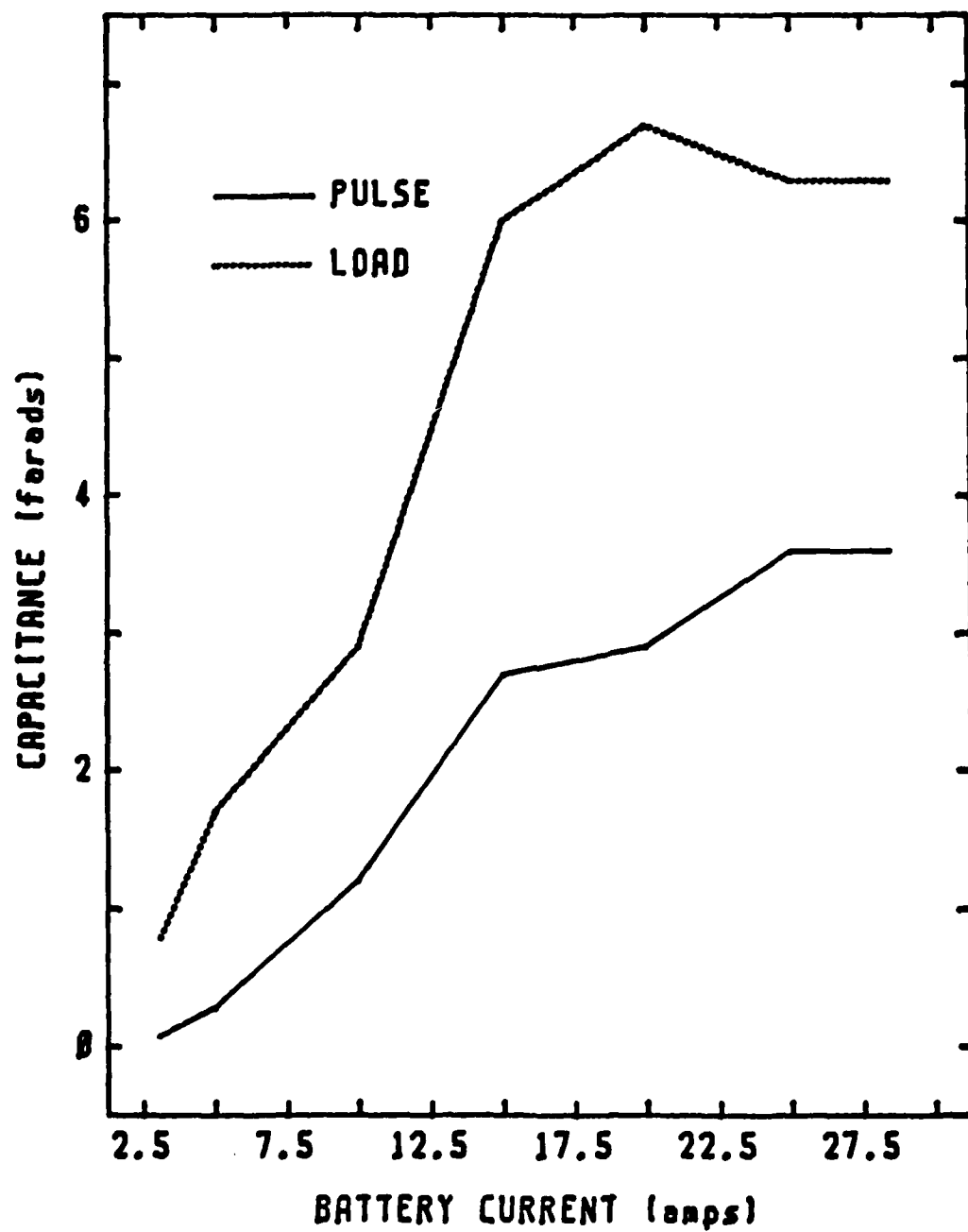


Figure 6-4. Current Load Test - Capacitance

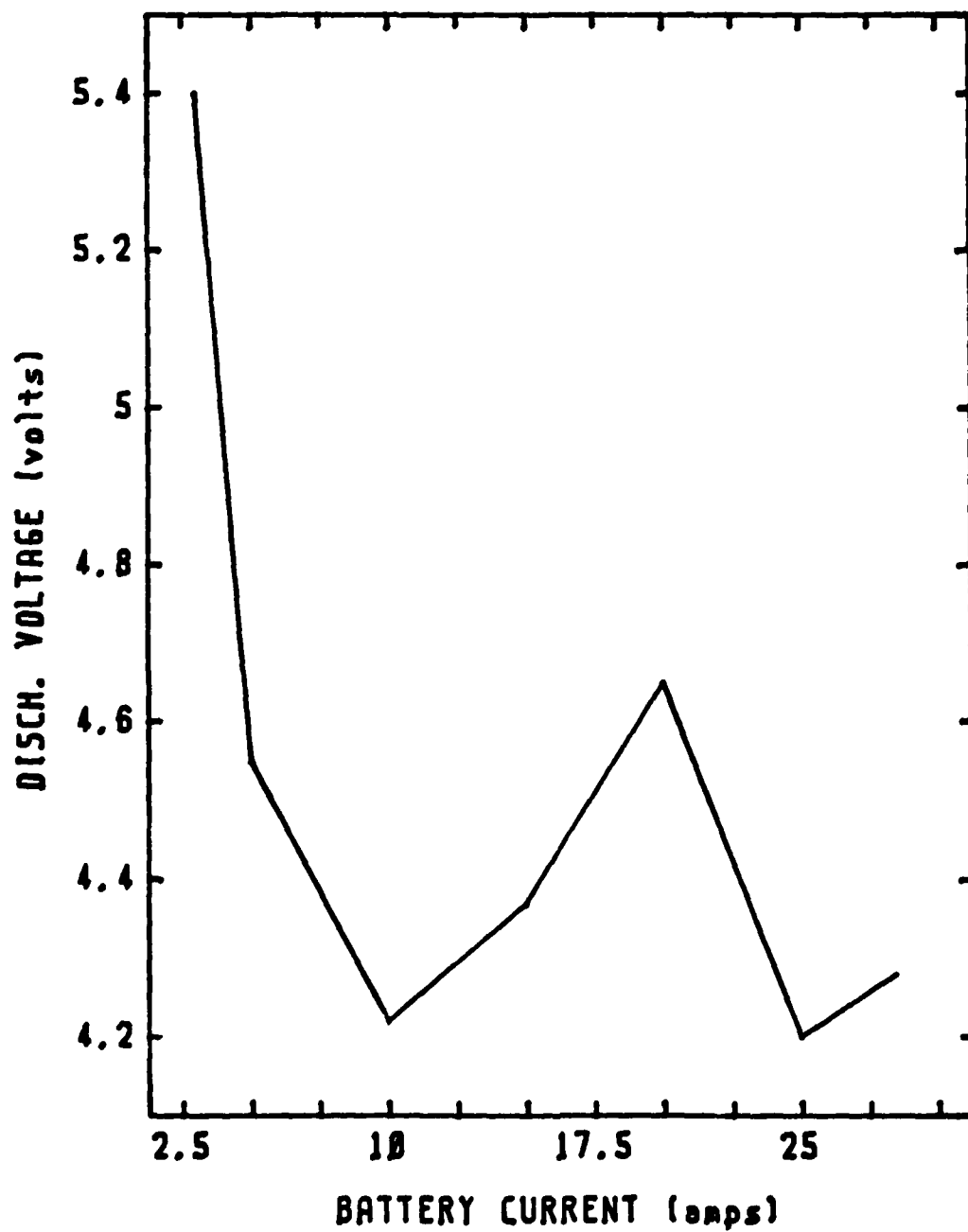


Figure 6-5. Current Load Test - Discharge Voltage

almost the same. Temperature did not appear to increase at higher cycle rates and remained more a function of the current.

End of Discharge Voltage. It had been suggested by Cimino and Gearing (5:36) that the end of discharge voltage might be a major determining factor of the efficiency and average capacitance exhibited by a Ni-Cd battery. Figure K-3 and K-4 show the load capacitance and efficiency as a function of the end of discharge voltage for Battery #2 at a battery current of 4.7 amperes and a cycle rate of 5 Hertz. Neither capacitance nor efficiency seemed to vary directly with the end of discharge voltage when varied from 3.7 to 4.6 volts at the above current and cycle rate. However, as the capacity of the battery decreased, the end of discharge voltage dropped. Changes in the charging current affected the battery end of discharge voltage more quickly when the battery capacity or state of charge decreased or individual cell voltages became unbalanced. Therefore, it was decided that the end of discharge voltage of a new battery would be maintained by the control network. This end of discharge voltage was determined as an average of the first three minutes of operation in lieu of any optimum voltage that was originally sought.

Based on the results from performance testing, two batteries were endurance tested at a state of charge of 75% and with the previously explained end of discharge voltage as the controlling voltage. Cycle rates of 5 and 10 hertz were

selected for comparison to past studies and because the batteries seemed to operate well as capacitive filters at these rates. A battery current of 3 amperes, or about a 10 C-rate, was chosen to keep the efficiency high and to prolong the life of the test batteries.

Endurance Testing

Cycle Life. Battery #3 failed after 1.6 million cycles. It had operated normally until the failure with no degradation in measured capacity. The average efficiency was 79% and an average load capacitance of 0.94 farads. Both efficiency and capacitance dropped dramatically as the battery developed an internal short. The failure of this battery negated the attempt to run a test bipolar battery for over a billion cycles. However, life cycle data for battery #2 was tracked along with that of the removeable cadmium electrode from battery #2. This data is presented in Figure 6-6. The overall measured capacity of battery #2 dropped significantly, but the capacity of battery #3, before the failure, and the removeable cadmium electrode remained constant. The average load capacitance of battery #2 varied between 0.6 and 1.5 farads and tended to be more a function of the state of charge and individual cell voltage balance of the battery rather than the cycle life. The efficiency of battery #2 varied between 87% and 93%. It also varied as a function of the battery's run-time since the last complete balancing discharge and charge of the

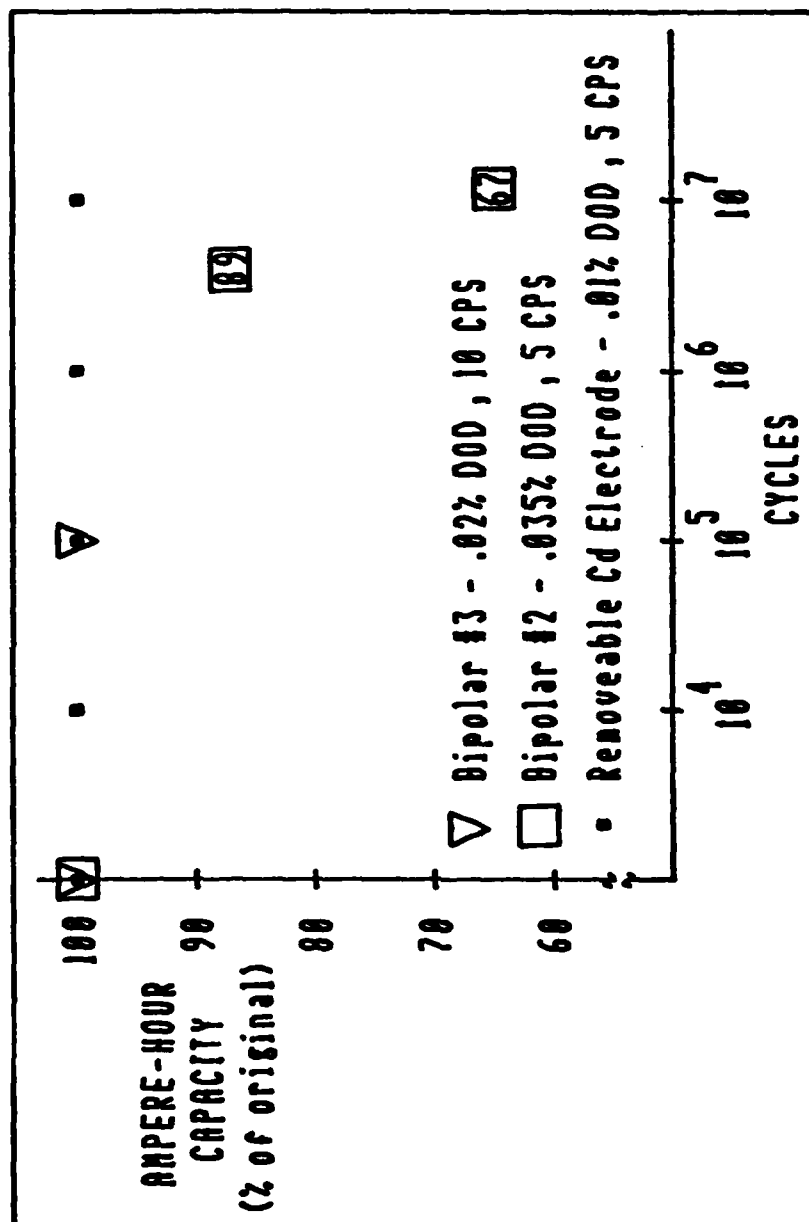


Figure 6-6. Endurance Test - Capacity Versus Cycles

battery. The more recent the charge, the more efficiently the battery operated.

Battery #3 was examined after its failure. The cadmium electrode in cell #3 had developed a circular, 2 centimeter diameter blister that had pushed outward through the separator to cause a short. A scanning electron microscope (SEM) examination and energy dispersive X-ray analysis revealed that the blister was mostly nickel. The fact that a cadmium electrode had blistered and that most of the blister was nickel was unusual. Further analysis revealed that the blister contained about 20% cadmium in the center, but the top and bottom contained 10% and 1% cadmium, respectively. The rest of the blister material was mostly nickel and nickel hydroxide. The blister was twice as thick as the original electrode (60 mils versus 30 mils) with most of the extra thickness occurring on the back side in the form of nickel hydroxide. Figures L-1 and L-2 are SEM photos of the blister. It appears that the nickel sinter in the failed cadmium electrode had corroded to form nickel hydroxide. The release of gaseous oxygen during cell overcharge was the probable cause of the sinter corrosion and formation of the blister.

Cadmium Electrode Study. Bipolar test battery #2 was cycled over ten million times at a 5 hertz rate. A battery current of 3 amperes was utilized to cycle the removeable cadmium electrode resulting in a 5 C-rate based on its measured capacity of 0.62 a-h. Even though about 9% of the

electrode was removed for analysis over the life of the test, the measured capacity of the electrode remained unchanged. Figures 6-7 through 6-9 are SEM photographs of the interior of the cadmium electrode before testing, after 10^3 cycles, and after 10^7 cycles. The initially large, impregnated cadmium hydroxide crystals were quickly broken down into smaller, more chemically active crystals. As the test progressed, isolated crystals of electrically insulating Beta $\text{Cd}(\text{OH})_2$ were formed within the electrode plaque (19). These Beta crystals are normal for cycled cadmium electrodes and indicate a reduction in the active cadmium available to provide electrochemical energy. The surface of the electrode remained clear and there were no signs of any sinter corrosion as illustrated in Figure L-3 through Figure L-6.

Battery #2 stopped working correctly after surpassing 10 million cycles and two months of testing. Its demise marked the failure of the last of the four experimental bipolar batteries. An examination of the electrodes of battery #2 revealed that one nickel electrode had formed a commonly seen blister and one cadmium electrode had formed a small blister similar to the one observed in battery #3. Another cell had a significant amount of cadmium migration throughout the separator and was extensively "soft-shortened." Two of the cells were dry and obviously electrolyte starved. The observed cell failure mechanisms were all normal failure modes, with the exception of the cadmium blister, and typical of what would be seen in a failed Ni-Cd battery that had

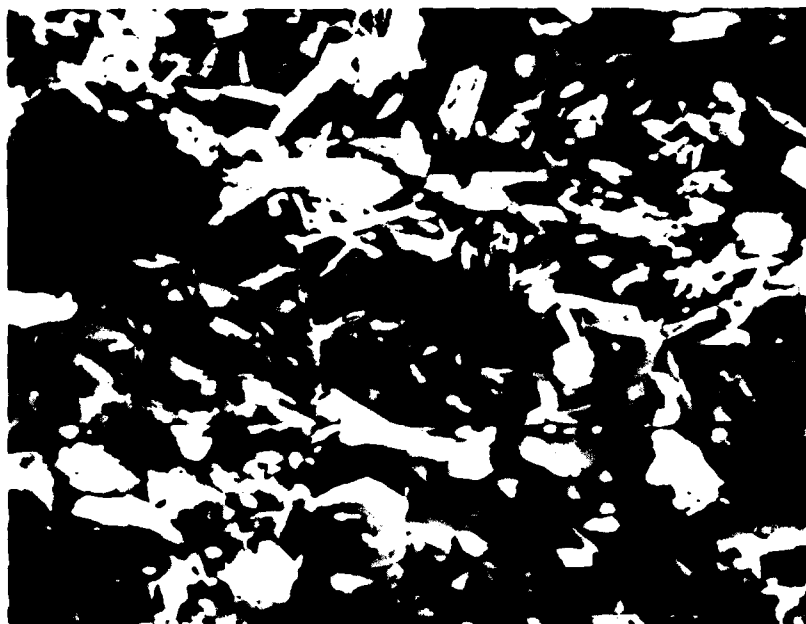


Figure 6-7. Cadmium Electrode Interior Before Cycling

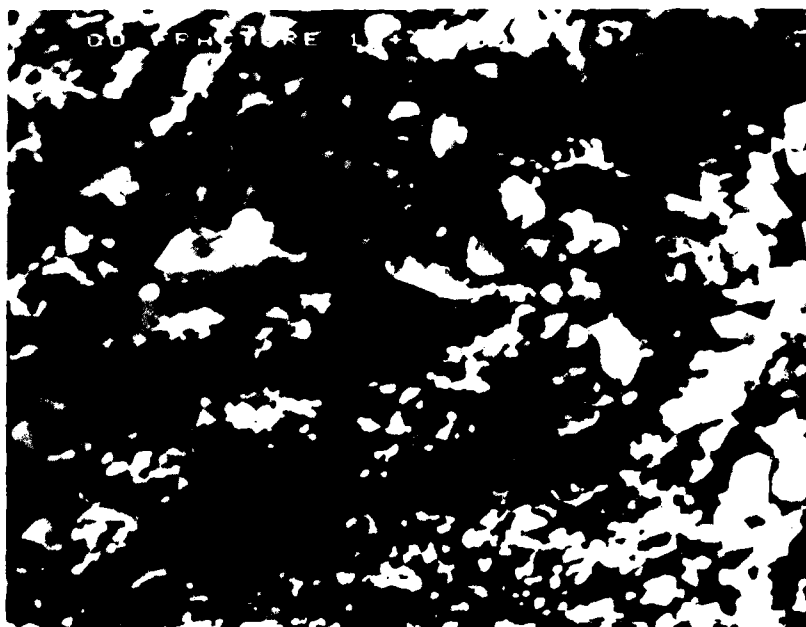


Figure 6-8. Cadmium Electrode Interior After Ten Thousand Cycles

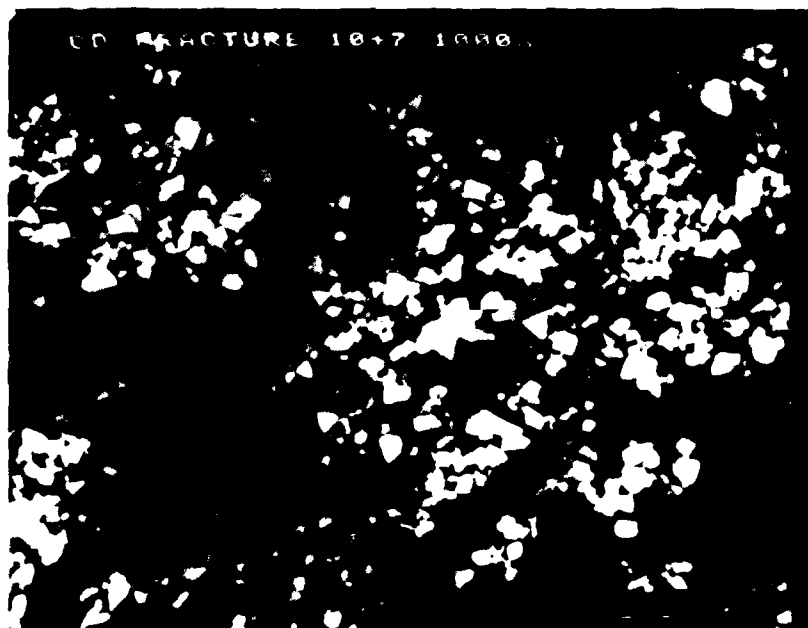


Figure 6-9. Cadmium Electrode Interior After Ten Million Cycles

undergone slow cycling rates.

The final chapter of this report presents the conclusions drawn from the experimental data obtained and observed over the nine months of this study. Recommendations are made where deemed appropriate in the pursuit of further knowledge and continued efforts in this area.

VII. Conclusions and Recommendations

Conclusions

The objectives of this limited study were to design, construct and test bipolar nickel-cadmium batteries to determine their suitability for use as relatively high frequency, pulsed load filter elements. One application could be their use in spacecraft pulsed power systems, replacing relatively heavier capacitors. The objectives were met. Four bipolar batteries were designed, constructed, and tested with the help of a computer controlled test network. Battery performance parameters to include energy density, efficiency, average capacitance, and capacity versus cycle life were obtained. A cadmium electrode was closely studied to determine the effects of this type of utilization on the structure of the electrode.

The following specific conclusions were made as a result of this study effort:

1. A functional bipolar Ni-Cd battery was designed and built. Total battery weight could be reduced with modern manufacturing techniques. Electrode manufacturing was inconsistent. Patented electrode manufacturing techniques utilized were not optimized for bipolar electrodes. An effective, open-cell seal was made, but no sealing method was found that would allow periodic assembly and disassembly without some leakage.

2. A Hewlett Packard HP-85A computer and HP-3497A Data Acquisition and Control System were successfully used to automatically control, monitor, and evaluate the test batteries. A computer program requiring minimal operator interface was highly successful.
3. A battery energy density of almost 75 joules per pound of equivalent battery weight was demonstrated. Test batteries were cycled at up to a 100 C-rate. An average capacitance of 6 Farads was achieved with one battery.
4. Battery charge and discharge cycle rates of 1 to 50 Hertz were investigated. Useful capacitance at 25 Hertz and above was less than 0.7 farads.
5. The end of discharge voltage was found not to be a major factor in the battery efficiency and capacitance. Rather, it was seen as an indication of the capacity and state of charge of the battery.
6. One battery was cycled over 10 million times as part of life cycle testing. Two cadmium electrodes developed blisters, a rare Ni-Cd battery failure mechanism. Nickel sinter corrosion, forming nickel hydroxide appeared to be the cause. The limiting battery failure mode experienced was the imbalance of the individual battery cells which caused overcharging of the nickel electrodes. This overcharging caused shedding of nickel hydroxide from the nickel electrode. Periodic full battery discharge and recharge were required

to prolong useful battery life and negate the more frequent occurrence of this common Ni-Cd battery problem.

7. A scanning electron microscope examination of a cycled cadmium electrode showed no unusual structure changes. An electrode cycled 10 million times had lost no capacity. The cadmium electrode itself was not seen as a limiting factor for a bipolar Ni-Cd battery utilized as a pulsed load filter element.

Recommendations

Rapid charge and discharge of bipolar Ni-Cd batteries is possible for extended periods of operation at a low depth of discharge. In this study, limitations in battery manufacture and mechanics overshadowed limitations in battery performance. Relatively high energy density and average capacitance with extended cycle lives indicate possible promise for bipolar Ni-Cd batteries as pulsed load filters. However, further study and testing should be accomplished before any large scale research is conducted.

The following specific recommendations are offered to further explore this idea:

1. Investigate Ni-Cd battery electrode impregnation processes to optimize procedures for bipolar electrode manufacturing.
2. Utilize better design and construction methods to make a bipolar Ni-Cd battery that is lighter, contains

ample electrolyte, and does not leak.

3. Study the effects of the pulsed load filter application of a Ni-Cd battery on the nickel electrode. Concentrate on efforts to avoid overcharge and the shedding of active material from the electrode surface.
4. Explore the possibility that nickel sinter corrosion is accelerated when Ni-Cd batteries are used as pulsed load filters.

Appendix A. Capacitance From Voltage Waveform

Figure A-1 illustrates how pulse and load capacitance were calculated. Load capacitance was based on the change in voltage from the knee of the voltage waveform to the end of discharge. Pulse capacitance was based on the initial slope of the voltage waveform at the knee.

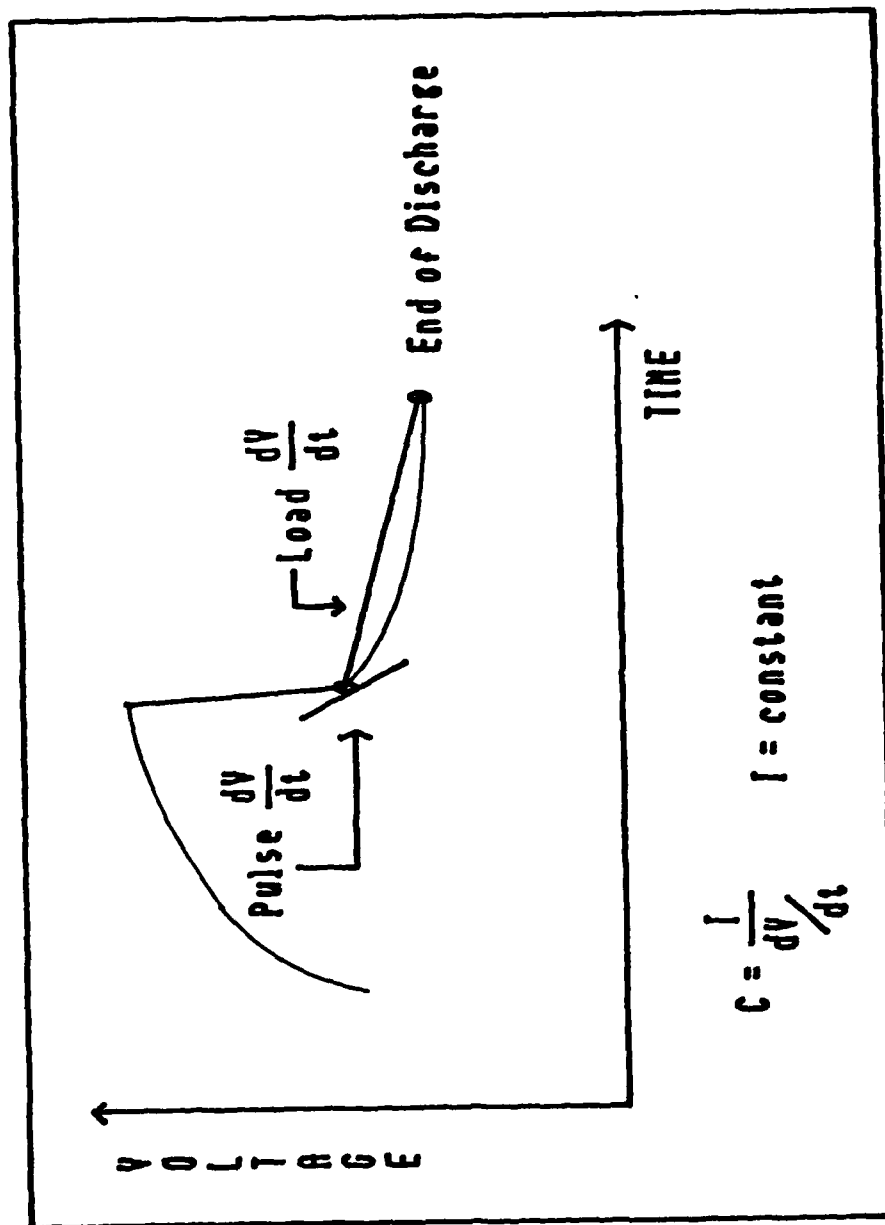


Figure A-1. Capacitance From Voltage Waveform

Appendix B. Battery Parameter Sample Calculations

1. Depth of Discharge (DOD in %) = $(I_b \times \text{Time} \times 100)/\text{Capacity}$

I_b = Discharge current through the battery (eg. 3 amperes)

Time = Discharge time in hours based on cycle rate

(eg. 5 Hz yeilds .1 sec x (1 hour/3600 sec))

Capacity = Measured capacity of test bipolar battery
before cycling (eg. 0.34 amperes)

$$\text{DOD (\%)} = (3 \times 2.78 \times 10^{-5} \times 100)/0.34 = 0.0245 \%$$

2. Energy Density (ED in joules/pound) =

$$(E \times I_b \times \text{Time})/\text{Weight}$$

E = Average Discharge voltage (eg. 5.4 volts)

I_b = Discharge current through battery (eg. 3 amperes)

Time = 5 Hertz yields a discharge time (eg. 0.1 sec)

Weight = Equivalent weight of the battery (eg. 0.32 pound)

$$\text{ED} = (5.4 \times 3 \times .1)/.32 = 5.1 \text{ joules/pound}$$

3. Efficiency (%) = $(V_b \text{ out} \times I_b \text{ out} \times 100)/(V_b \text{ in} \times I_b \text{ in})$

$V_b \text{ out}$ = Average battery discharge voltage (eg. 5.4 volts)

$I_b \text{ out}$ = Battery discharge current (eg. 3 amperes)

$V_b \text{ in}$ = Average battery charge voltage (eg. 5.7 volts)

$I_b \text{ in}$ = Battery charge current (eg. 3.1 amperes)

$$\text{Efficiency} = (5.4 \times 3 \times 100)/(5.7 \times 3.1) = 92\%$$

4. Average Capacitance (C in farads) = $I_b / (dV/dT)$

I_b = Battery discharge current (eg. 3 amperes)

dV/dT = Change in battery discharge voltage over a time interval during the discharge of the battery (eg. 4 volts/sec).

$$C = (3/4) = 0.75 \text{ farads}$$

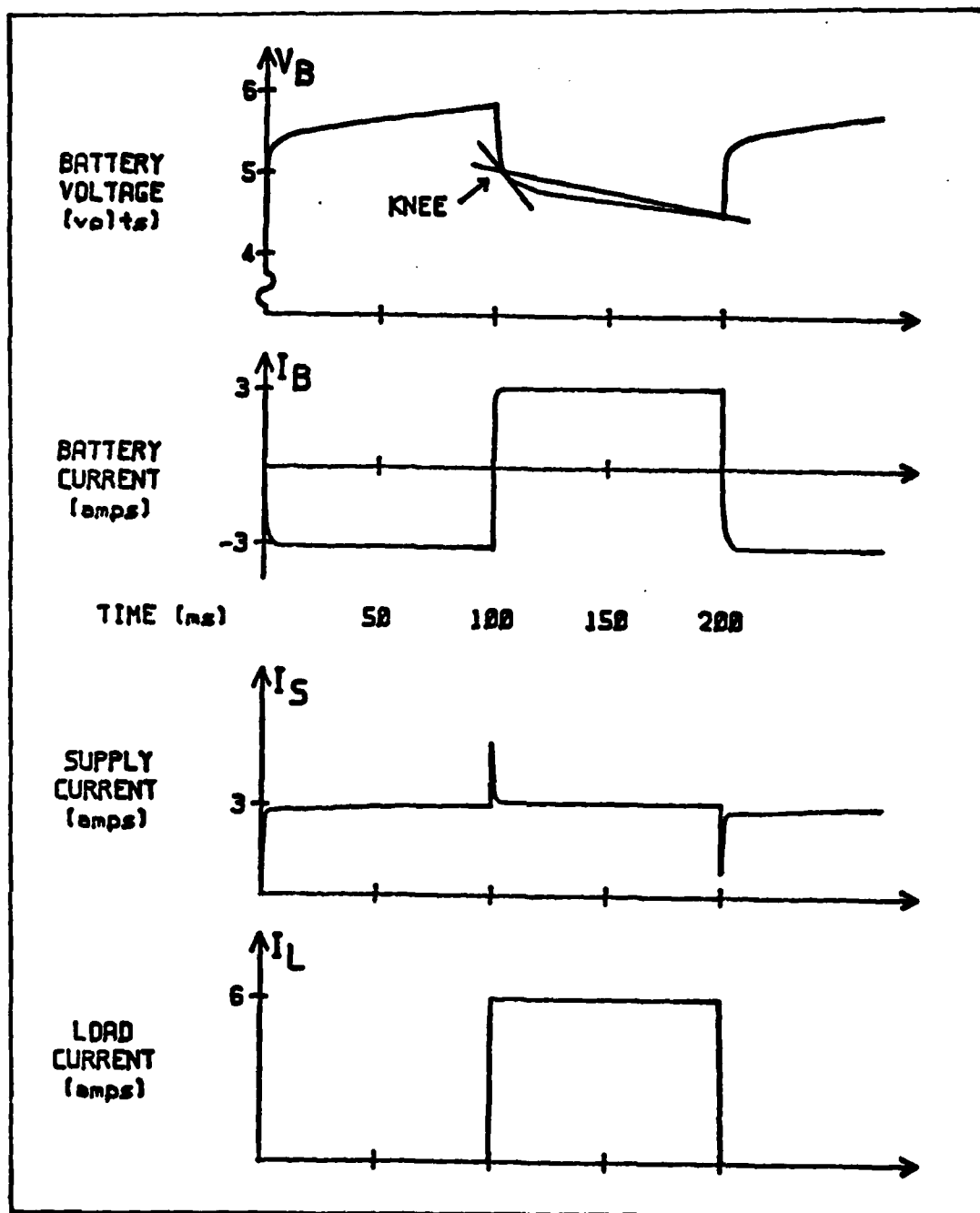


Figure B-1. Typical Waveforms

Appendix C. Battery Components

The drawings in this appendix provide physical specifications of the battery components used in the construction of bipolar batteries.

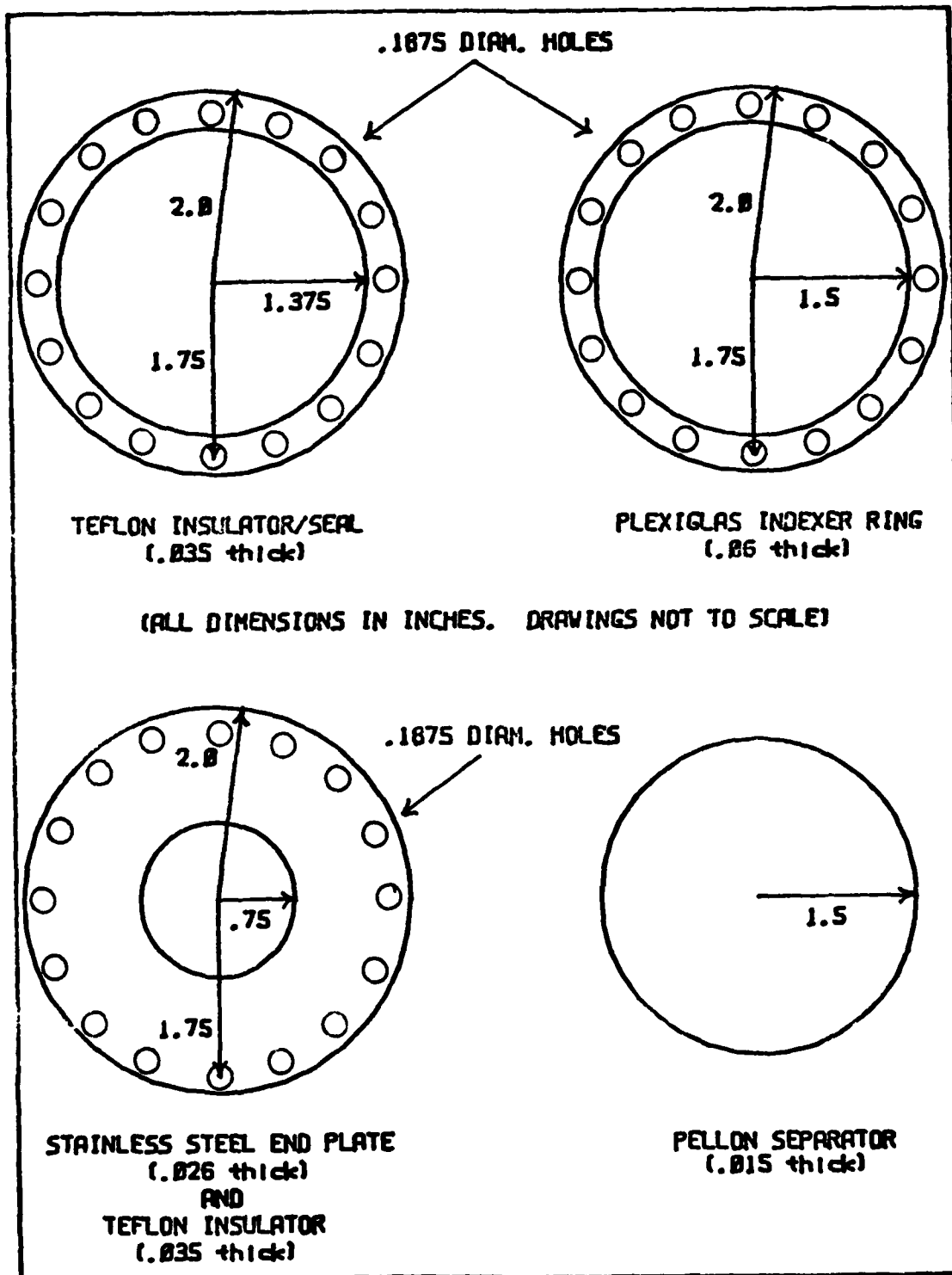


Figure C-1. Dimensions of Battery Components

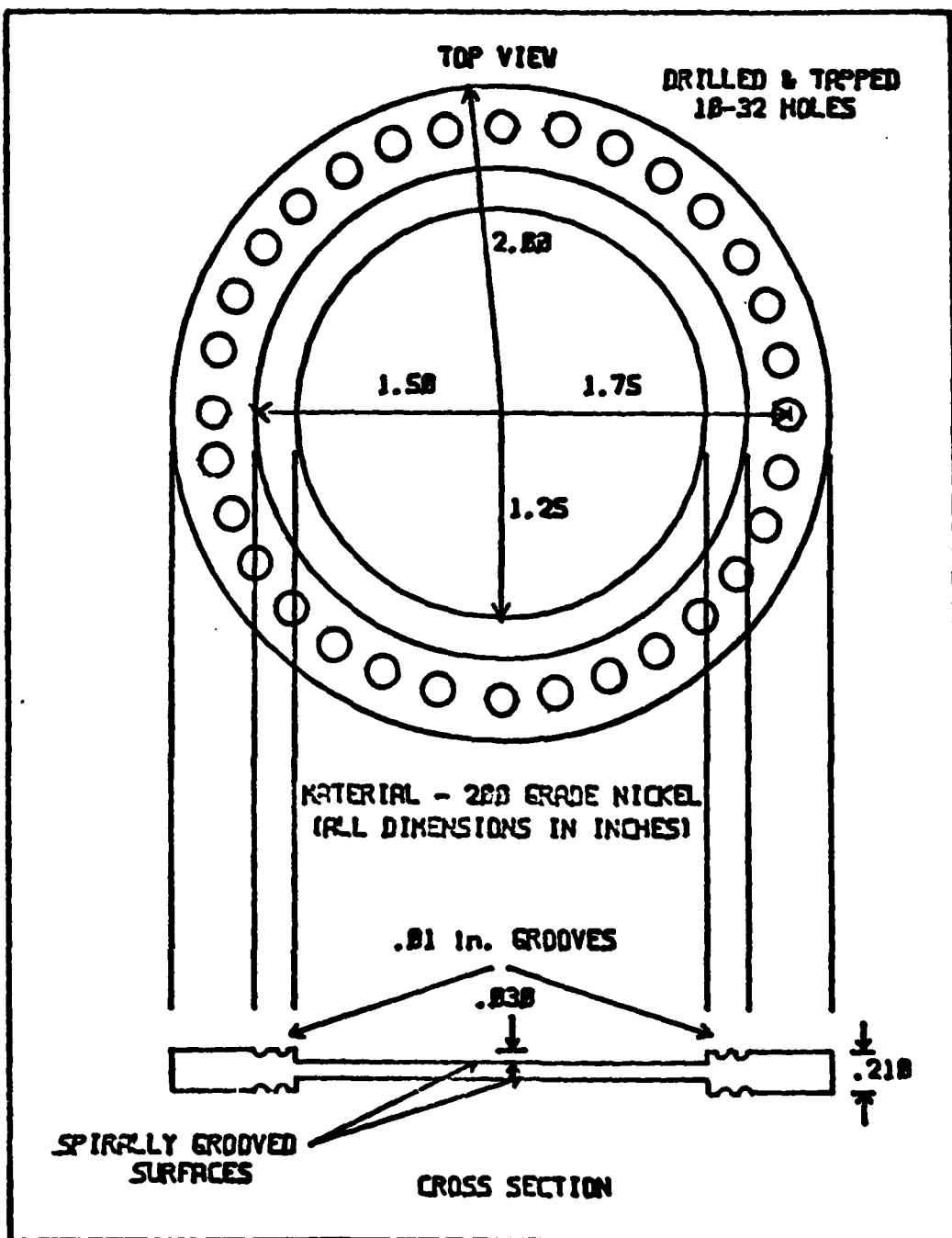


Figure C-2. Inner End Plate for Removeable Electrode Battery

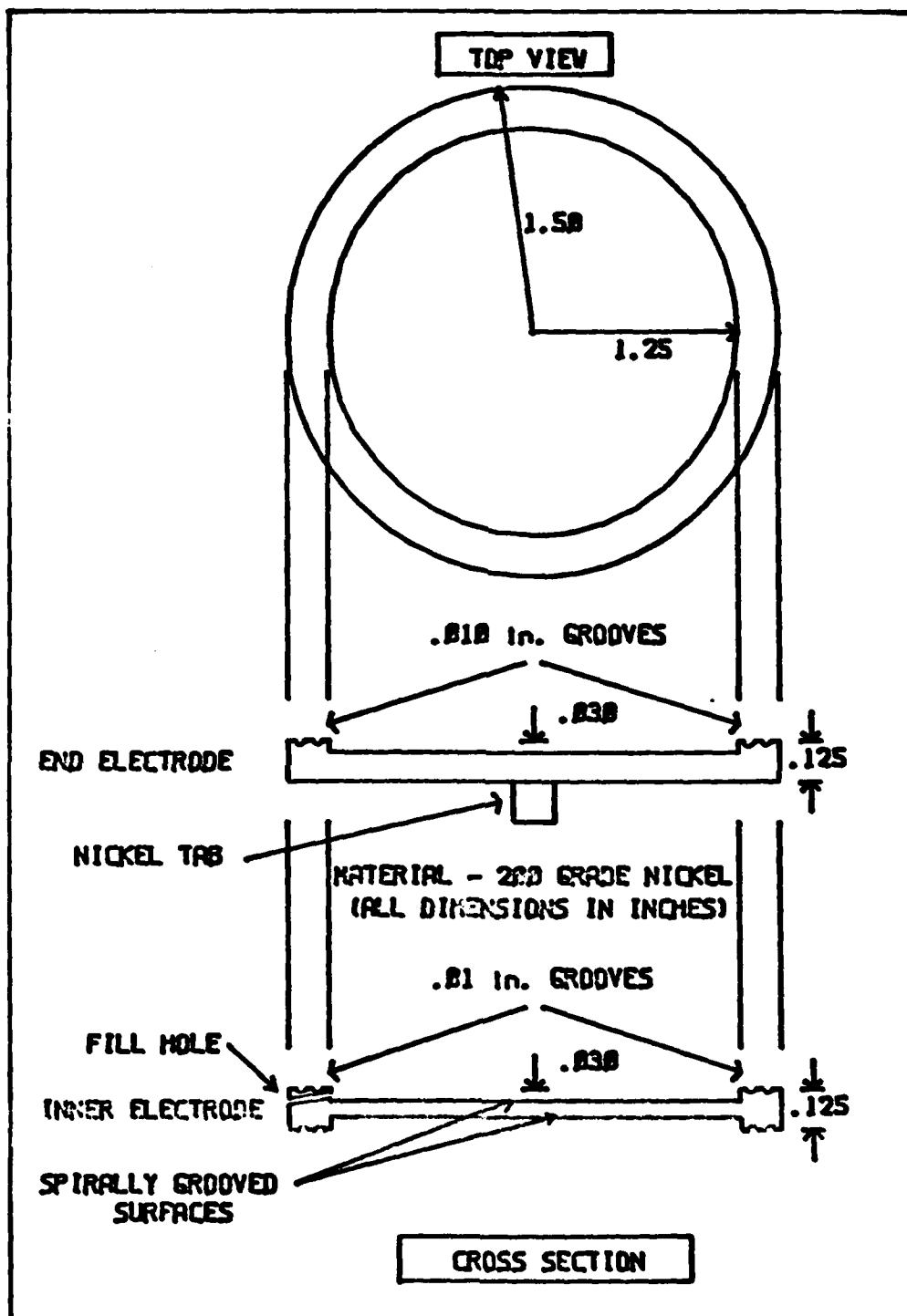


Figure C-3. Standard Electrode Substrates

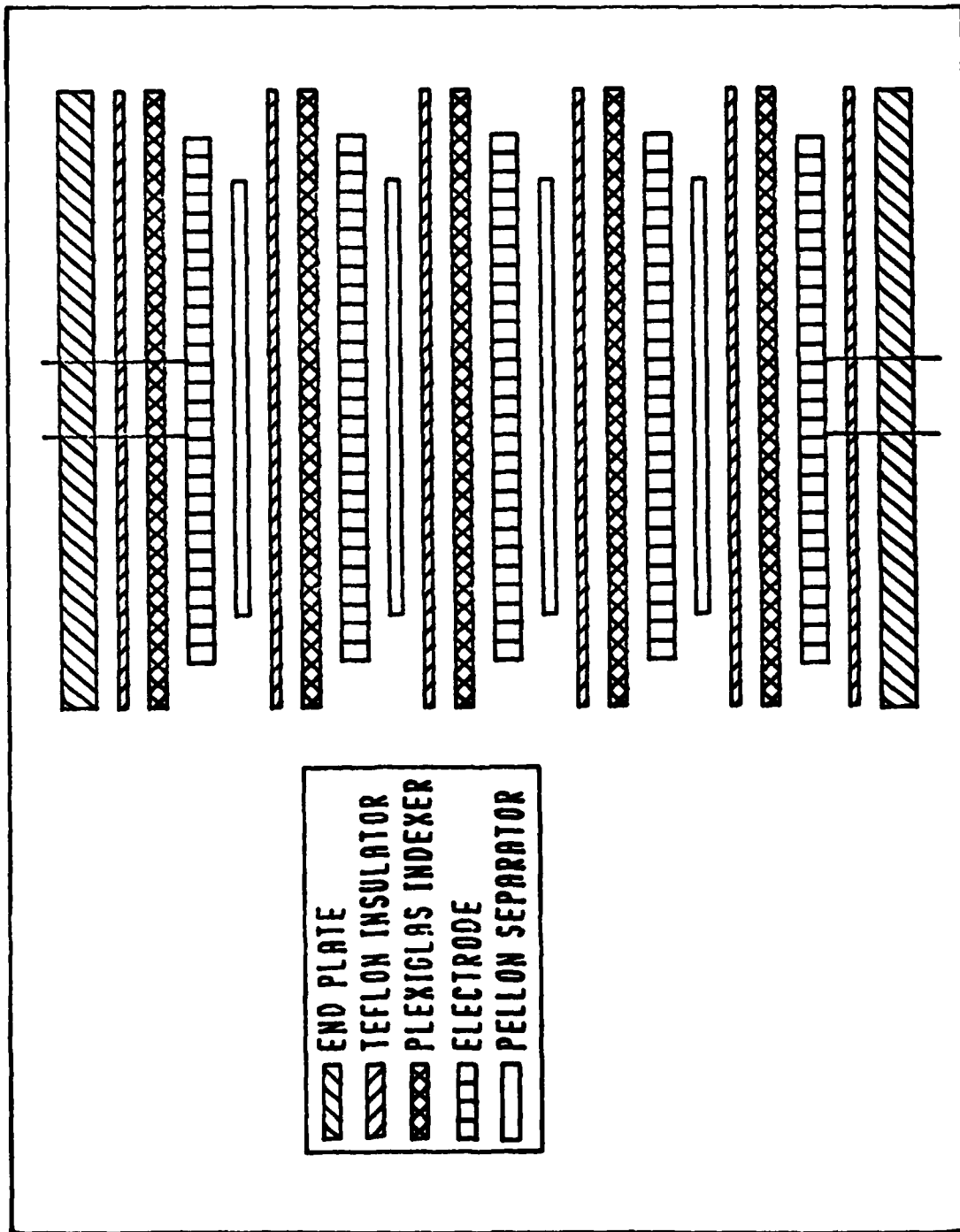
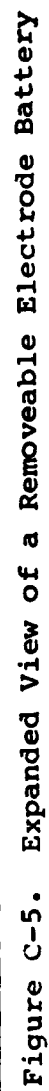


Figure C-4. Expanded View of a Test Bipolar Battery



Appendix D. Electrode Sintering Checklist

1. Knock off or file any metal burrs.
2. Acid etch slug for a few minutes until it just starts to speckle. Rinse with distilled water and dry thoroughly.
3. Weigh accurately.
4. Fill one side of the slug cavity with type 287 Mond brand nickel powder, 200 mesh sift, and smooth with a glass rod. Make a growth groove in the powder around the outside with a knife.
5. Place the slug in a 6 inch Lindberg tube furnace (9400 watt) on a quartz glass plate and slide it to the middle of the tube. Preheat the oven to 500 degrees C with a 5% hydrogen and 95% nitrogen gas flow. Turn oven up to 980 degrees C and sinter slug for 8 to 12 minutes after reaching the set temperature(8 minutes if the first side of a double-sided slug). Turn oven and hydrogen off. Leave the nitrogen on, slide the slug to the end of the tube, open the oven door, and let it cool to below 200 degrees C before removing.
6. Weigh accurately.
7. Test porosity of the sinter by dropping distilled water drops on it. This sintering process normal yields 82% porous plaque. Inspect carefully for any blisters, bubbles, cracks, or looseness.
8. Repeat 4-7 for the other side of a double-sided slug. Cook for 10 to 12 minutes.

AD-A163 949

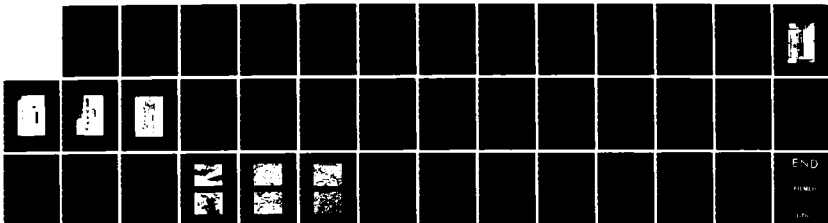
STUDY OF BIPOLAR NICKEL-CADMIUM BATTERIES AS PULSED
LOAD FILTERS(U) AIR FORCE INST OF TECH WRIGHT-PATTERSON
AFB OH SCHOOL OF ENGI.. R W CHEDISTER ET AL. NOV 85
AFIT/GE/ENG/85D-6 F/G 10/3

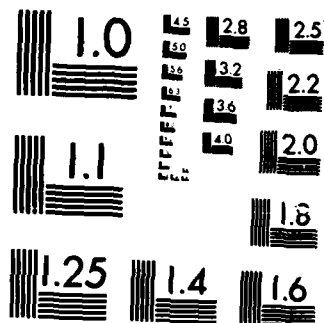
2/2

UNCLASSIFIED

F/G 10/3

NL





MICROCOPY RESOLUTION TEST CHART
NATIONAL BUREAU OF STANDARDS 1963-A

9. Use the double-cooked side for the cadmium electrode if possible because nickel stresses the sinter more during impregnation.

10. Weigh accurately. Slugs averaged 2.5 grams of powder per electrode.

Appendix E. Electrode Impregnation Checklist

Cadmium Impregnation

1. The theoretical capacity for a cadmium electrode is 0.366 a-h per gram of cadmium impregnated into nickel sinter.
2. Make a solution of 2 molar $\text{Cd}(\text{NO}_3)_2$. Two times the atomic weight of $\text{Cd}(\text{NO}_3)_2$ in grams (472g) mixed with 1 liter of water makes a 2 gram mole of solution.
3. Heat the cadmium nitrate solution to 80°C while continuously stirring. Maintain a pH of 3.5 with a 7.5 molar nitric acid drip.
4. Mount the cadmium electrode (to cover the nickel side) or cover an end plate backside with RTV. This insures that current passes through the sintered plaque only. See Figure E-2 for drawings of the impregnation mounts.
5. Place a cadmium metal plate along with the slug to be impregnated into the solution. Run a 0.5 ampere current (0.1 ampere per square inch of sinter surface) through the circuit for 4 hours. Run the current with the slug at the negative lead for 50 seconds then reverse leads and run for 10 seconds. See Figure E-1 for a schematic of the impregnation apparatus.
6. After the impregnation, rinse the slug in distilled water, stir bath for a few hours to remove any solution left in the plaque.
7. Take the slug out of the mount and dry it in a vacuum oven for a few hours and then clean off deposited materials

outside the sintered area of the electrode.

8. Weigh the electrode accurately. The increased weight is the amount of cadmium impregnated and is used to figure a theoretical cadmium electrode capacity.

Nickel Impregnation

1. Make a solution of 1.8 molar nickel nitrate and 0.2 molar cobalt nitrate by mixing 523.4 grams (1.8×290.8) of nickel nitrate and 58.21 grams (0.2×291.05) of cobalt nitrate into 1 liter of distilled water.
2. Heat the solution to 80 degrees C, continuously stir, and maintain a pH of 3.5 with a nitric acid drip.
3. Mount the slug if required or cover its back with RTV.
4. Place a nickel plate and the electrode slug into the bath. Run a 0.875 ampere (0.175 ampere per square inch) current through the solution for 4 hours.
5. Take out the electrode, rinse quickly in distilled water to remove debris and place in a KOH formation bath with another nickel plate. Cycle 0.5 amperes (0.1 ampere per square inch) of current through the bath and plates, reversing the current every 20 minutes for at least 5 cycles. Take the electrode out fully discharged.
6. Rinse the electrode in a stir bath of distilled water a few hours to remove excess nitrates and KOH.
7. Dry the electrode in a vacuum oven at 50 degrees C for a few hours.

8. Clean off any excess deposits of nickel hydroxide and weigh it accurately. The increase in weight is used to figure the nickel hydroxide electrode capacity (0.289 a-h per gram).

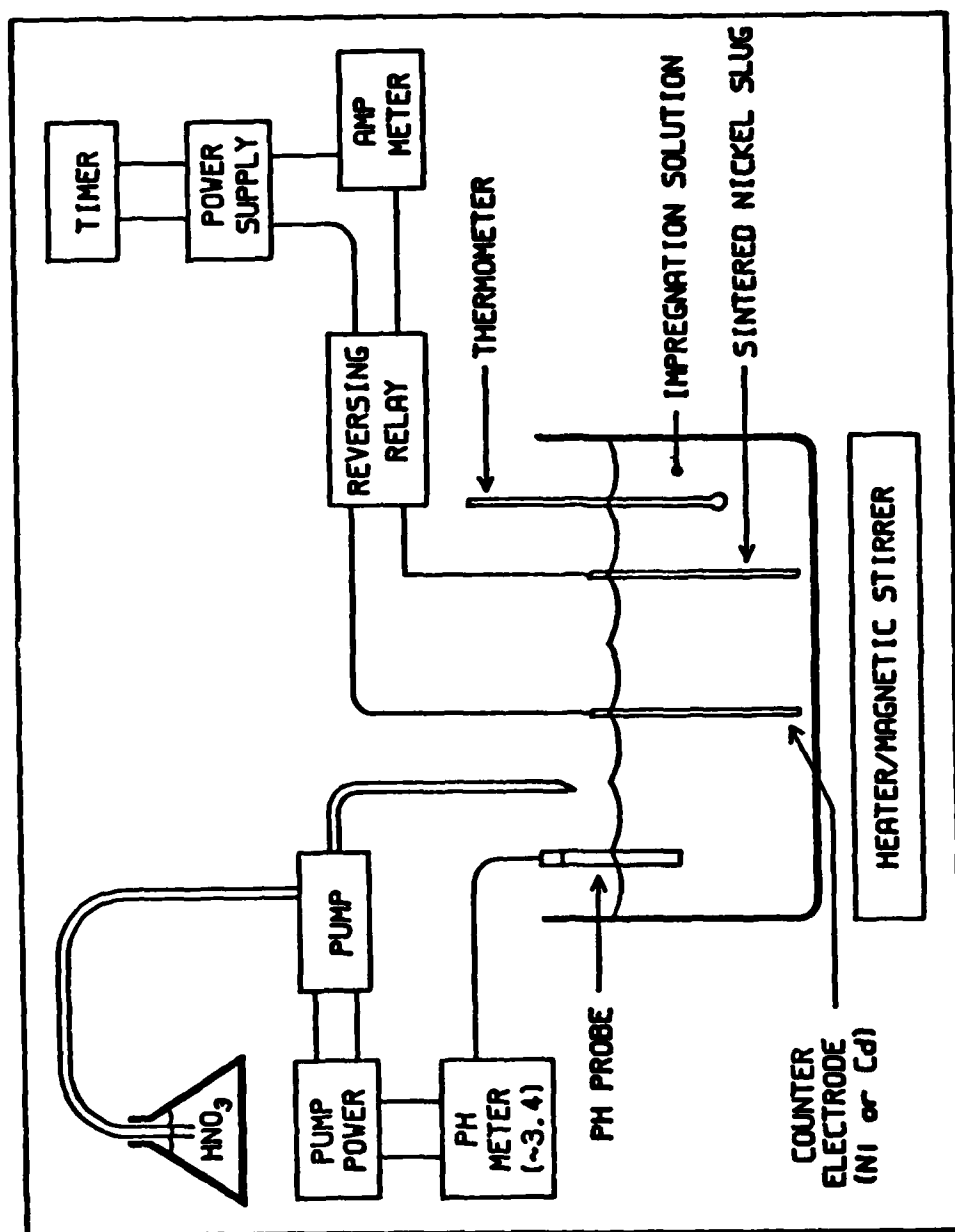


Figure E-1. Electrode Impregnation Apparatus

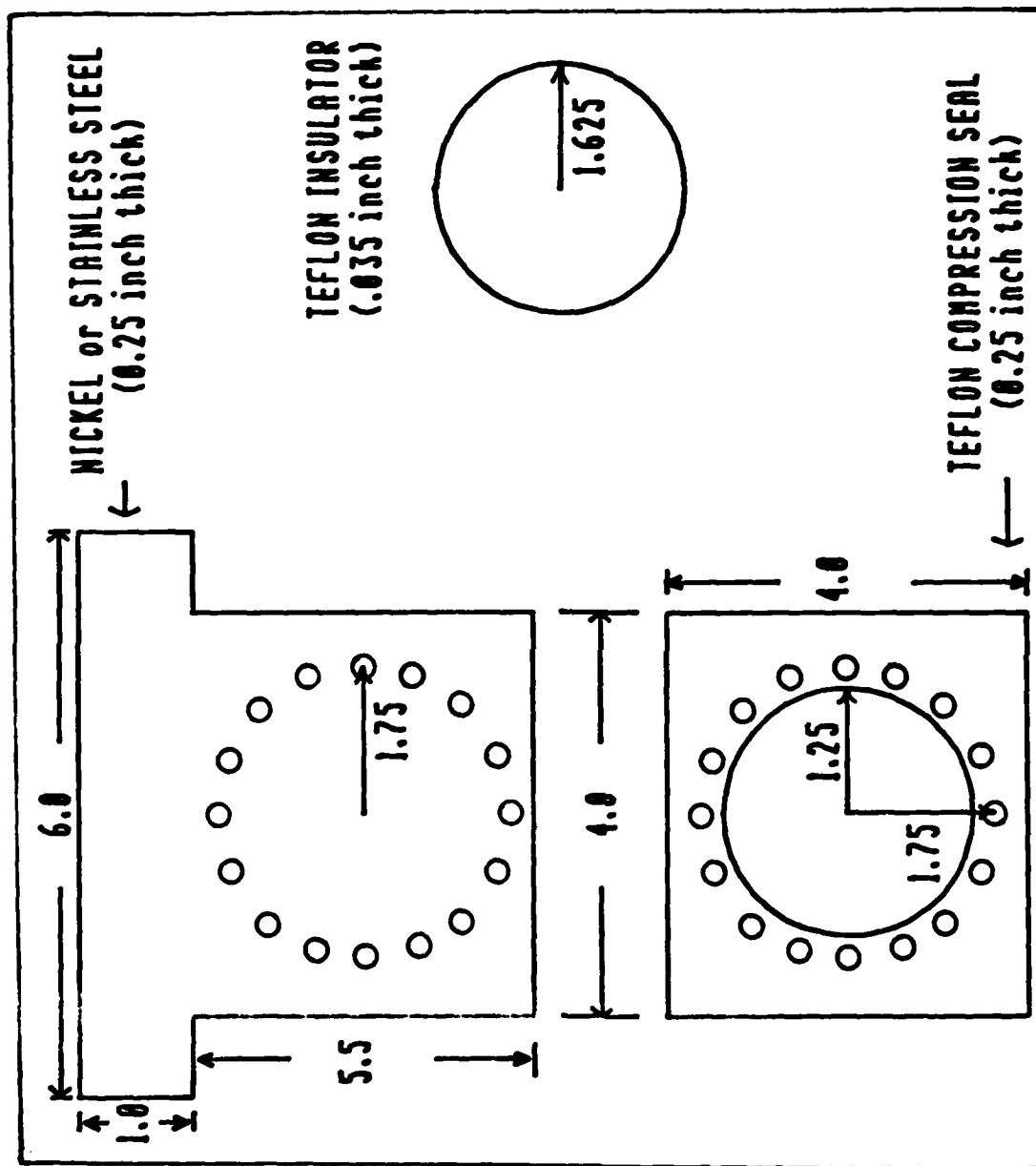


Figure E-2. Impregnation Mount Components

Appendix F. Battery Equivalent Weights

1. Electrode weight was considered 57.9% of the total equivalent battery weight. This was based on a standard aircraft Ni-Cd battery (4,5:75).
2. The electrode wall weight between the positive and negative sides was estimated using data from the Seiger study (8:975). Using a 0.03 thick wall of nickel, the weight of each wall was approximated to be 8.3 grams. This value was used because it was achievable and closer to that which would be used in commercial manufacturing to minimize battery weight.
3. Battery electrode weight calculations example:

8 x sinter weight	=	20 g
Nickel impregnated	=	8.3 g
Cadmium impregnated	=	13.5 g
5 x intercell wall	=	41.5 g
Total electrode weight (ELW)	=	83.3 g
Total equivalent weight	=	0.32 pounds

$$\text{Equivalent Weight} = (\text{ELW (g)} / 0.579) \times (1 \text{ lb} / 453.6 \text{ (g)})$$

4. The four test battery equivalent weights are listed below:

<u>Battery</u>	<u>Weight in pounds</u>
0	0.31
1	0.32
2	0.28
3	0.30

5. Assuming 82% porosity of the sinter, the void volume available in the sintered slugs for impregnation was 1.98 cubic centimeters (cc). A figure of merit for the impregnation process is to typically get 1.6 to 1.7 grams per cc of nickel impregnated. The process in this study averaged around 1 gram per cc.

$$\text{Void volume} = \text{Volume of sinter} \times 0.82$$

$$\text{Grams per cc of void volume} = \text{grams impregnated} / \text{void volume}$$

Appendix G. Equipment

This appendix contains an equipment list, calibration log, and apparatus pictures.

Equipment List

CONDITIONING and CHARGING

HP-6263	DC Power Supply (2 each)
HP-7132A	2-Channel Chart Recorder
173A	Timer/Relay Unit
HP-4328A	Keithley Multimeter
	Mili-ohmmeter

PERFORMANCE

HP-85A	Computer
HP-3497A	Data Acquisition/Control Unit
HP-6012A	DC Power Supply
HP-3314A	Function Generator
DLP-50-60-1000	Solid State Load Controller
	25 amp - 50 mv Current Shunts (2 each)
	50 amp - 50 mv Current Shunts
HP-1201A	Dual Trace Oscilloscope
173A	Keithley Multimeter
HP-7418A	8-Channel Recorder

ENDURANCE

1. REMOVEABLE CADMIUM ELECTRODE STUDY

Same as Performance.

2. LONG TERM

HP-9915	Computer
HP-3497A	Data Acquisition/Control Unit
HP-6012A	DC Power Supply
HP-3314A	Function Generator
DLP-50-60-1000	Solid State Load Controller
	25 amp - 50 mv Current Shunts (2 each)
	50 amp - 50 mv Current Shunts
HP-1201A	Dual Trace Oscilloscope
173A	Keithley Multimeter
HP-7418A	8-Channel Recorder

Equipment Calibration Log

26 June 1985

0830 HP-7418A channels 5-8 calibrated

5 - 50.5V/Div; 0.2V/Div; 0-6 Volts

6 - 2.0 mV/Div; 5.0 mV/Div

7 - 1000 uV/Div; 2000 uV/Div

8 - 1000 uV/Div; 2000 uV/Div

0900 All remaining equipment checked for valid calibration

28 August 1985

1100 HP-7418A channels 1-4 calibrated

1 - 2.0V/Div; 0-6 Volts

2 - 0.005 V/Div; 0.01 V/Div; 0-6 Volts

3 - 0.005 V/Div; 0.01 V/Div; 0-6 Volts

4 - 0.005 V/Div; 0.01 V/Div; 0-6 Volts

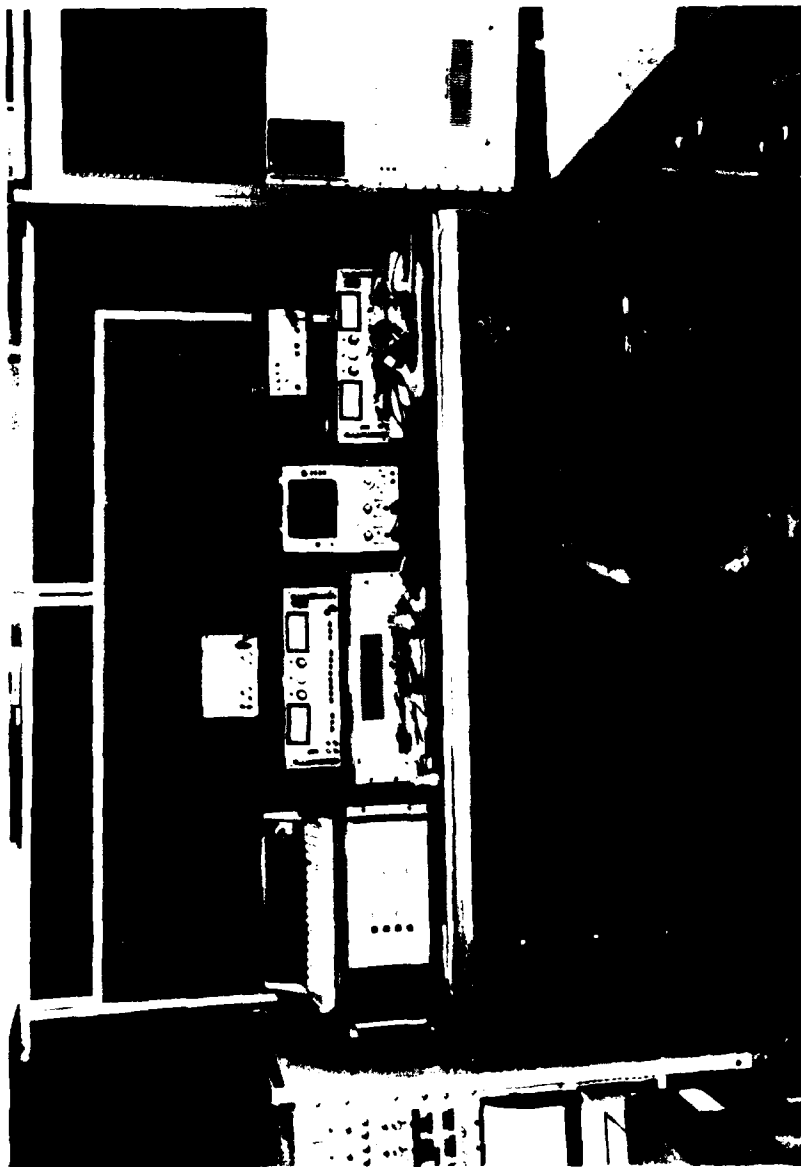


Figure G-1. Test Equipment Layout

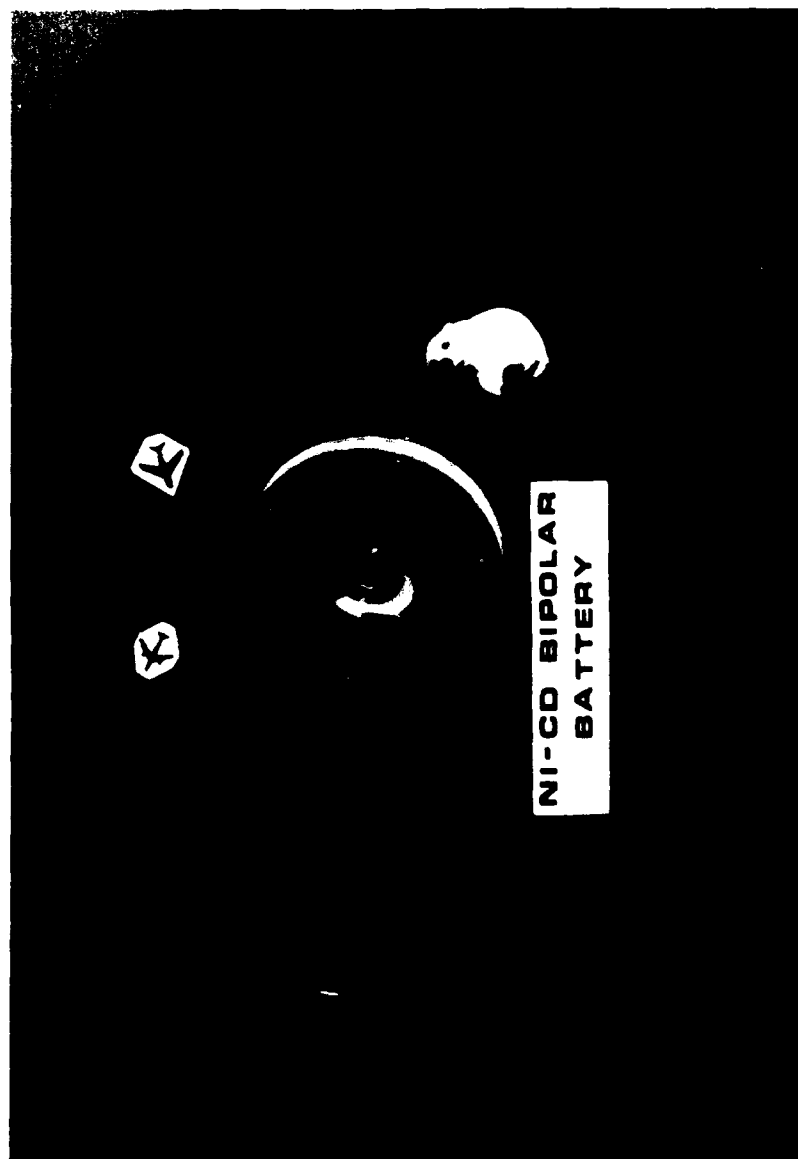


Figure G-2. Bipolar Ni-Cd Battery



Figure G-3. Bipolar Ni-Cd Battery Parts

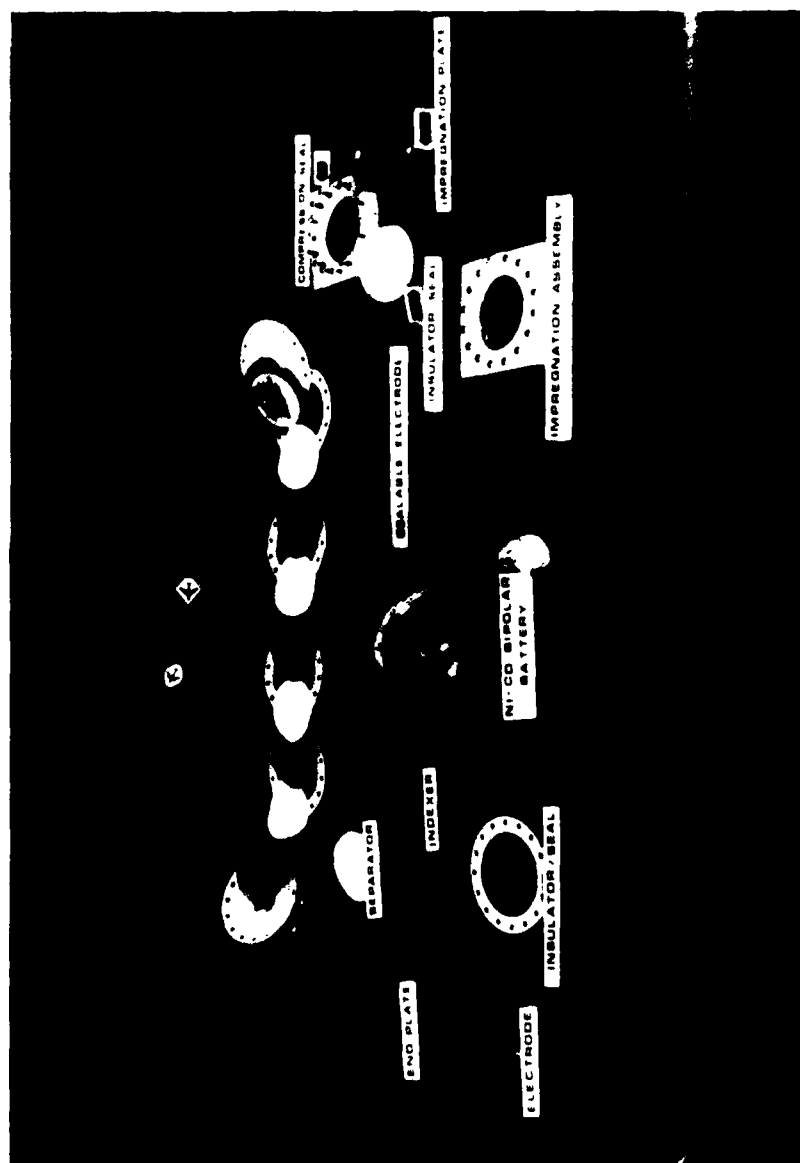


Figure G-4. Miscellaneous Battery Parts

Appendix H. Computer Program

Due to existing governmental regulations, the computer program is not contained within this report. Copies may be obtained from the Power Technology Branch, Aero Propulsion Laboratory, Air Force Wright Aeronautical Laboratory, or the Air Force Institute of Technology, Wright-Patterson AFB, Ohio.

Figures H-1 and H-2 illustrate the logic behind the computer program used to control battery end of discharge voltage.

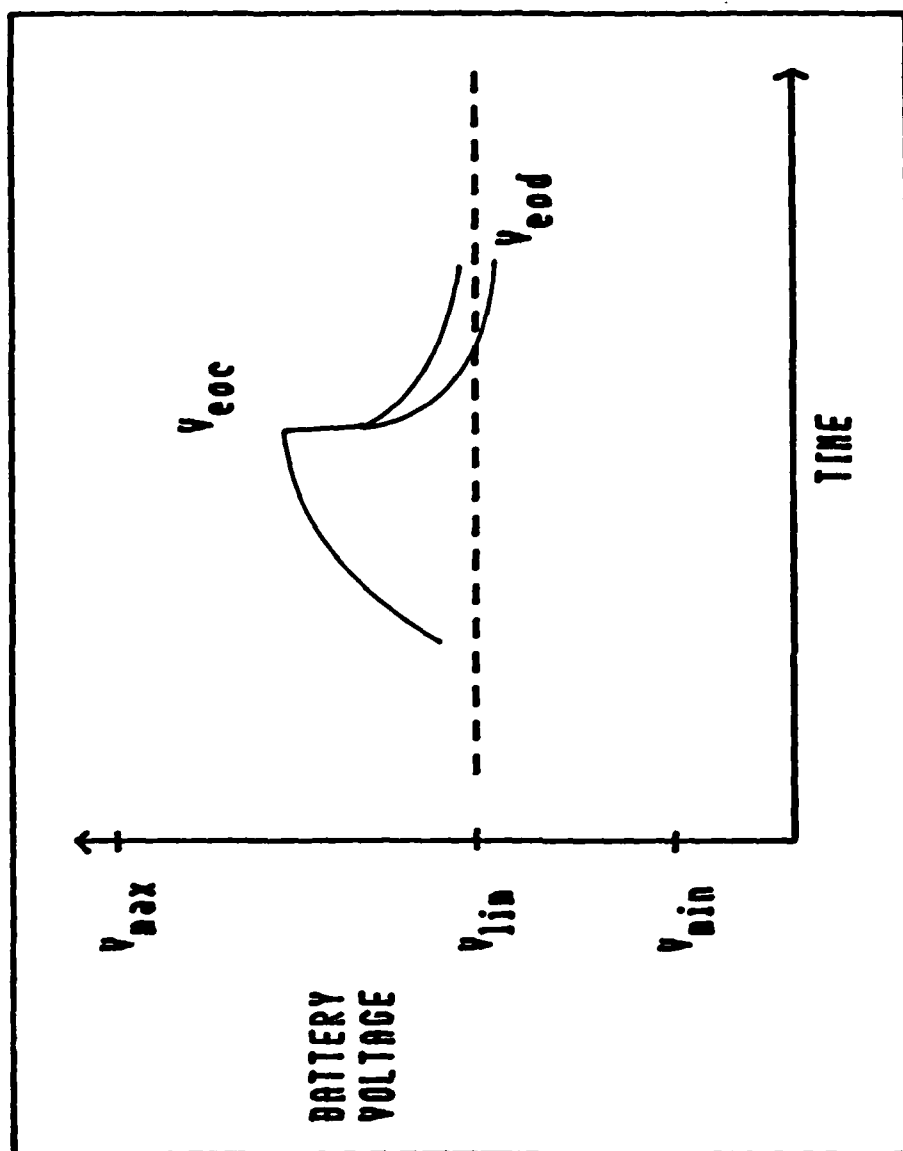


Figure H-1. Endurance Test Battery Control Parameters

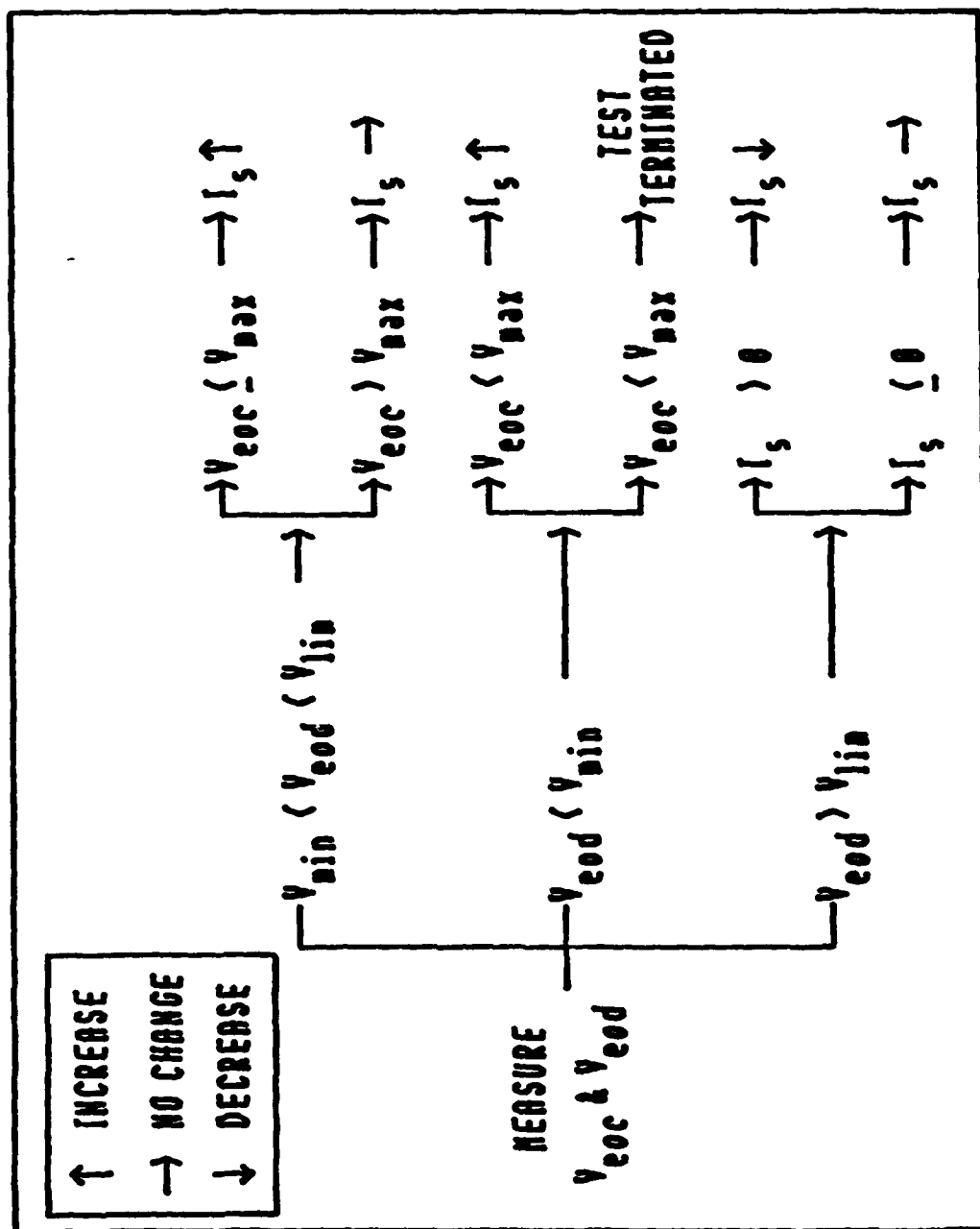


Figure H-2. Endurance Test Control Logic

Appendix I. Electrode Specifications

This appendix provides detailed impregnation data for all of the battery electrodes in tabular form.

Table II
Electrode Specifications

Battery #	Slug #	Type (C=Cadmium) (N=Nickel)	Grams Impregnated	Capacity (Amp-Hour)
0	1	C	3.1	1.13
	2	N	2.7	0.78
		C	2.4	0.88
	3	N	2.4	0.68
		C	1.9	0.70
	4	N	2.4	0.69
		C	2.4	0.89
	5	N	1.9	0.56
1	1	N	2.1	0.61
	2	C	4.8	1.80
		N	1.8	0.53
	3	C	3.1	1.10
		N	2.2	0.64
	4	C	3.3	1.20
		N	2.1	0.61
	5	C	2.4	0.87
2	1	N	1.9	0.55
	2	C	3.6	1.30
		N	1.7	0.50
	3	C	2.4	0.89
		N	1.7	0.50
	4	C	2.1	0.77
		N	1.7	0.49
	5	C	2.7	0.97
3	1	C	1.9	0.68
	2	N	2.0	0.57
		C	2.1	0.78
	3	N	3.0	1.10
		C	2.4	0.87
	4	N	1.8	0.53
		C	2.3	0.85
	5	N	2.0	0.58

Appendix J. Internal Resistance

Figures J-1 and J-2 illustrate the change in the internal resistance of battery #1 as it was charged and discharged.

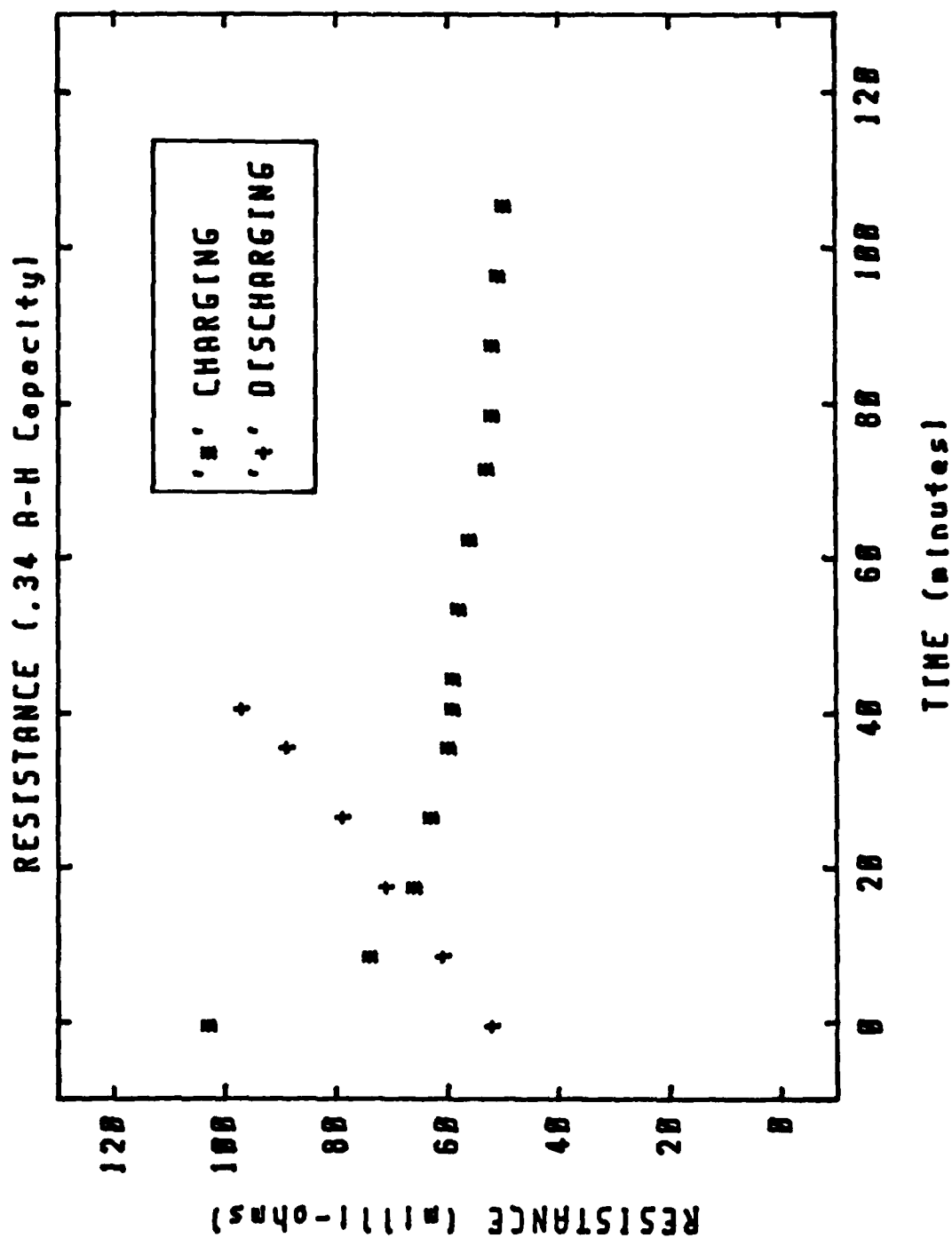


Figure J-1. Internal Resistance of Battery #1 at Full Capacity

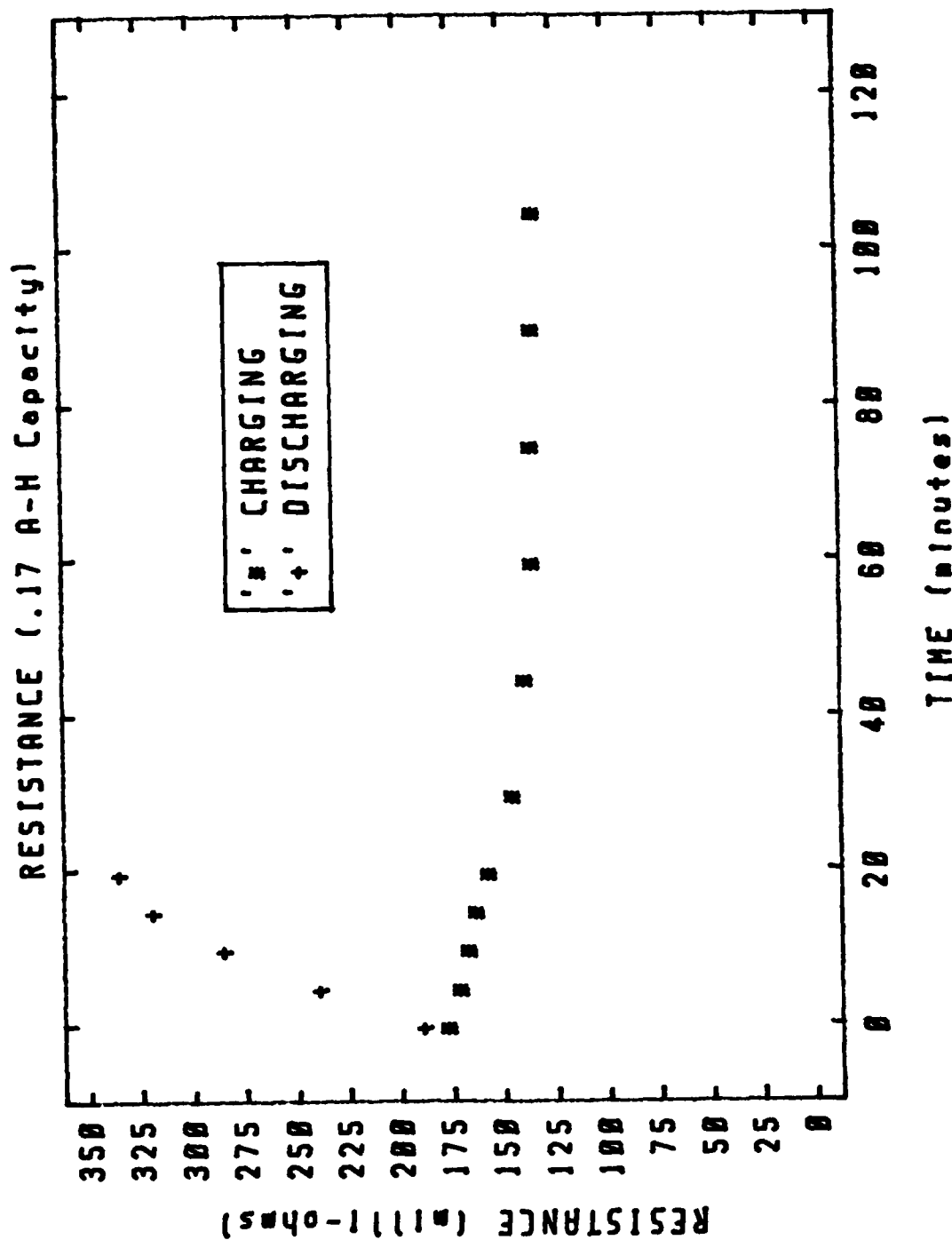


Figure J-2. Internal Resistance of Battery #1 at One-Half Capacity

Appendix K. Performance Data

The graphs in this appendix present additional performance test data.

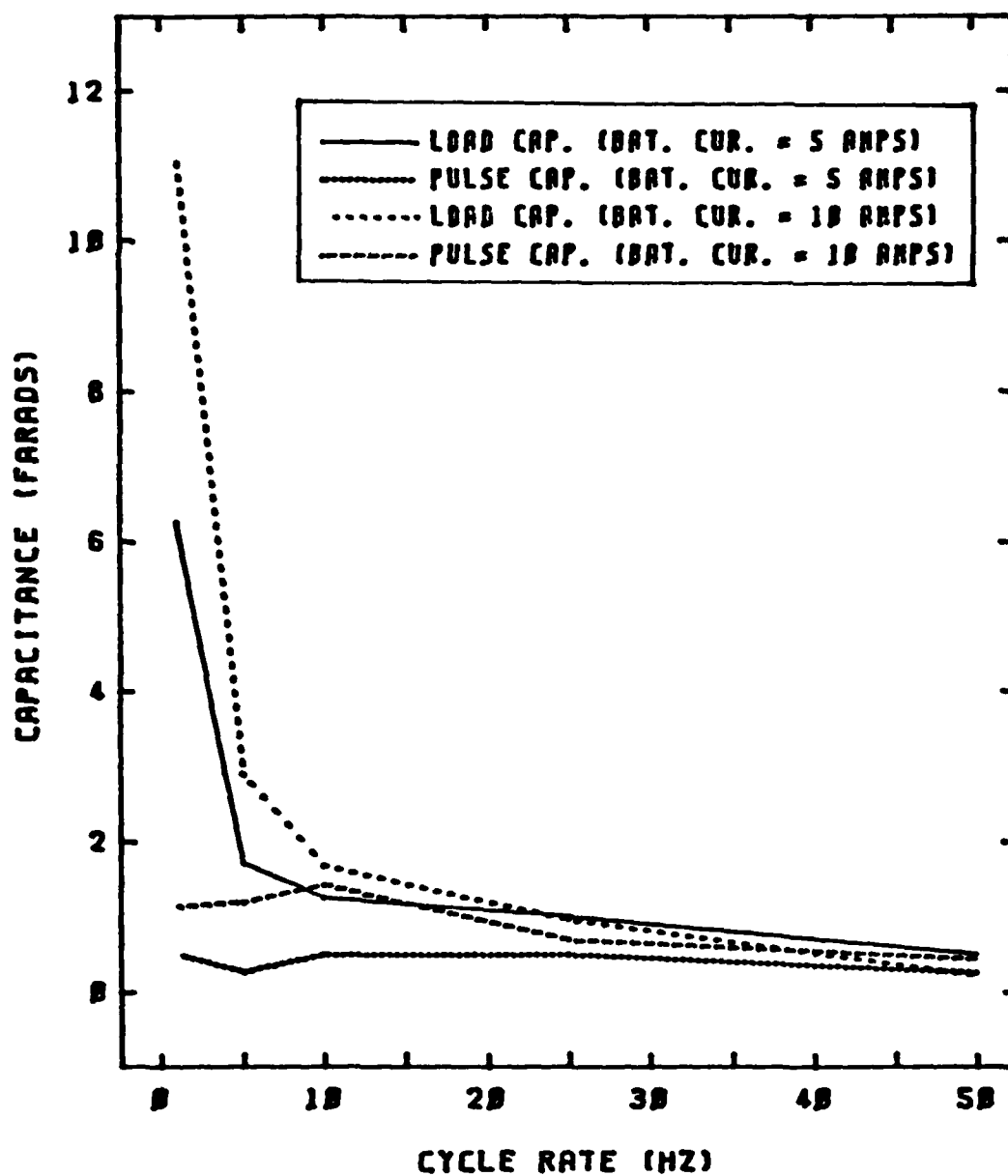


Figure K-1. Battery #1 Capacitance Versus Cycle Rate

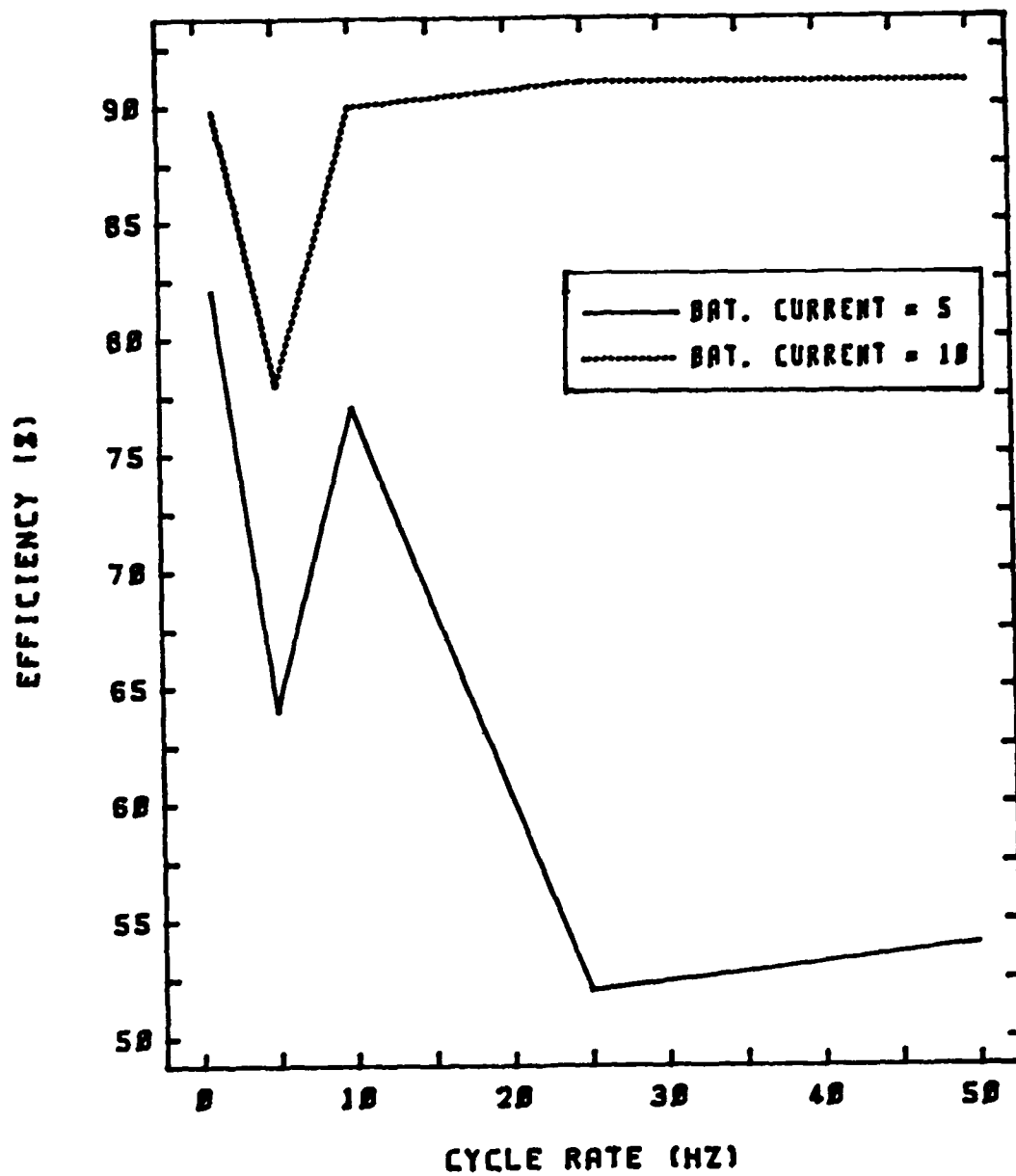


Figure K-2. Battery #1 Efficiency Versus Cycle Rate

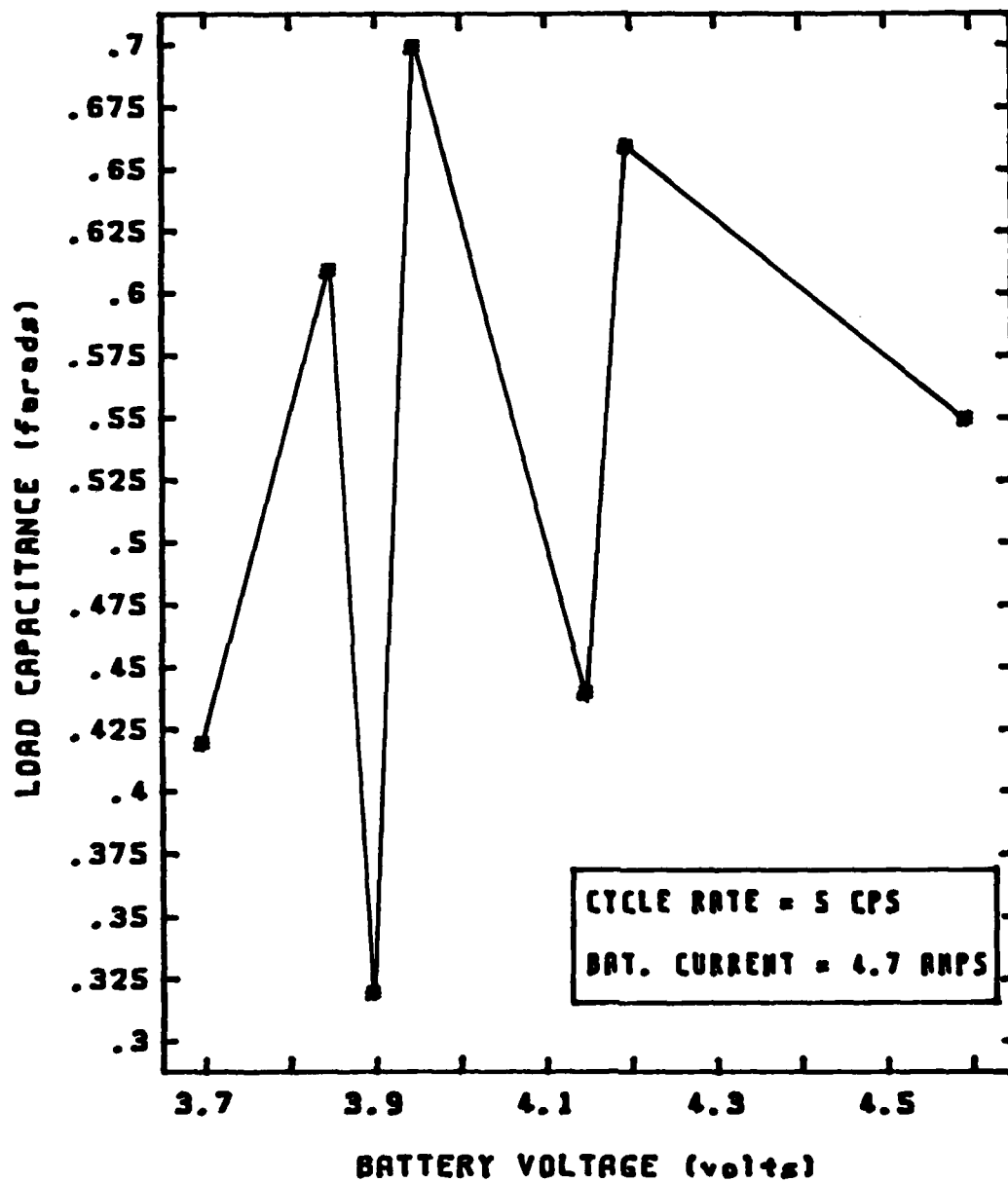


Figure K-3. Battery #2 Capacitance Versus End of Discharge Voltage

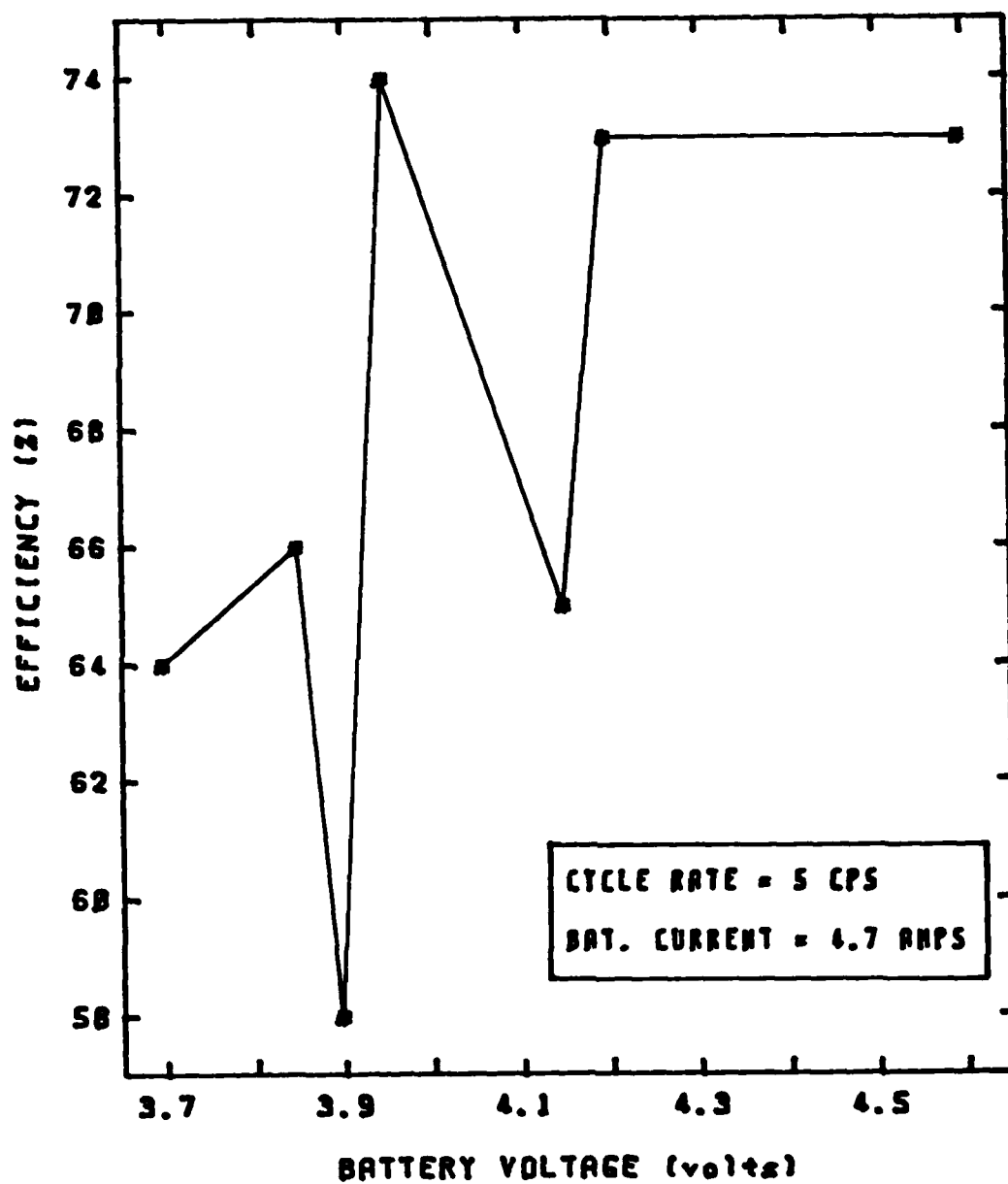


Figure K-4. Battery #2 Efficiency Versus End of Discharge Voltage

Appendix L. Scanning Electron Microscope Photographs

The photographs in this appendix illustrate various changes in the cadmium electrode morphology resulting from battery testing.

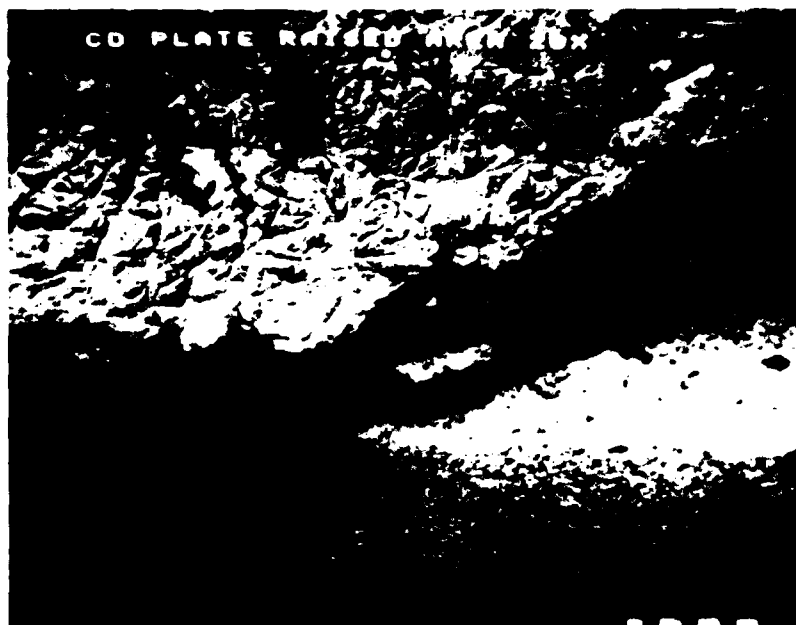


Figure L-1. Cadmium Electrode Blister - Top View



Figure L-2. Cadmium Electrode Blister - Side View

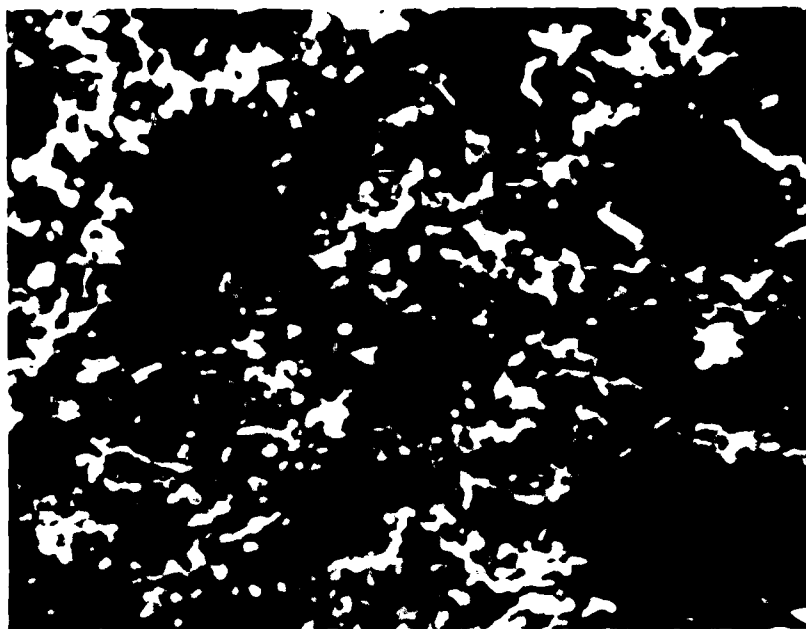


Figure L-3. Cadmium Electrode Surface Before Cycling

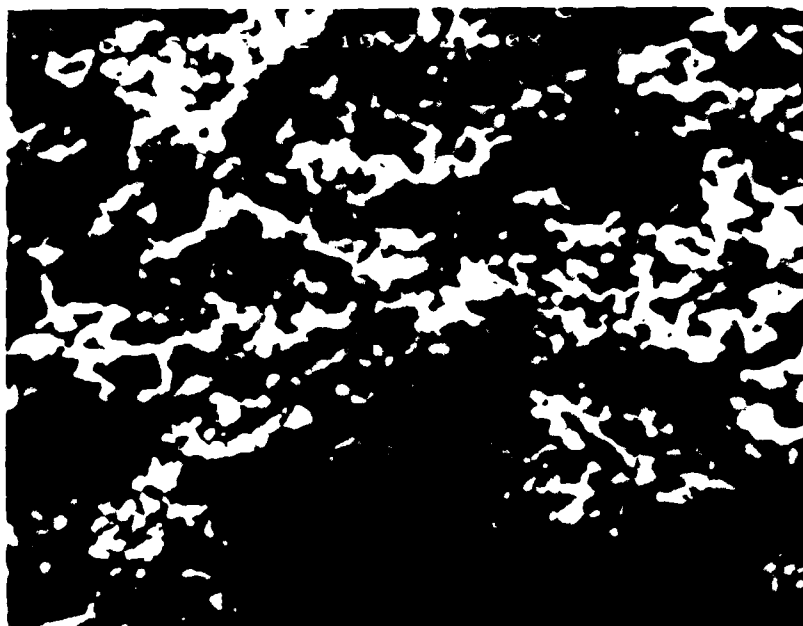


Figure L-4. Cadmium Electrode Surface After Ten Million Cycles



Figure L-5. Cadmium Electrode Back Before Cycling

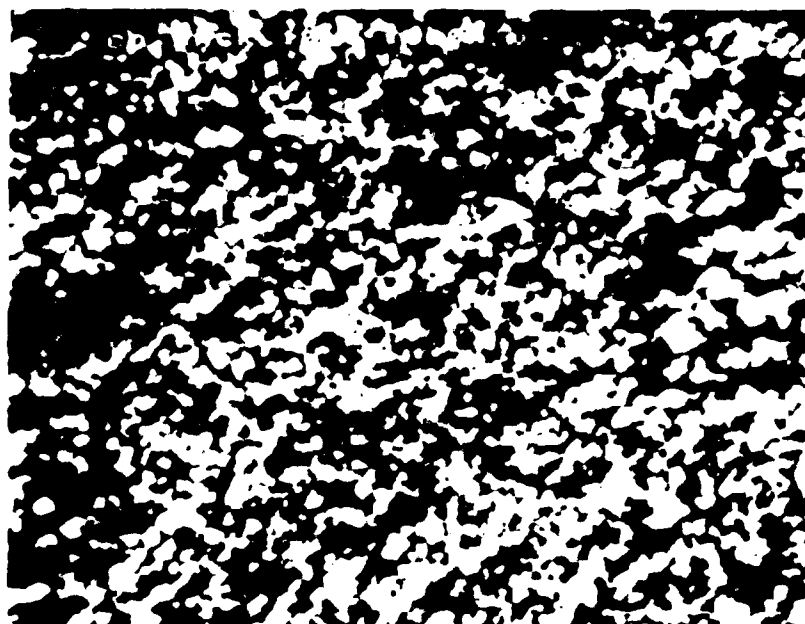


Figure L-6. Cadmium Electrode Back After Ten Million Cycles

Bibliography

1. Allen, Douglas M. and Wayne S. Bishop, "A Forecast of Air Force Requirements for Electrochemical Power Source Development," Proceedings of the 30th Power Sources Symposium, 249-252, Atlantic City, NJ, 7-10 June 1982.
2. Ford, Floyd E. and Gerald Halpert. "Future Needs for Energy Storage," Proceedings of the 30th Power Sources Symposium, 255-259, Atlantic City, NJ, 7-10 June 1982.
3. Weldon, William F. "Pulsed Power Packs a Punch," IEEE Spectrum, Vol. 22:59 (Mar 1985).
4. Bishop, Wayne S. and David C. Stumpff. Evaluation of Nickel-Cadmium Batteries for Long Life, High Repetition Rate Cycling Applications. Unpublished Test Report. Aero Propulsion Laboratory, Air Force Wright Aeronautical Laboratories, Wright-Patterson AFB, Ohio, December, 1982.
5. Gearing, Gregory M. and Michael B. Cimino. Pseudo Bipolar Nickel-Cadmium Batteries Used as Filter Elements To Pulsed Current Loads. Technical Report AFWAL-TR-84-2094, Aero Propulsion Laboratory, Air Force Wright Aeronautical Laboratories, Air Force Systems Command, Wright-Patterson AFB, Ohio, November 1984.
6. Clifford, J.E. Study of Bipolar Batteries. BATTELLE, Columbus Laboratories, Columbus, Ohio, June 1984, (SAND84-7108).
7. Seiger, Harvey N. et al. "Study of High Current Densities in Nickel-Cadmium Bipolar Batteries." Final Report to U.S. Army Missile Command, Contract No. DA-01-021-AMC-12509(Z) with US Army Missile Command. Gulton Industries, Inc., October, 1966.
8. -----, "Bipolar Nickel-Cadmium Cells for High Energy Pulses," Journal of Spacecraft and Rockets, 4:974-977 (Aug 1967).
9. Mantell, Charles L. Batteries and Energy Systems (Second Edition). New York: McGraw-Hill Book Company, Inc. 1983.
10. Bauer, Paul. Batteries for Space Power Systems. Washington D.C.: National Aeronautics and Space Administration, 1968 (NASA SP172).

11. Bishop, Wayne S. "Batteries and Fuel Cells for Pulsed Power Applications." Pulsed Power Lecture Series (15). Plasma and Switching Laboratory, Dept. of Electrical Engineering, Texas Tech University, Lubbock, Texas, 1981.
12. GET-3119A, Battery Application Manual. General Electric Battery Product Section, Gainesville, Fla. undated.
13. Milner, Paul C. and Upton, B. Thomas. "The Nickel-Cadmium Cell," Advances in Electrochemistry and Electrochemical Engineering, 5. 1-86, New York: Interscience Publishers, 1967.
14. Fritts, David H. Project Engineer, (Personal Interview). Aero Propulsion Laboratory, Air Force Wright Aeronautical Laboratories, Wright-Patterson AFB, Ohio, 23 July 1985.
15. Seiger, Harvey N. "Electrical Characteristics of a Sealed Nickel Cadmium Battery Having a Bipolar Construction," Proceedings 4th Intersociety Energy Conversion Engineering Conference: 710-714, Washington, D.C. September 22-26, 1969.
16. Gileadi, Eliezer et al. Interfacial Electrochemistry An Experimental Approach. Reading, Massachusetts: Addison-Wesley Publishing Company, Inc. 1975.
17. Delnick, Frank M. and Donald E. Amos, Battery Response to Pulse Loads: A Mathematical Model. Sandia Report. Sandia National Laboratories, Albuquerque, NM, August 1984 (SAND 83-1770).
18. Goddard Space Flight Center. Acceptance Test of Nickel-Cadmium Cells. Evaluation Program for Secondary Spacecraft Cells. Quality Evaluation Laboratory, Naval Ammunition Depot, Crane, Indiana, 15 July 1969 (QE/C 69-553).
19. Fritts, David H. and Ross E. Dueber, "A Discussion of the Mechanism of Cadmium Migration in Sealed Nickel-Cadmium Cells," Journal of the Electrochemical Society, Vol 132, No. 9 : 2039-2043 (Sept 1985).
20. General Electric. Nickel-Cadmium Battery Application Engineering Handbook. Gainesville, Florida, General Electric Company, 1975.

21. Warnock, Don R. Advanced Nickel-Hydrogen Battery Technology, United States Air Force Report. Air Force Aero Propulsion Laboratory, Wright-Patterson AFB, Ohio, October, 1977 (AD-B030652-L).
22. NASA Lewis Research Center. Nineteenth Annual Report of Cycle Life Test, Evaluation Program for Secondary Spacecraft Cells. Naval Weapons Support Center, Crane, Indiana, January, 1983 (WQEC/C 83-1).
23. Bishop, Wayne S. Technical Area Manager, Battery/Fuel Cells, (Personal Interview). Aero Propulsion Laboratory, Air Force Wright Aeronautical Laboratory, Wright-Patterson AFB, Ohio, 5 July 1985.
24. Fleischer, Arthur. "Sintered Plates for Nickel-Cadmium Batteries." Transactions of the Electrochemical Society, 94: 289-299 (Dec 1948).
25. Pickett, David F. US Patent 3,827,911, 1974, Preparation of Nickel Electrodes.
26. Fritts, David H. et.al. US Patent 4,242,179, 1980, Method of Fabricating Cadmium Electrodes.
27. Leonard, John F. Engineering Technician, (Personal Interview). Aero Propulsion Laboratory, Air Force Wright Aeronautical Laboratories, Wright-Patterson AFB, Ohio, 11 June 1985.
28. Fritts, David H. "A Discussion of the Causes of Blistering of Sintered Nickel Hydroxide Electrodes," Journal of Power Sources, 6 : 327-336 (1981).

Vita

Major Robert W. Chedister was born on October 27, 1949 in Little Rock, Arkansas. He graduated from Hazen High School in 1967 and attended Arkansas Tech University and the University of Arkansas where he received the degree of Bachelor of Science in Electrical Engineering in May 1972. Upon graduation he received a commission in the United States Air Force (USAF) through the ROTC program and entered undergraduate pilot training at Moody Air Force Base (AFB), Georgia. After earning his wings in May 1973, he was assigned to the 23rd Tactical Fighter Wing Flying Tigers where he flew the A-7D Corsair II. Following a tour in West Germany flying OV-10A Broncos and a Masters in Management degree from Troy State University, he attended the USAF Test Pilot School. As a USAF Fighter Test Pilot he flew F-16, F-4, and F-111 aircraft at Eglin AFB, Florida for four years until entering the School of Engineering, Air Force Institute of Technology, in May 1984.

Permanent addrees:

Box 343
Hazen, Ark. 72064

Vita

Captain John M. Ulmer was born on January 24, 1955 in Bellfontaine, Ohio. He graduated from Lakeland Senior High School, Lakeland, Florida in 1973. He received a Bachelor of Science degree in Electrical Engineering from the University of Florida, Gainesville, Florida in 1981 and received a commission in the United States Air Force upon completion of Officer's Training School the same year. He was assigned to the Air Force Cryptologic Support Center, Electronic Security Command in San Antonio, Texas where he served as a COMSEC Electronic Engineer until May 1984 when he entered the School of Engineering, Air Force Institute of Technology.

Permanent address: 2715 French Ave
Lakeland, Fla. 33801

REPORT DOCUMENTATION PAGE

1a. REPORT SECURITY CLASSIFICATION UNCLASSIFIED			1b. RESTRICTIVE MARKINGS			
2a. SECURITY CLASSIFICATION AUTHORITY			3. DISTRIBUTION/AVAILABILITY OF REPORT Approved for public release; distribution unlimited.			
2b. DECLASSIFICATION/DOWNGRADING SCHEDULE						
4. PERFORMING ORGANIZATION REPORT NUMBER(S) AFIT/GE/ENG/85D-6			5. MONITORING ORGANIZATION REPORT NUMBER(S)			
6a. NAME OF PERFORMING ORGANIZATION School of Engineering Air Force Institute of Technology		6b. OFFICE SYMBOL (If applicable) AFIT/ENG	7a. NAME OF MONITORING ORGANIZATION			
6c. ADDRESS (City, State and ZIP Code) Wright-Patterson AFB, Ohio 45433			7b. ADDRESS (City, State and ZIP Code)			
8a. NAME OF FUNDING/SPONSORING ORGANIZATION Aero Propulsion Laboratory AF Wright Aeronautical Labs		8b. OFFICE SYMBOL (If applicable) AFWL/POOS	9. PROCUREMENT INSTRUMENT IDENTIFICATION NUMBER			
8c. ADDRESS (City, State and ZIP Code) Wright-Patterson AFB, Ohio 45433			10. SOURCE OF FUNDING NOS.			
11. TITLE (Include Security Classification) see box 19			PROGRAM ELEMENT NO. 61102R	PROJECT NO. 2303	TASK NO. S4	WORK UNIT NO. 02
12. PERSONAL AUTHOR(S) Robert W. Chedister, Major USAF and John M. Ulmer, Captain USAF						
13a. TYPE OF REPORT MS Thesis		13b. TIME COVERED FROM _____ TO _____		14. DATE OF REPORT (Yr., Mo., Day) 1985 November		15. PAGE COUNT 134
16. SUPPLEMENTARY NOTATION						
17. COSATI CODES			18. SUBJECT TERMS (Continue on reverse if necessary and identify by block number)			
FIELD	GROUP	SUB. GR.	Nickel-Cadmium Battery, Bipolar Nickel-Cadmium Battery, Capacitive Filter, Life Cycle Testing			
10	03					
09						
19. ABSTRACT (Continue on reverse if necessary and identify by block number)						
Thesis Advisor: Dr. Andrew Terzuoli						
Title: STUDY OF BIPOLAR NICKEL-CADMIUM BATTERIES AS PULSED LOAD FILTERS						
<div style="text-align: right;"><i>Approved for public release LAW AFB 198-17</i> LYNN E. WOLAVER 16JAN86 Dean for Research and Professional Development Air Force Institute of Technology (AFIT) Wright-Patterson AFB OH 45433</div>						
20. DISTRIBUTION/AVAILABILITY OF ABSTRACT UNCLASSIFIED/UNLIMITED <input checked="" type="checkbox"/> SAME AS RPT. <input type="checkbox"/> DTIC USERS <input type="checkbox"/>			21. ABSTRACT SECURITY CLASSIFICATION UNCLASSIFIED			
22a. NAME OF RESPONSIBLE INDIVIDUAL Dr. Andrew Terzuoli			22b. TELEPHONE NUMBER (Include Area Code) 513-255-2024		22c. OFFICE SYMBOL AFIT/ENG	

ABSTRACT

Bipolar nickel-cadmium batteries were designed, built, and tested for use as capacitive filter elements for possible pulsed power applications. Electrodes were made by electrochemically impregnating sintered sides of nickel cell walls. Four-cell batteries were constructed by compressing together the electrodes separated by Teflon seals. A computer controlled test circuit charged and discharged the test batteries at frequencies of 1 to 50 Hertz and at depths-of-discharge of less than one percent. A special test battery was constructed with a removeable cadmium electrode for scanning electron microscope study. Battery energy density, effective capacitance, and efficiency were investigated as a function of current load or depth-of-discharge, cycle-rate, and end-of-discharge voltage. Energy densities of nearly 75 joules per pound were demonstrated. Current loads of up to a 100 C-rate were demonstrated and an average capacitance of 6 Farads was achieved. Cadmium electrode morphology was photographed and studied as a function of the charge and discharge cycle life and no crystalline anomalies were discovered. Sinter corrosion, nickel electrode overcharging, and individual cell voltage imbalances were discovered as areas for further study.

END

FILMED

3-86

DTIC